

AD 654718

ARC DISCHARGE SOURCES

FINAL REPORT

16 OCTOBER 1964 TO 28 FEBRUARY 1967

31 MARCH 1967

CONTRACT Nonr 4647(00)

ARPA ORDER NO. 306-62

CODE 4730

REQ: NO. NR-012-511, 7 JANUARY 1966

A 28-MONTH CONTRACT

EXPIRATION DATE 28 FEBRUARY 1967

COST \$195,933

Charles H. Church, Principal Investigator (412) 256-3678

B. W. Swenson

E. Geil

J. Lowke

L. Armstrong

R. Liebermann

G. Basi

P. Buchhave

D. Sun

I. Liberman

R. S. de Voto

This document has been approved
for public release and its
distribution is unlimited.

DDC
RECEIVED
JUL 17 RECEIVED
JUL 21 1967
CESTI

190

DISCLAIMER NOTICE

THIS DOCUMENT IS THE BEST
QUALITY AVAILABLE.

COPY FURNISHED CONTAINED
A SIGNIFICANT NUMBER OF
PAGES WHICH DO NOT
REPRODUCE LEGIBLY.

ARC DIS LARGE SOURCES

FINAL REPORT
16 OCTOBER 1964 TO 28 FEBRUARY 1967

31 MARCH 1967

CONTRACT Nonr 4647(00)
ARPA ORDER NO. 306-62
CODE 4730
REQ: NO. NR-012-511, 7 JANUARY 1966

A 28-MONTH CONTRACT
EXPIRATION DATE 28 FEBRUARY 1967
COST \$195,933

Charles H. Church, Principal Investigator (412) 256-3678

B. W. Swanson	E. Geil
J. Lowke	L. Armstrong
R. Liebermann	G. Basi
P. Buchhave	D. Sun
I. Liberman	R. S. de Voto

BLANK PAGE

TABLE OF CONTENTS

	<u>Page</u>
PREFACE	111
ABSTRACT.	iv
I. INTRODUCTION.	1
II. BASIC PRINCIPLES OF HIGHLY RADIATIVE ARCS	4
2.1 Electrical and Thermal Conductivity.	6
2.2 The Spectral Absorptivity.	6
2.3 The Arc Models	8
III. COUPLING THE PUMP INTO THE LASER ROD.	14
IV. RECENT EXPERIMENTAL MEASUREMENTS ON THE ARC	19
V. SUMMARY AND CONCLUSIONS	28
VI. ACKNOWLEDGMENTS	29
VII. REFERENCES.	30
VIII. APPENDICES.	
A. A Program for the Calculation of the Electrical and Thermal Conductivity of Xenon as a Function of Temperature and Pressure. By R. S. DeVoto.	
B. Calculation of Bound-Bound Transition Probabilities. By D. Sun	
C. Calculation of the Optical Radiation Emitted by a Cylindrical Arc of Known Temperature Profile. By R. Liebermann	
D. Whittaker and Gamma Functions-Description of Two ALGOL Procedures. By G. Basi	
E. Radiative Transport in a Xenon Arc. By B. W. Swanson.	
F. Analysis of Xenon Discharges. By J. J. Lowke	

LIST OF FIGURES

	<u>Page</u>
Figure 1 - The equations relating the electrical power input to the optical radiation and the thermal conduction.	5
Figure 2 - The information flow for the calculation procedures in the appendices.	7
Figure 3 - The calculated spectral absorptivity of xenon I over a range of temperature for a pressure of 5 Atm.	9
Figure 4 - The calculated spectral radiance along a .8 cm diameter homogeneous temperature xenon plasma at 12000°K and 5 Atm pressure.	11
Figure 5 - The calculated spectral radiant emittance for .8 cm and 1.4 cm diameter homogeneous cylindrical plasmas in xenon at 12000°K and 5 Atm pressure.	12
Figure 6 - Simplified representation of laser rod-coaxial laser pump system.	15
Figure 7 - Multiple rod coaxial laser pump.	17
Figure 8 - Geometry of the spherical reflector.	18
Figure 9 - Black body temperatures corresponding to measured spectral radiances.	21
Figure 10 - Black body temperatures corresponding to same spectral radiance as 13 mm flash tube as a function of input power density.	22
Figure 11 - Spectral radiance of linear cylindrical Xe flash tubes of different diameters as a function of power density input.	23
Figure 12 - Spectral radiance of linear cylindrical Xe flash tubes of different diameters as a function of power input.	24
Figure 13 - Spectral radiance distribution for an EG & G Inc. FX-52 flash tube single & double pulsed.	25
Figure 14 - The spectral radiance at 3000Å viewed end on and side on for a 13 mm diameter arc tube.	27

PREFACE

This report presents the work since the previous semiannual report on Contract Nonr 4647(00). It also summarizes the previous work on the contract toward the development of quantitative models for high energy pulsed arcs of the type that are used for the optical pumping of high energy lasers. The studies in this contract have been concerned primarily with xenon as this gas has been used most successfully for high energy laser pumping; the principles contained in the models for the arcs are applicable to other highly radiative arcs, though in many cases the necessary quantitative descriptions of the physical properties of the arc plasma are not available at the present time.

Recent developments in pumping geometries and in additive lamps, arising, in part, from this work and from work in a closely related area, the optical pumping of continuous lasers, under Contracts DA-28-043-AMC-00292(E) and DA-28-043-AMC-02097(E), indicate new promise for efficient optically pumped lasers. The principles discussed in this report provide a basis for an understanding of the optical pumps for lasers.

ABSTRACT

This report summarizes the studies made on Contract Nonr 4647(00) towards the development of models for the highly radiative arcs used for the high energy pumping of lasers. The report also presents the experimental and theoretical studies since the last semi-annual report. The experimental investigations were primarily concerned with more extensive measurements of the spectral radiance of the plasma to provide verification for the models. The theoretical work has resulted in computer methods, described in the appendices, to calculate the transport properties, the spectral absorptivities for the lines and the continuum of xenon, and the spectral radiance and temperature profiles in cylindrical arcs. Also included as an appendix is a theoretical analysis of the xenon arc using radiative transport techniques developed in other studies.

ARC DISCHARGE SOURCES

Charles H. Church, Principal Investigator (412) 256-3678

B. W. Swanson	E. Geil
J. Lowke	L. Armstrong
R. Liebermann	G. Basi
P. Buchhave	D. Sun
I. Liberman	R. S. de Voto

I. INTRODUCTION

The optically pumped solid state laser provides the highest peak power and highest peak energy available from coherent sources. This report summarizes the work on Contract Nonr 4647(00) toward the development of quantitative models for the highly radiative arcs used to excite these lasers. Contained in the appendices to this report are computer programs developed in this work for the calculation of many features of these arcs. The calculation procedures are for xenon, though in principle, they are applicable to other atomic systems.

The theoretical and the experimental research on this contract has been directed towards the creation of quantitative models for the flash lamps that in turn would be useful in the improvement of high energy lasers. The development of the models required basic studies of the many aspects of highly radiative arcs, and lead to considerable expansion of the experimental techniques available for the study of these dense plasmas. These plasmas may be encountered in many situations other than the flash tubes for pumping high energy lasers, including re-entry shock waves and high voltage switch gear.

The effort in this contract can be divided into three areas: (1) the development of theoretical techniques to calculate the necessary physical properties of arc plasmas, (2) the applications of these techniques to create models for the high radiative arcs, and (3) the experimental measurements required to formulate and then to verify the models.

The earlier reports (references 1, 2, 3 & 4) described many aspects of the problem more fully. The computer programs resulting from this work are all in the ALGOL language for a Burroughs B5500 DISK computer.

The development of the models required techniques for calculating the transport properties (electrical and thermal conductivity), and the spectral absorptivity (the broadened spectral lines plus the continuum) as a function of temperature and pressure. In addition, methods for handling energy transport within highly radiative inhomogeneous temperature arc plasmas were required.

For the transport properties of xenon, we were fortunate in obtaining the assistance of Dr. R. S. de Voto of Stanford University, who has developed computer programs for calculating the properties of partially ionized monatomic gases. His program for the calculation of the electrical and thermal conductivities of xenon as a function of temperature and pressure is in Appendix A.

The calculation of the spectral absorptivity of xenon required consideration of the broadened lines and the continuum. The final program given in Appendix B is due to the efforts of many people, particularly D. Sun of California Institute of Technology, E. Corinaldesi, now at Boston University, and R. G. Schlecht, now at Aeroneutronics Division of Ford Motor Company. Appendix C uses the bound-bound transition probabilities and other information on xenon to calculate the optical radiation emitted by a cylindrical arc of a given temperature profile and pressure. Appendix D presents calculations for Whittaker functions of real and imaginary argument for use in calculations of the matrix elements for bound-free and free-free transitions. We will discuss details of these calculations in a later section.

Two approaches were followed in the creation of the models for the arc. In one approach, we assumed the arc to be homogeneous in temperature and neglected thermal conduction to the walls. Experimental measurements had indicated that this was a reasonable assumption for the central core. Such model would explain a number of the observed characteristics, such as the arc radiant emission saturation in the infrared and in the visible, and account for a major portion of the input power.

The pressure to be used for this homogeneous temperature model is open to question due to the actual temperature gradient which exists near the walls. In the other approach, the electric field across the arc, the inside diameter of the arc tube, and the pressure of heavy particle number density are to be specified and the radial absolute temperature distribution is to be sought. With the temperature distribution, we could calculate all of the observed properties of the arc including the spectral radiance at the walls (Appendix C). This calculation required the solution to the energy balance equation for a non-grav, nonhomogeneous temperature plasma. An approximate analysis described in Appendix E was applied to this problem to obtain a better initial temperature distribution. The final program developed in this work is given in Appendix F.

The experimental measurements were intended to aid in the formulation and verification of the models. In the course of the work, the flash lamp or more completely, the confined wall-stabilized pulsed arc discharge, was found to be a useful vehicle to study high power density, high pressure, highly radiative plasmas. Plasmas with these characteristics in gases other than xenon are of interest to workers in many fields or research and applications. In the course of this work and in the closely associated company sponsored research, techniques have been and are being developed to study these plasmas. These techniques have included two rapid scanning spectrometers, one of high resolution scanning over a limited range⁽⁶⁾ the other of decreased resolution but with a much wider spectral range⁽⁷⁾.

A problem still exists in the accurate measurement of the instantaneous pressure. The pressure is crucial to an accurate description of the arc as the pressure varies widely with the temperature gradient near the wall. Currently a laser interferometer similar to that of Gerardo et al.⁽⁸⁾ is being set up to allow electron density measurements. These electron density measurements will serve to check the values we have assumed in the calculations.

II. BASIC PRINCIPLES OF HIGHLY RADIATIVE ARCS

The arcs used for pumping high energy lasers have many features in common with arcs used for continuous laser pumping. The primary difference between these arcs lies in the size of the arc column and the power density in the arc. In both cases, the arcs are near or above atmospheric pressure. As the efficiency of the laser systems increase, the differences between the two arc applications are becoming less marked.

The usual form of the arc used in high energy laser pumping is a cylindrical arc surrounded by a wall. We have only investigated this wall stabilized arc. In the arc, current flow carries power into the arc; radiation external to the arc and thermal conduction to the arc surroundings (i.e.: the wall) carry power away from the arc. Convective power transport can be neglected in this type of wall stabilized confined arc unless there is gas flow--which we have not considered in this work. A wall stabilized highly radiative arc such as those used for high energy laser pumping has a central plasma core at the temperature of the fully ionized plasma (the actual temperature varying with the composition of the plasma) with the temperature at the wall dependent upon the rate at which power is carried away from the walls. (A fully ionized plasma may be only .01% ionized. It is characterized by the dominance of the electron-electron and electron-ion interaction over the other particle interaction).

The relation between the input power and that carried away from the arc by radiation and conduction can be put into equation form. Figure 1 presents the family of equations that relate the power input per unit volume to the power carried away by radiation and conduction. We consider the arc to be in local thermal equilibrium (LTE) and thus describable by Boltzmann's equation, Saha's equation and a simple radiation law. The electrical and thermal conductivities as well as the spectral absorptivities are functions of the local temperature and pressure for each constituent. The various constituents of the plasma interact with each other through the ionization law

The Energy Balance

$$\tau \cdot (\bar{F}_{RAD} + \bar{F}_{TC}) = \sigma (p, T) E^2$$

where E is the electric field in Volts cm^{-1} , σ is the electrical conductivity in $(\text{ohm cm})^{-1}$ and is dependent upon the pressure (p) and the temperature (T). $\bar{F}_{T.C.}$ is the thermally conducted power flux in Watts cm^{-2} and is given by

$$\bar{F}_{T.C.} = -K(p, T) \text{grad } T$$

K is the thermal conductivity in Watts $\text{cm}^{-2} \text{ } ^\circ\text{K}^{-1} \text{ cm}$. \bar{F}_{RAD} is the radiant emittance (i.e. radiative flux) in Watts cm^{-2} and is expressed in terms of $F_{\nu, RAD}$, or $F_{\lambda, RAD}$. The spectral radiant emittance

$$\bar{F}_{RAD} = \int_0^\infty \bar{F}_{\nu, RAD} d\nu = \int_0^\infty \bar{F}_{\lambda, RAD} d\lambda$$

where ν is the frequency and λ the wavelength in consistent units. Consider the x component of $\bar{F}_{\nu, RAD}$; it is expressed in terms of I_ν

$$F_{\nu, x} = \int_\omega I_\nu(\bar{S}) \cos(x, \bar{S}) d\omega$$

I_ν is the spectral radiance (i.e. specific intensity) in Watts cm^{-2} Steradian frequency unit $^{-1}$ along the \bar{S} direction. ω is the solid angle over which the integral is to be taken. I_ν is the solution to the equation of transfer for the geometry being considered:

$$\frac{dI_\nu(\bar{S})}{ds} = \kappa_\nu'(p, T) [B_\nu(T) - I_\nu(\bar{S})]$$

in which s is the magnitude of the direction vector \bar{S} and κ_ν' is the spectral absorptivity including stimulated emission in cm^{-1} and is given by

$$\kappa_\nu' = \kappa_\nu(p, T)(1 - e^{-h\nu/kT})$$

$B_\nu(T)$ is the Planck distribution function. h is Planck's constant, k is Boltzmann's constant and are to be in units consistent with T and ν . κ_ν is the spectral absorptivity in cm^{-1} which in turn is the sum of the spectral absorptivities for bound-bound transitions, κ_ν^{bb} , the spectral absorptivity for bound-free transitions, κ_ν^{bf} , and the spectral absorptivity for free-free transitions, κ_ν^{ff} :

$$\kappa_\nu = \kappa_\nu^{bb} + \kappa_\nu^{bf} + \kappa_\nu^{ff}$$

The relations between the spectral absorptivities and the transition probabilities for these processes will be presented in Appendix C.

FIGURE 1

The equations relating the electrical power input to the optical radiation and thermal conduction.

(Saha's equation) and thus the electron density, and in broadening the lines through electron, ion, and Van der Waals mechanisms.

2.1 Electrical and Thermal Conductivity

The transport properties (i.e., the electrical and thermal conductivities) of partially ionized gases are currently under extensive investigation in many laboratories. We have used de Voto's calculations^(9, 10) as applied to xenon using the momentum transfer cross section of Frost and Phelps.⁽¹¹⁾ The program for the electrical and thermal conductivities of xenon is given in Appendix A.

2.2 The Spectral Absorptivity

The spectral absorptivity of atomic species can now be calculated (in theory) to a relatively high precision without exorbitant computer time using "quantum defect" methods to obtain the transition probabilities for bound-bound transitions and the cross sections of the bound-free and free-free transitions. The electron broadening was calculated using the line broadening theory outlined by Griem⁽¹²⁾ as applied by Corinaldesi.⁽¹³⁾ Figure 2 shows schematically the calculation⁽³⁾ of the spectral absorptivities which are carried out in appendices C and D and how they relate to the other programs.

The population of the initial level is one of the most important determinants of the strength of an absorption as the population in the initial level can vary in orders of magnitude as the temperature changes a few thousand degrees. If the line in bound-bound transition arises from a ground or very low lying state, the population in the level is very high in the cooler gas near the walls, thereby leading to a high spectral absorptivity. Examples for these ground state transition are the resonances lines of xenon lying in the vacuum ultraviolet and the yellow doublet of sodium. The high spectral absorptivity will be manifested in the arc discharge by very broadened and self reversed emission bands.

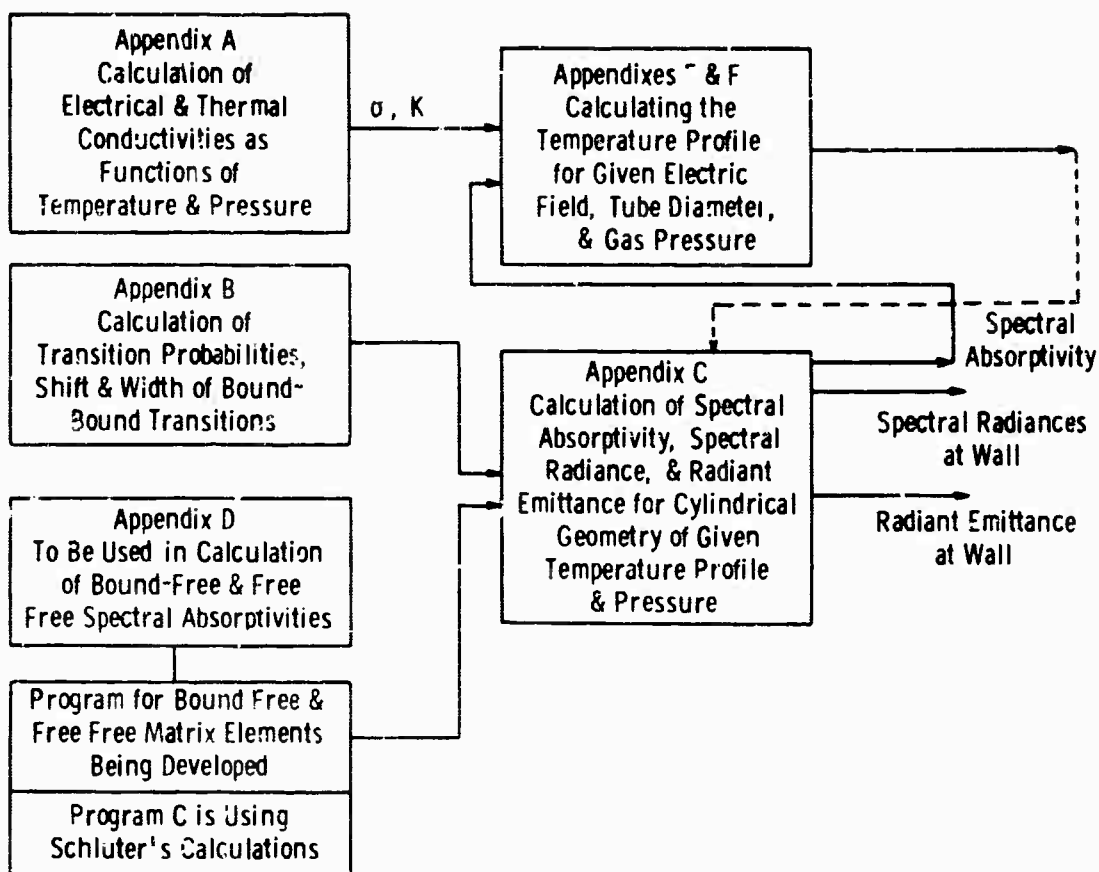


Fig. 2—The information flow for the calculation procedures in the appendices

The shape of the line determines how the absorption varies with wavelength. We have considered the lines in the dense highly radiative plasmas treated herein to have a Lorentzian shape. The line width, w , and the shift, d , arises in the cases being considered from electron broadening in the center of the arc (Stark broadening theory), and neutral particle broadening near the edge (Van de Waals or resonance broadening).

The various broadening mechanisms are calculatable (in theory at least) for atomic systems such as xenon. Figure 3 shows the spectral absorptivities for xenon for a range of temperatures at the same pressure; 5 atm. The program for this is in Appendix C. The spectral absorptivities shown in Figure 3 include the broadened lines and the continuum. The lines were calculated using an intermediate coupling program described in the last report⁽⁴⁾ and in Appendix B which was the extension to xenon of the calculation of Garstang and Van Blerkom.⁽¹⁴⁾ The continuum was that calculated by Schluter⁽¹⁵⁾ and is described in an earlier report and in Appendix C. The upper limit on the spectral absorptivities that may be calculated by this program is limited to below those temperatures for which Xenon II becomes appreciable ($\sim < 14,000^\circ\text{K}$) (We are modifying the programs to include XeII, but this work was not available for this report.) The effect of the XeII will be to increase the continuum and the emission in the blue and ultraviolet as XeII does not have the strong infrared lines that XeI exhibits.

2.3 The Arc Models

Two approaches were used in the creation of models for the arc. In the simplest, the arc was assumed to be homogeneous in temperature and thermal conduction to the walls was neglected. In the more complete approach, the absolute temperature profile is calculated for a given electric field and tube diameter. From the temperature profile, the spectral radiance through the arc, the radiation external to the arc, and the thermal conduction to the walls can be calculated.

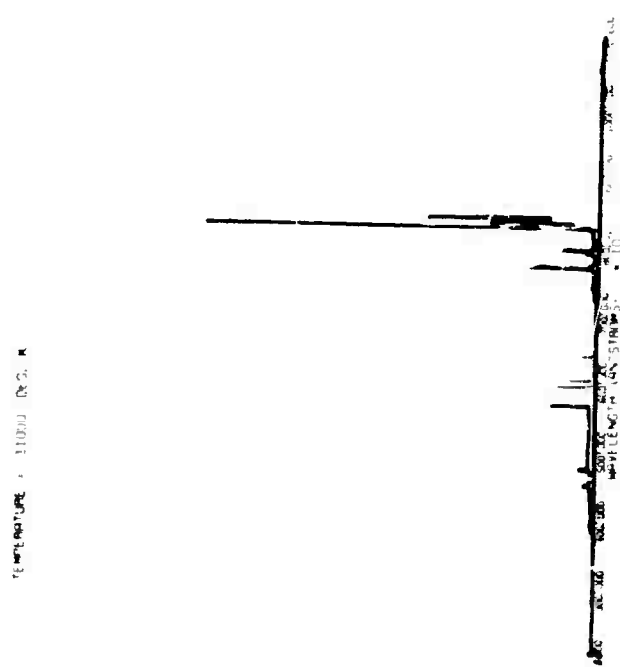
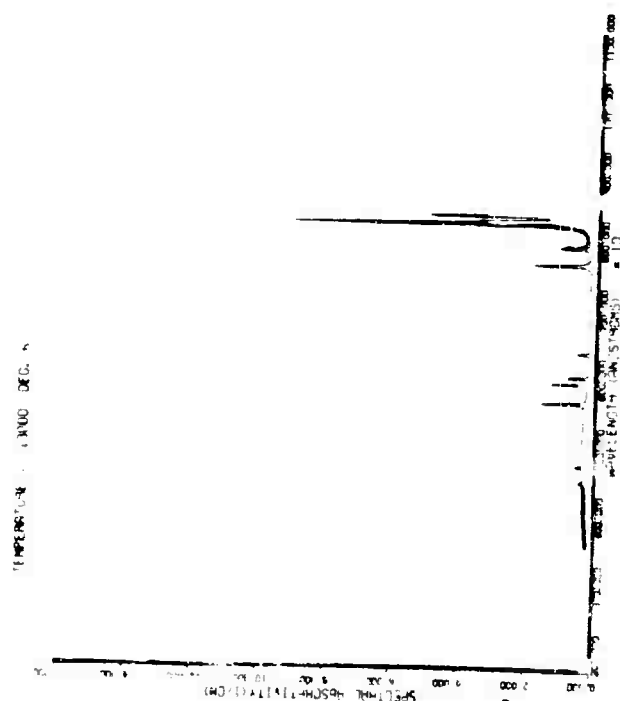
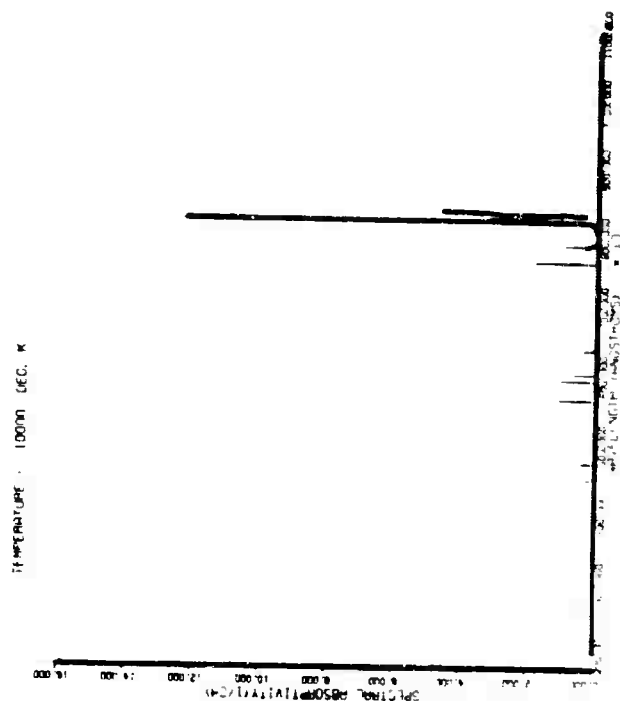
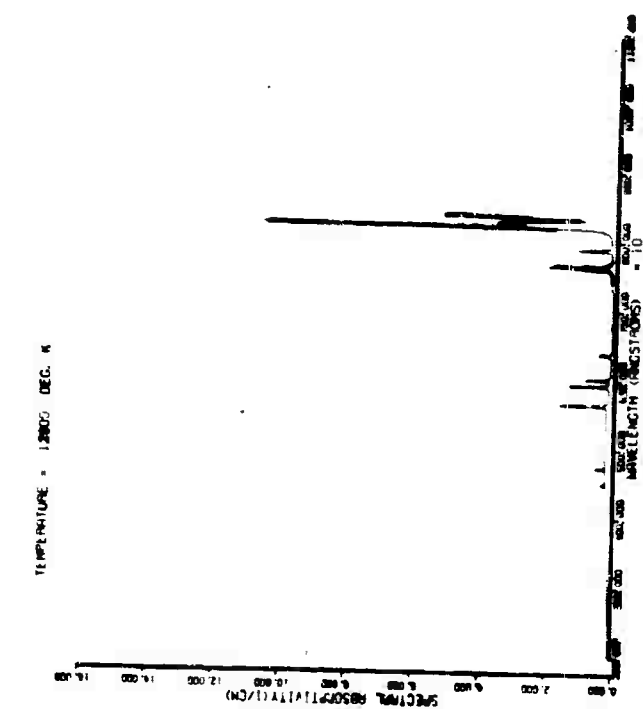


Fig. 3—The calculated spectral absorptivity of Xenon I over a range of temperatures for a pressure of 5 atm

The inclusion of the free-free transitions and the more complete calculations of the bound-free transitions required more extended application of the quantum defect methods of Seaton⁽¹⁶⁾, and Burgess and Seaton⁽¹⁷⁾. Peach^(18,19), Schlüter⁽¹⁵⁾, and a series of papers by Biberman and Norman and their collaborators⁽²⁰⁾ have indicated improvements using the Coulomb field; Stewart and Rotenberg⁽²¹⁾ and McGuire⁽²²⁾ have extended the theory to the non-Coulomb potential found in the inner part of the atom. The rise of these methods required programs for calculating Whittaker functions⁽²³⁾ of real and imaginary argument. Appendix D presents ALGOL translation of and corrections to the FORTRAN programs of McGuire⁽²⁴⁾. These programs are to be used as entry points for the numerical integrations of the radial matrix elements for bound-free and free-free transitions.

The homogeneous temperature models considered the arc to be a cylinder of uniform temperature with the arc diameter to be an input parameter. The homogeneous temperature models for the pulsed arcs were found to give reasonable agreement with experiment if the arc diameter were properly chosen. In the previous report, the electrical conductivity determined from a .41 cm bore tube was used to calculate the arc core diameters for the larger tubes at the same temperatures using temperatures measured from a region of the spectrum that was assumed to be radiating like a black body. The radiant emittances (neglecting lines) calculated for the respective core diameters at the temperatures studied were found to account for the major portion of energy delivered to the flash tube.

The spectral radiance along a .8 cm diameter for a homogeneous temperature discharge of 12,000°A and 5 atm. is shown in Figure 4.

The spectral radiant emittances for two homogeneous temperature cylindrical arcs of .8 and 1.4 cm diameter are shown in Figure 5. The radiant emittance (i.e. radiative flux) is shown in the figure. The radiated power per unit length is simply the product of the radiant emittance and the surface area of the arc. The program for the calculation of the radiant emittance is part of Appendix C.

SPECTRAL RADIANCE AT SURFACE OF CYLINDRICAL PRC COLUMN
FROM ALONG LINE OF SIGHT OF DIAMETER HAVING A SPATIAL
TEMPERATURE GRADIENT
PRESSURE = 5.000 ATM

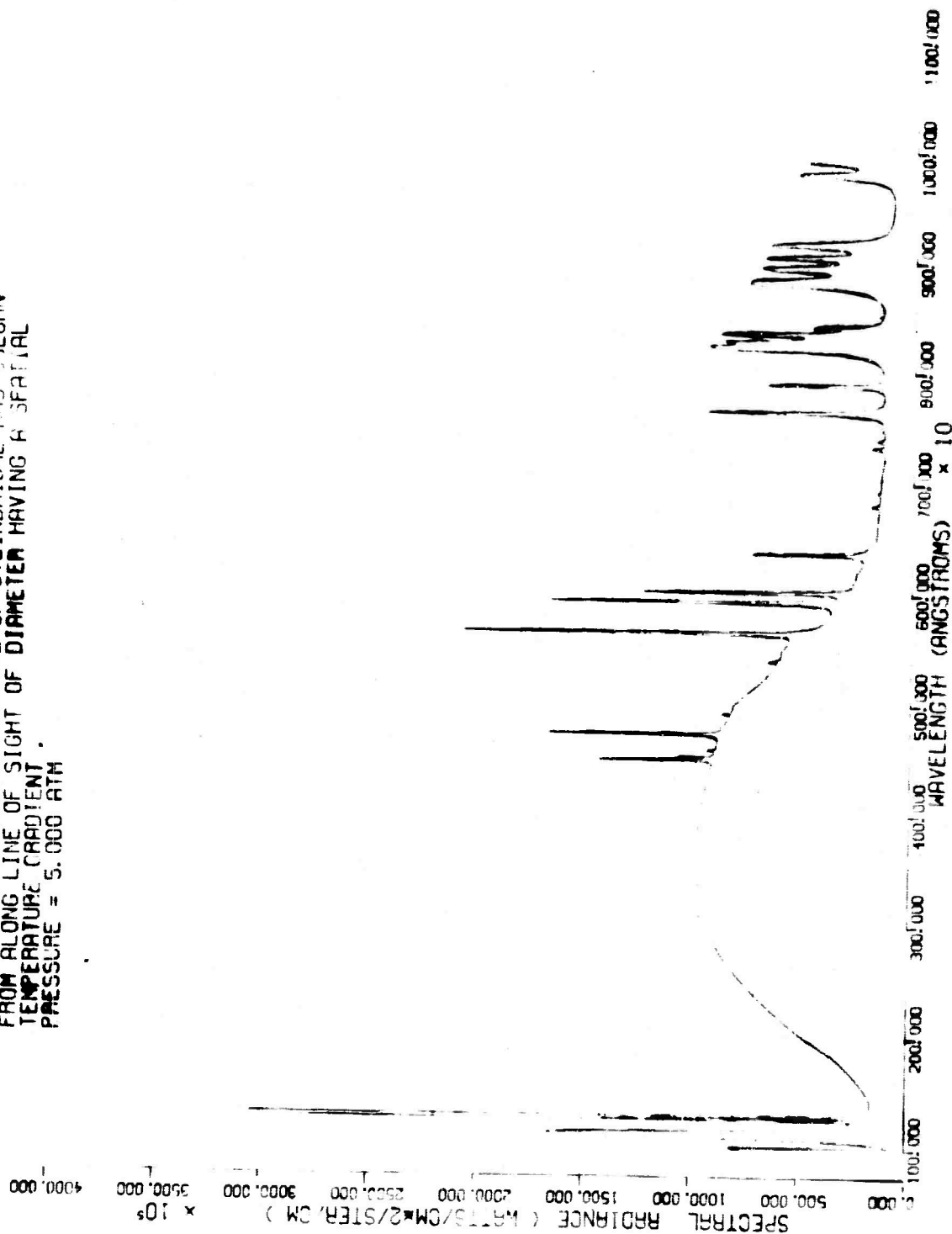


Fig. 4—The calculated spectral radiance along a .9 cm diameter homogeneous temperature Xenon plasma at 12000°K and 5 atm pressure

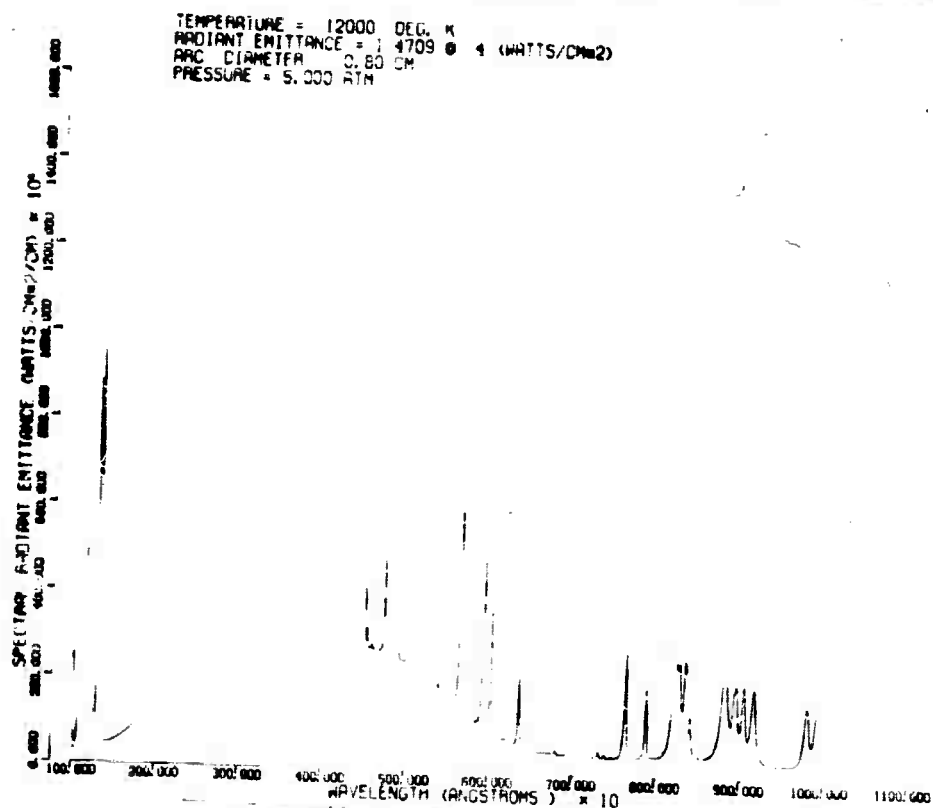
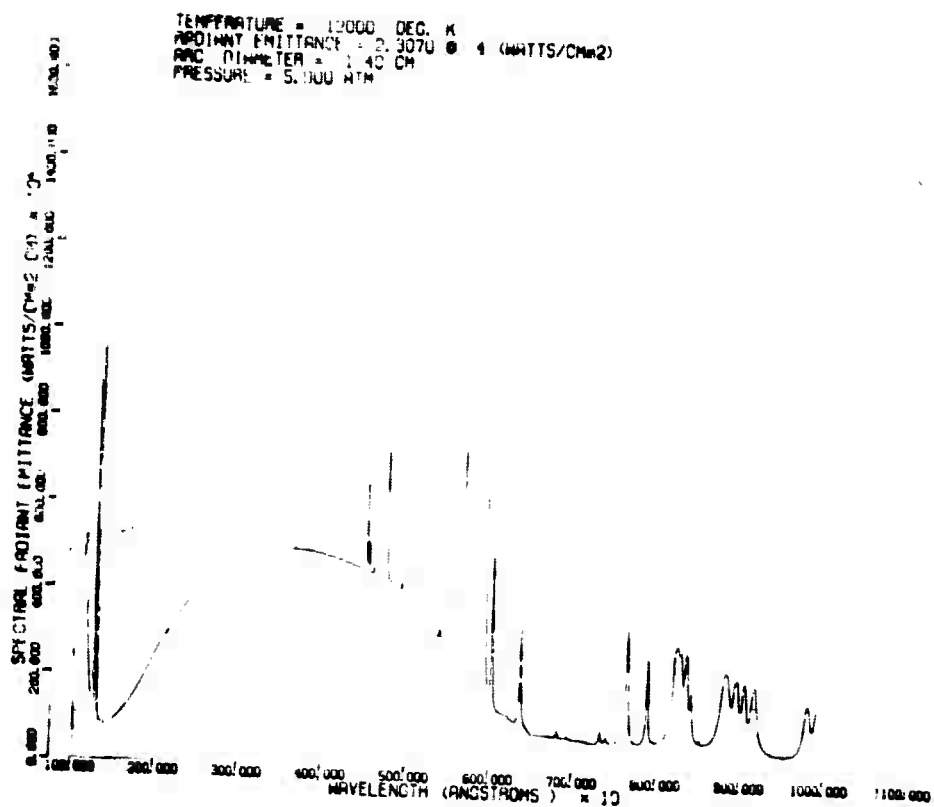


Fig. 5—The calculated spectral radiant emittances for .8 cm and 1.4 cm diameter homogeneous temperature cylindrical plasmas in Xenon at 12000°K & 5 atm pressure

The ideal model for the arc is one in which the characteristics of the arc discharge are determined by the input parameters: the electric field across the arc, the geometry of the arc container (i.e., the inside diameter of the cylinder), and the pressure and composition of the fill gas. But this model requires the solution to an integral-differential equation, called the energy balance equation, shown in part in Figure 1. The result of the application of the equation is simply the temperature distribution within the arc column.

We have explored a few methods for solving the energy balance equation for non-gray, nonhomogeneous plasma. The problem may be divided into two phases: determining the radiative flux (i.e., radiant emittance) throughout the arc column, and using the radiative flux together with the transport properties to find the temperature profile that satisfies the integral differential equation.

In this work, on Contract Nonr 4647(00), the radiative flux was calculated using an exact integration (described in Reference 2 and 25) and an approximate integration based upon a technique of Sampson⁽²⁶⁾. The latter method was approximately ten times faster to compute than the former, and has given good agreement for the cases tested though it does not as yet include lines nor very steep ionization edges.

The temperature profile is calculated by using a relaxation method applied to the energy balance equation. In this, the radiative flux for an assumed (best guess) temperature profile is calculated. Using this radiative flux in a time dependent energy balance equation, the contributions of the other components of the energy balance equation are then calculated. By iterating the process over and over, a temperature profile that satisfies the equation could be calculated (i.e., where the time dependent part equals zero). This is described in Appendix E.

A program has been developed which combines the exact and approximate calculations to obtain a profile. The results of a sample calculation together with the program are given in Appendix E also.

To provide further insight into this calculation, an analysis procedure devised in other work⁽⁵⁾ was applied to the xenon arc. The complete analysis together with calculated fluxes and temperature profiles is in Appendix F.

In all of these calculations, the pressure throughout the discharge is considered to be constant; that is, radiation and magnetic effects upon the pressure were neglected^(1,2). The gas pressure before the initiation of the discharge is known (typically, it is 150 to 300 torr for the xenon-filled flash tubes). Recent calculations have indicated that the final pressure in the fully developed arc is strongly dependent upon the temperature profile. A simple example will illustrate this dependence. Consider a simple two temperature confined arc in which the arc core is at $10,000^{\circ}\text{K}$, the volume near the walls is at 1000°K , and neglect the electron contribution to the pressure. It is simply shown that a cool arc volume of only 10% of the central core volume will reduce the arc pressure by a factor of two from the pressure that would occur if the central core occupied the whole volume as we had assumed in the earlier homogeneous temperature models^(1,2,3). This consideration in the pressure becomes very important for the larger diameters with larger cool portions⁽⁴⁾.

III. COUPLING THE PUMP INTO THE LASER ROD

The ideal pump for optical lasers is one in which a major fraction of the energy radiated can be coupled or at least incident upon the laser rod. There are two general methods to do this: the diffusely reflecting cavity and the focussing cavity. We have investigated a particular diffusely reflecting cavity, the coaxial laser pump, which is well suited for use with large high energy pulsed laser, and a high image quality focussing system, the spherical cavity, which has demonstrated high efficiency in continuously operating laser systems⁽²⁸⁾.

Figure 6 shows a cross sectional drawing transverse to the rod of a current design coaxial lamp. The radiation from the plasma surrounds the laser rod. The MgO layer diffusely reflects the radiation back toward the laser rod. As Whitile and Skinner⁽²⁹⁾ point out, in a recent paper, the efficiency of the system may be obtained roughly by comparing the product of the area and energy absorbed by the rod with the sum of the products of areas and absorptions for the whole system. In this analysis

Dwg. 746A824

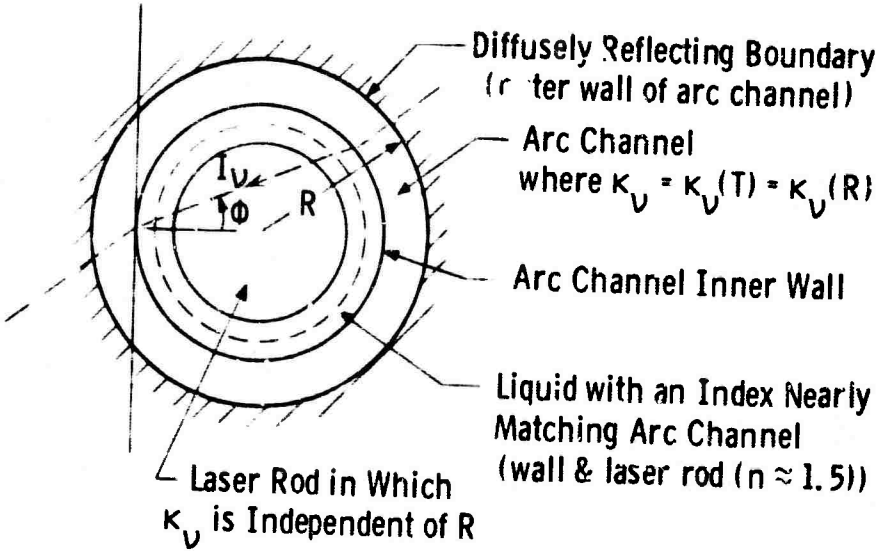


Fig 6-Simplified representation of laser rod-coaxial laser pump system

an open area is considered to be complete absorption. Good laser pump design would seek to minimize openings (as for electrodes) and minimize non-laser rod area. This line of reasoning is counter balanced partially by the need to minimize thermal conduction which varies with the gradient and may vary with plasma thickness. An unknown quantity in the analysis of an MgO reflector coaxial lamp is the reflectivity of the MgO layer under the conditions in the flash tube. This important parameter would need to be determined for a quantitative analysis of this pumping geometry.

Figure 7 is of a possible evolution of the coaxial laser pump which minimizes thermal losses, and allows very high energy outputs from energy limited laser rods. The minimizing of the thermal losses arises from the reduction per unit laser rod area of absorbing diffusely reflecting surfaces and of thermally conducting walls

To date our efforts on the use of the spherical cavity have been with small rods though the geometry need not be limited to them. Figure 8 from Reference 28 shows the geometry of the spherical cavity with the laser rod and laser pump symmetrically disposed about the radius of curvature. If the laser rod length is small enough relative to the diameter of this sphere (and the spherical mirrors are of optical quality), the image of the lamp can be placed upon the rod for a very large fraction of the total solid angle. The data we have at present were obtained on 3 x 30 mm laser rods in which were obtained an efficiency of 1.15% and a total power of 3.6 watts for a Nd:YAG rod with external resonators. The application of this high efficiency system to larger laser rods is underway.

The spherical cavity has many advantages for laser pumping and a major disadvantage, this being the size sphere required for a rod of a given length (the diameter of the sphere should be considerably larger than the rod length). Some of the advantages include a high transfer efficiency (that can be calculated and ray traced readily), and a relatively remote reflecting surface (less subject to radiation damage).

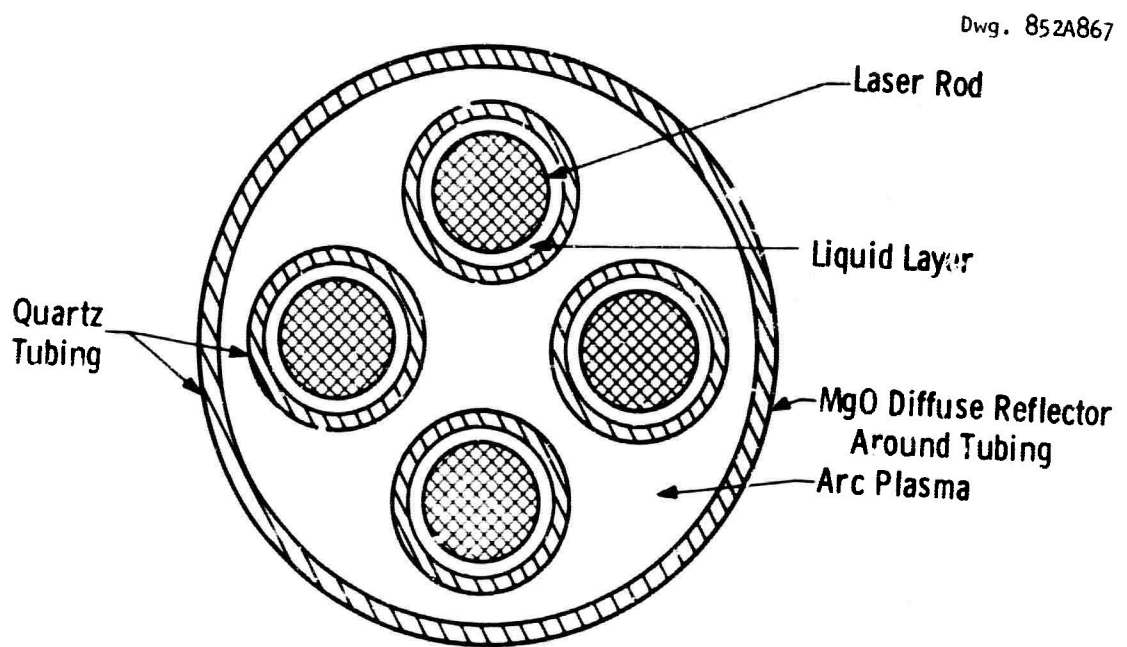


Fig. 7—Multiple rod coaxial laser pump

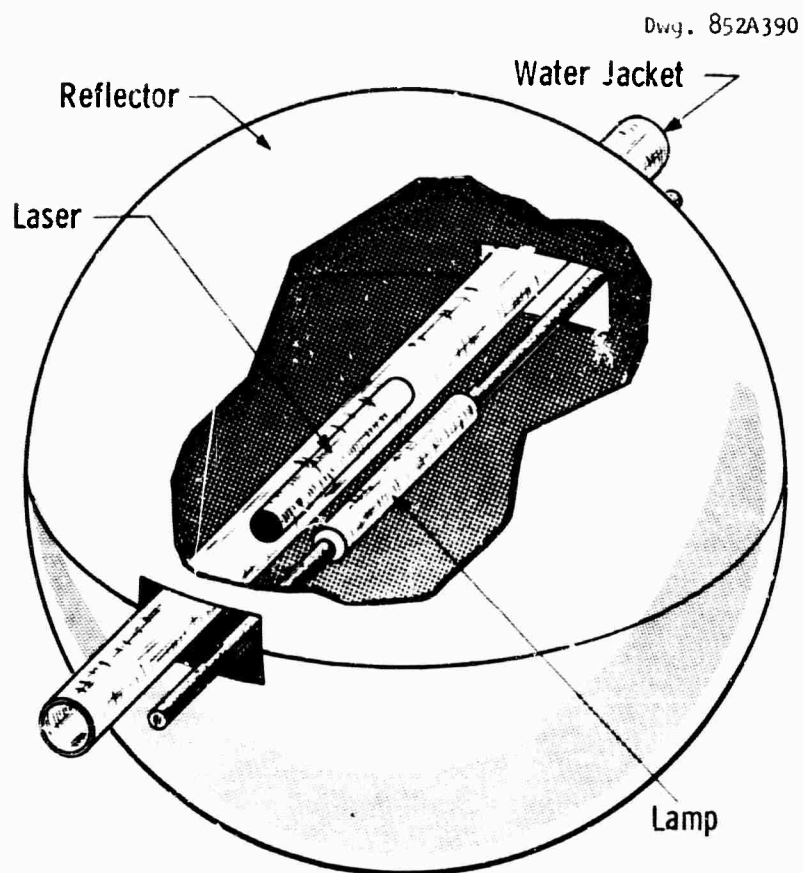


Fig. 3—Geometry of the spherical reflector

The sphere may be fabricated in large sizes readily to optical tolerances. The results obtained with the spherical cavity indicate promise for use in high energy laser pumping.

IV. RECENT EXPERIMENTAL MEASUREMENTS ON THE ARC

The experimental measurements taken throughout this work have been directed towards improving and verifying the information used in the models. Early in the work, we developed a technique to measure the temperature of the plasma (More correctly we developed a technique to measure the lower bound of the temperature - we will treat this more thoroughly in the discussion in double pulsed arcs). To calculate the spectral properties, we needed to know the pressure in the discharge. As we had the initial pressure of the gas (typically 150 torr) and the arc filled the tube to a first approximation, we initially assumed a homogeneous temperature. The arc was measured from the radial distribution of the spectral radiance in the ultraviolet to be relatively homogeneous for a large fraction of the radius - though subsequent estimates from the electrical conductivity discussed in the last semi-annual report⁽⁴⁾ indicated this fraction varied with flash tube inside diameter. Recent analysis of the effect upon the pressure of the temperature profile within the tube indicated that measurements of the pressure or the electron density were required.

The experimental work in the past few months has been concerned with measurements of the pressure using a piezoelectric transducer, a Kistler Instrument Co. 603A, and of the spectral radiance in the vicinity of some lines and in various continuum regions for the arc under power densities over 1.5 MW/cm^3 (using pulse preionization⁽⁵⁻⁷⁾). Measurements were also made of the spectral radiance in the ultraviolet (at 3000 Å) for the arc viewed side on and viewed end on. These measurements from the side and end would give a path length difference of ten or more depending upon the tube.

The pressure measurements for the 12.7 and 19 mm inside diameter tubes had shown a pressure considerably lower than that calculated for a homogeneous temperature distribution. The transducer output was very oscillatory reducing the accuracy. These measurements indicated that there was a cool volume near the walls which could change considerably during the arc cycle. A laser interferometer is being set up to measure the electron density in the center of the arc, but no final results are available for this report. The interferometer is similar to that of Gerardo et. al.⁽⁸⁾ in which the flash tube is inside a reference cavity which is in series with the laser cavity. Measurements of the electron density with the interferometer together with those of temperatures will characterize more fully the arc plasma.

The measurements of the temperature in the double pulsed arc required finding spectral regions in which the emission from the arc was not self-reversed but still optically thick. The 8231.6 Å line of XeI was suspected to be self-reversed at power densities above about .1 MW/cm³. This was confirmed using the high resolution rapid scanning spectrometer⁽⁶⁾. Calculations of the spectral radiance (using the program in Appendix C) for a temperature profile similar to that expected in the arc showed self reversal in the immediate vicinity of the 8231.6 Å lines.

The spectral radiances measured for the lines and the continuum are shown in Figures 9 through 12 for power densities over 1.5 MW/cm³. In Figures 9 and 10, the spectral radiance is plotted in terms of the equivalent black body temperature. The power is the input power dissipated in the lamp per unit volume. The flash tube diameters ranged from .41 cm to 1.94 cm. The tubes were preionized with a .5 ms pulse (100-600 μF in series with 100 μHy). The main pulse was about 50 μs long (50-100 μF and the residual inductance ~3 μH). The main pulse was switched in by means of an ignitron using the circuit shown in Reference 6. The self reversal of the 8231.6 Å line of XeI was considered to be the primary reason for the reduction in the spectral radiances for the larger diameter flash tubes. Figure 13 gives the spectral radiance distribution for an EG & G Inc. FX-52 flash tube under single and double pulsed conditions. The data was taken with a spectral width of about 1 Å at the wavelengths indicated.

Doc # 581515-A

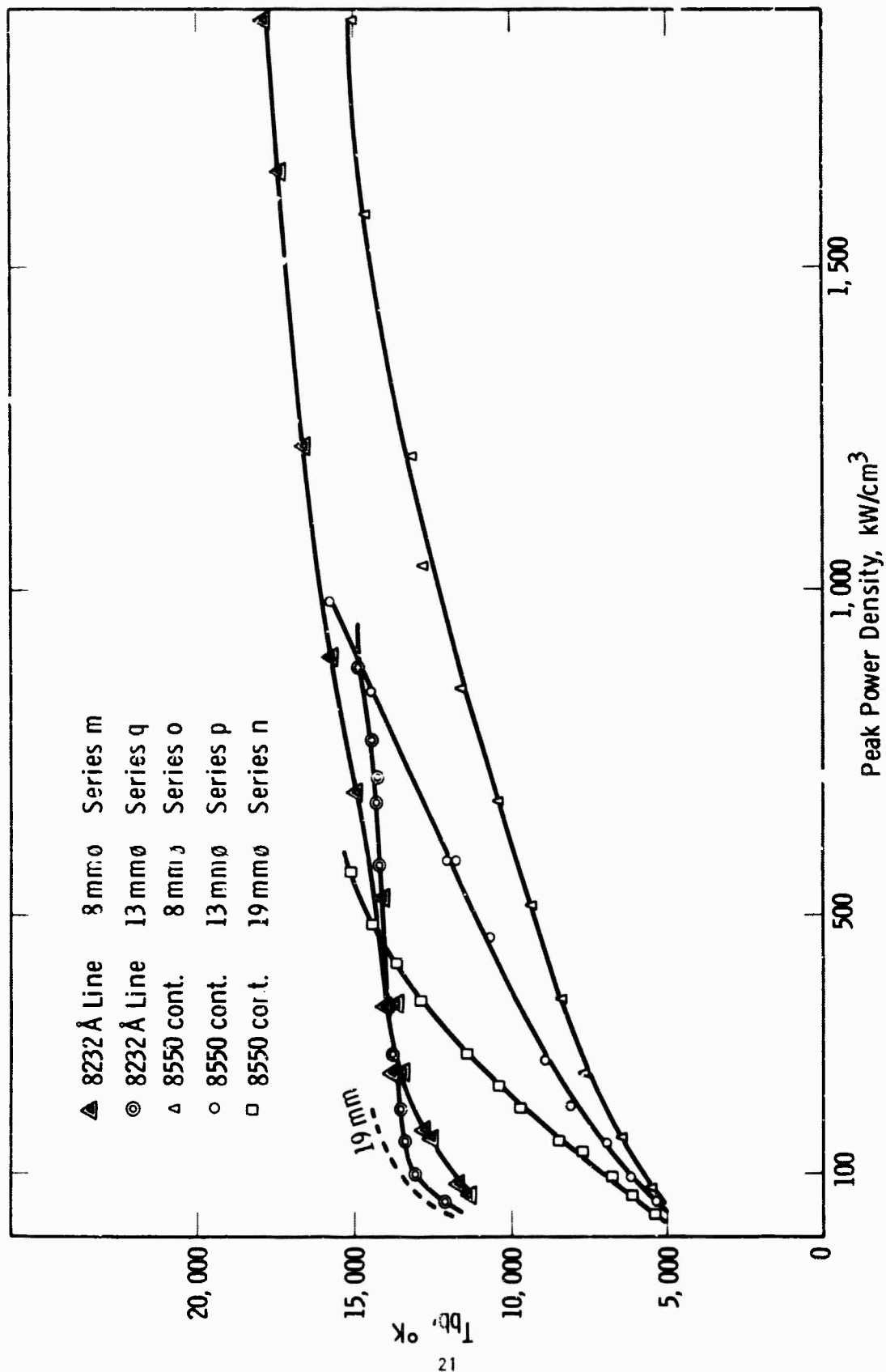


Fig. 9—Black body temperature corresponding to measured spectral radiance as a function of input power density

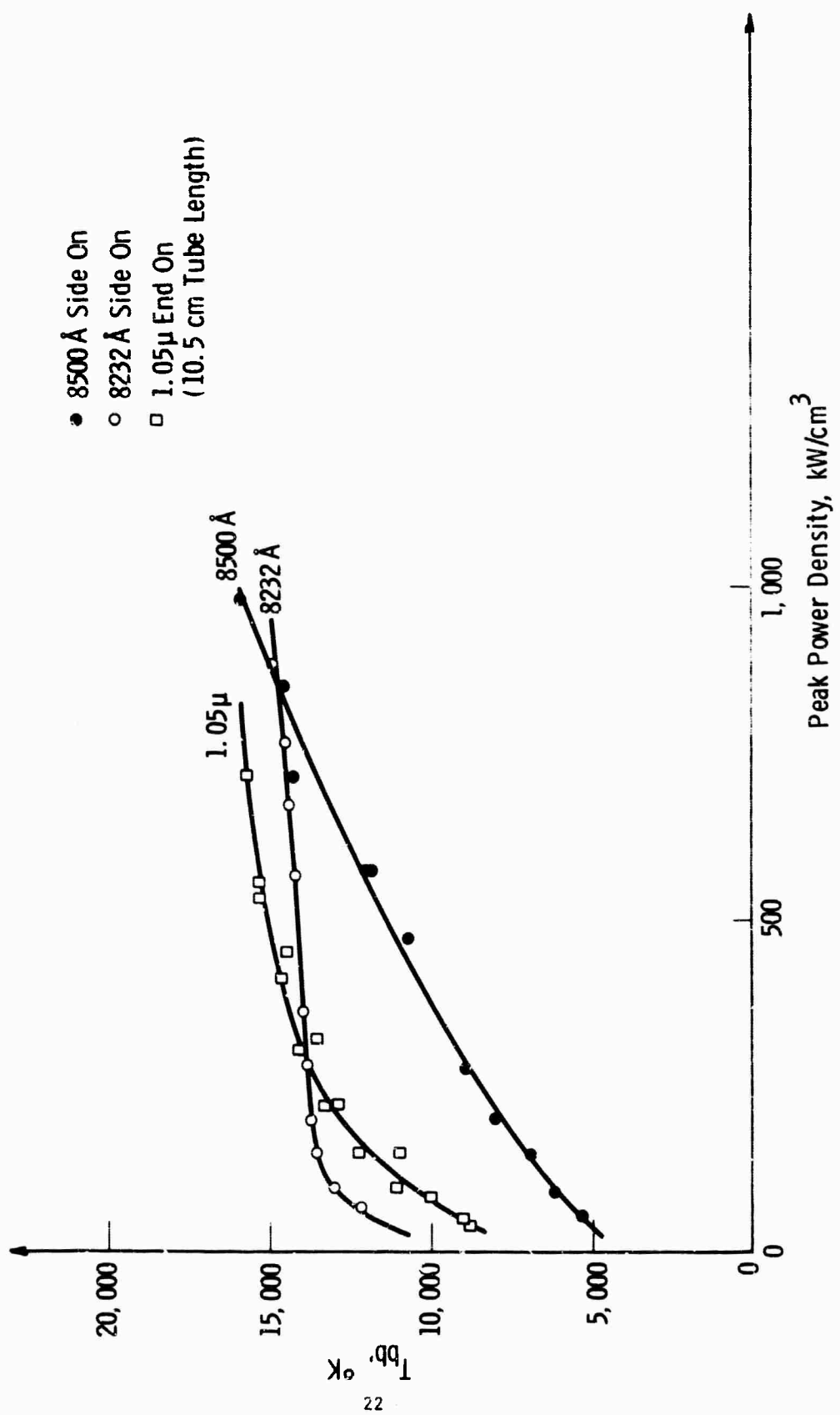


Fig. 10—Black body temperature corresponding to same spectral radiance as 13 mm flash tube as a function of input power density

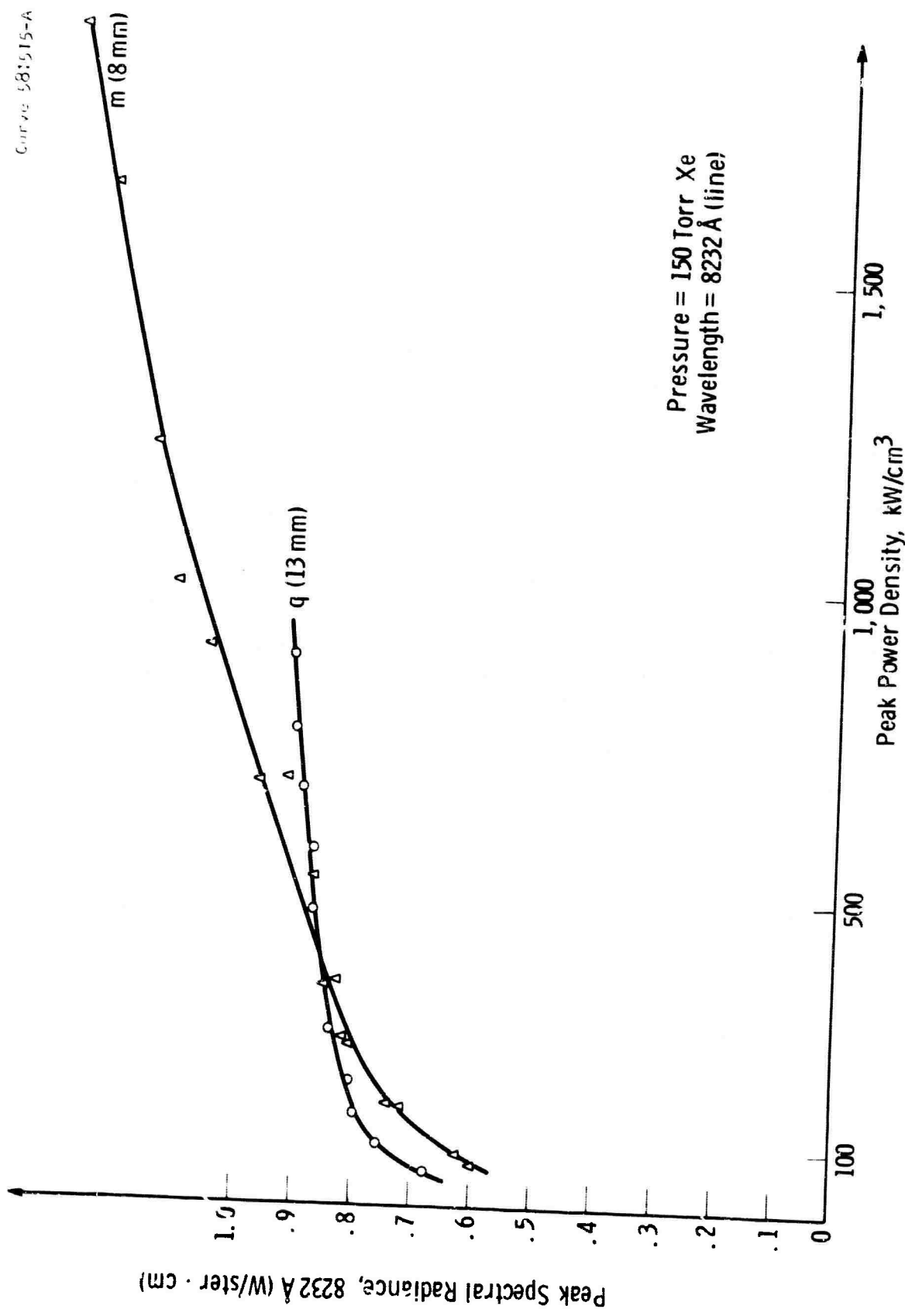


Fig. 11—Spectral radiance of linear cylindrical Xe flash tubes of different diameters as a function of power density input

Curve 58151(-A

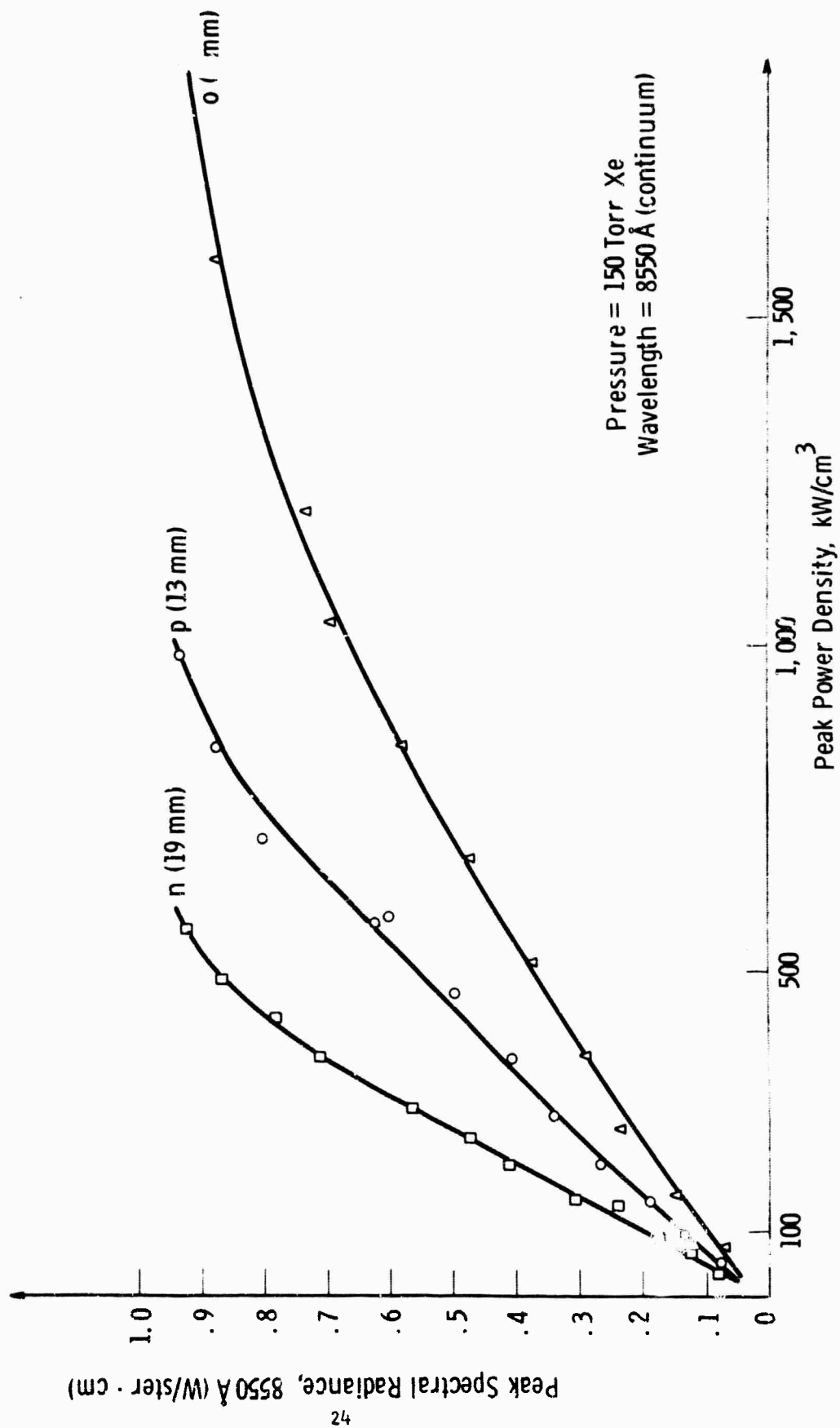


Fig. 12—Spectral radiance of linear cylindrical Xe flash tubes of different diameters as a function of power input

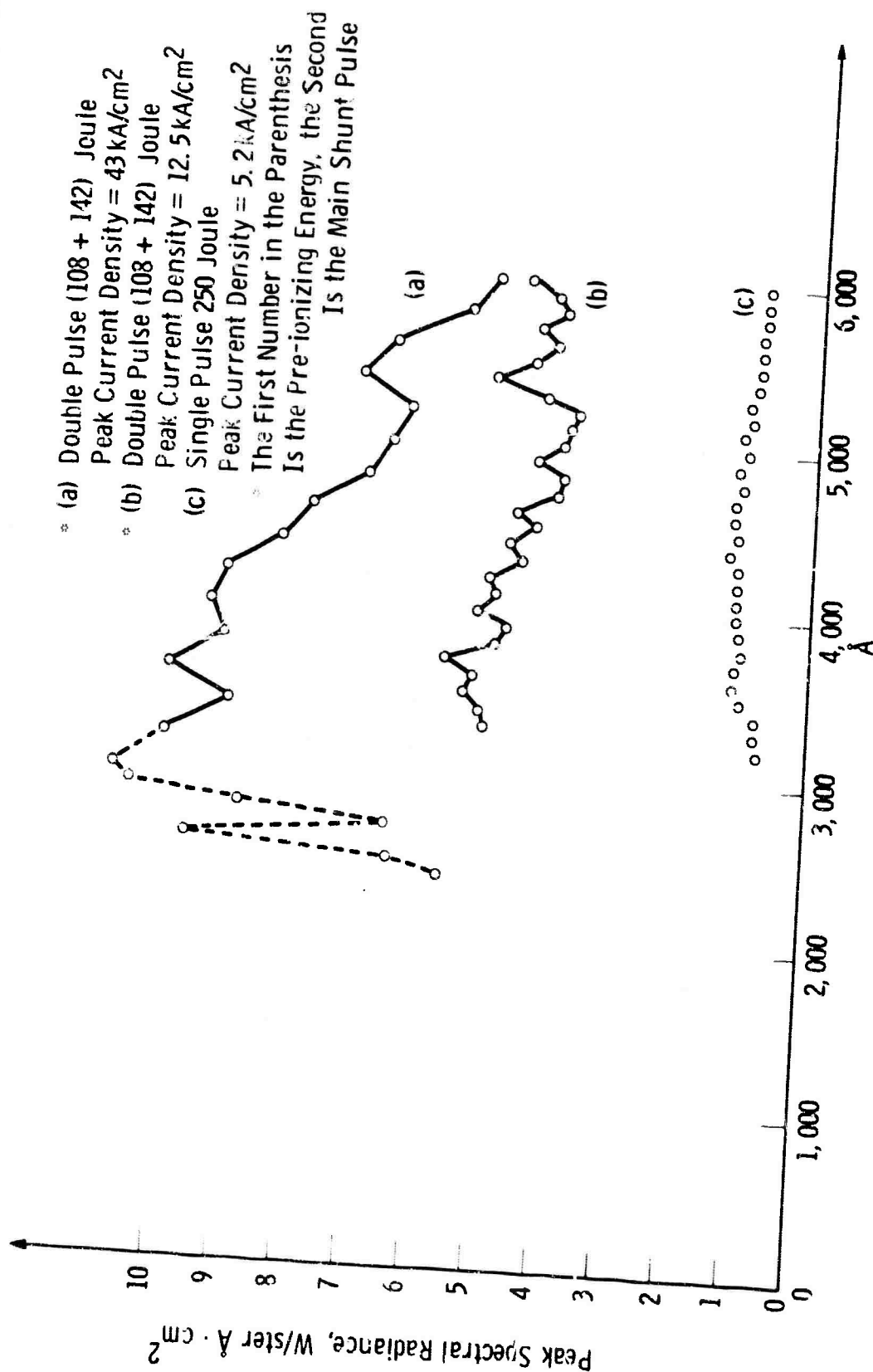


Fig. 13—Spectral radiance distribution for an EG & G Inc. FX-52 flash tube single & double pulsed

The measurements of the spectral radiance at 3000 \AA on flash tubes viewed side on and viewed end on yielded the theoretical ratio of the length of the tube to diameter of the tube for lower energies only when the tungsten electrodes were moved back out of the arc. The ratio again deviated at the higher currents as shown in Figure 14. This may arise in part from further tungsten injection, but also may be due to the plasma becoming thick for the flash tube length being viewed.

We have not yet made a detailed comparison of the calculated radiances with those measured experimentally. This requires a more accurate knowledge of the pressure and/or the electron density than we currently have. We shall be making these comparisons after the laser interferometer is completed. To compare the spectral radiances observed in Figure 13 with the calculated values in Figure 4, multiply the values in Figure 13 by 10^8 to obtain the values in Figure 4 ($\text{W/cm}^2 \text{ Ster cm}$). The single pulsed values correspond with those for the plot in Figure 4; the exact agreement requiring better values of pressure than we currently have.

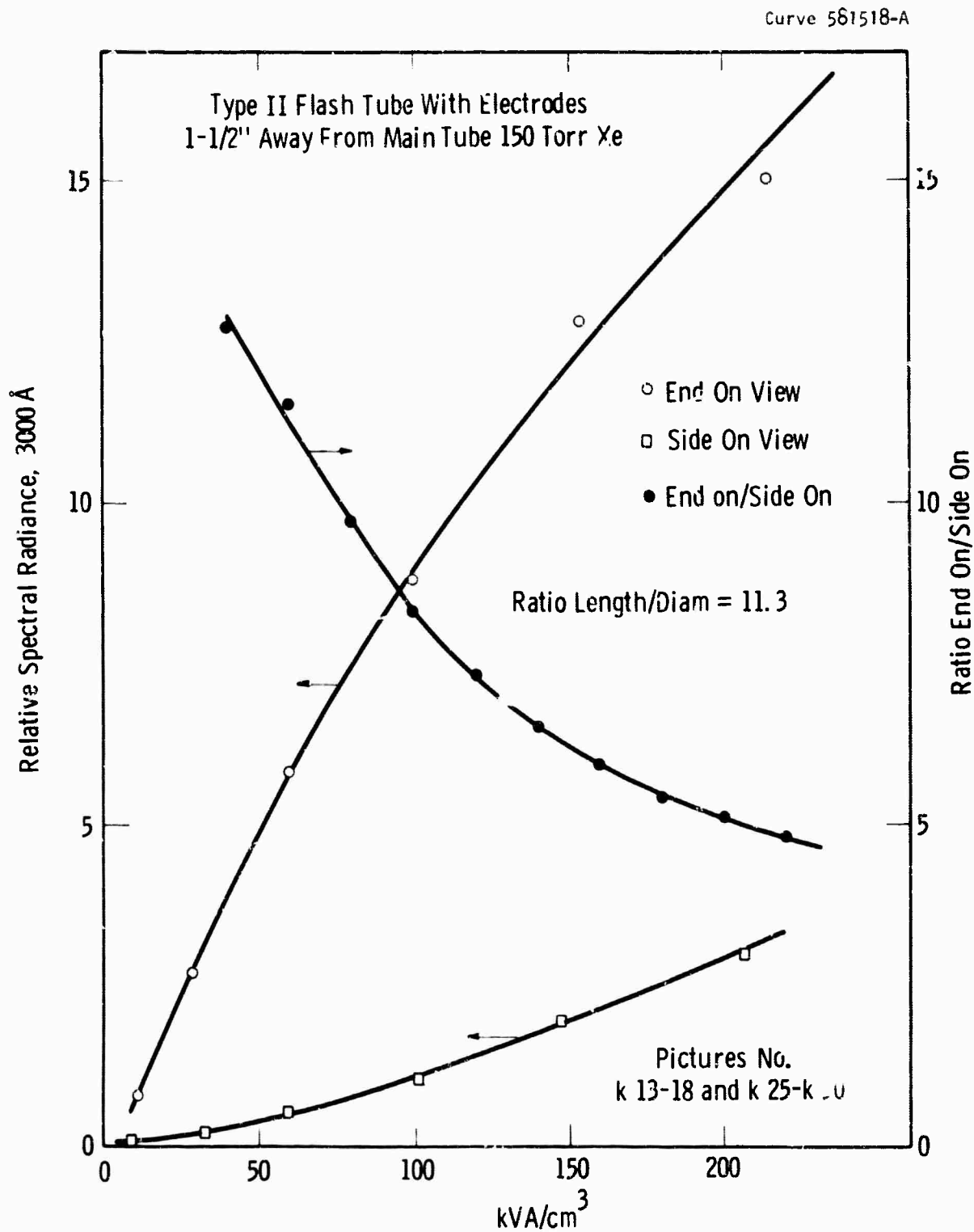


Fig. 14—The spectral radiance viewed at 3000 Å end on and side on for a 13 mm diameter arc tube

V. SUMMARY AND CONCLUSIONS

This report presents a description of the work carried out on Contract Lbr 4647(00) towards the creation of quantitative models for the pulsed arc discharge that is used for the optical pumping of high energy solid state lasers. The primary results of these studies are computer programs for the calculations of the physical properties of the arc plasma, using xenon as the working gas, and for determining the balance within the arc between radiation external to the arc and thermal losses to the walls. The experimental results obtained since the last semiannual reports are also described. The experimental studies have been concerned with measurements of the pressure within the arc, and the characterization of the arcs at very high power densities.

The models for the arc developed in this work are at present only semi-quantitative. They possess the main features of the arc, exhibiting the saturation of the radiation in the infrared, the strong dependence upon power density of the radiation emitted in the ultraviolet; and the nearly homogeneous temperature distribution that have been observed in these arcs. To improve the accuracy of the models, more complete and accurate measurements of the physical properties need to be made. Through the use of the model calculations, quantitative comparisons can be made between the power input, the average electrical conductivity, the spectral absorptivities in various regions of the continuum and in the vicinity of selected lines, and of the pressure and electron density to make a consistent picture.

The full implications of these models are still being explored. The models are allowing a new insight into the behavior of the high density arc. The arc models help to remove the high density plasma - the light emitting plasmas - from the "art" area of technology.

We hope that the work described in this series of reports will assist the designer of optically pumped lasers in the development and improvement of this area of laser technology.

Through this work, we hope that we are bring to bear on an old problem-- light sources--some of the new techniques in both theory and experiment that were developed by a wide variety of people working in areas far removed from the optical pumping of lasers.

VI. ACKNOWLEDGMENTS

We wish to acknowledge the assistance and real contribution of many people to this series of research programs. R. D. Haun, Jr., of Westinghouse Research Laboratories, J. McNall of the Lamp Division of Westinghouse Electric Corp., and Elliot Weinberg of ONR-San Francisco, contributed encouragement of both the moral and physical varieties. Contributors to this work other than the listed include E. F. G. Arrott, A. V. Phelps, L. S. Frost, R. G. Schlecht (now at Aeroneutronics), and L. Gampel (now at Electro Optical Systems, Inc.). We would also like to thank E. Corinaldesi of Boston University, D. Sun of California Institute of Technology, R. A. Day of Harvard College Observatory, and R. S. de Voto of Stanford University for their share of the developing of the computer programs used on this work. The technicians involved in the measurements included R. L. Grassell, J. Humphreys, J. Russell. J. Nee, and R. Webb.

The reproduction of the man reports for this work was carried under the directions of Miss E. Marko, with the assistance of Mrs. M. Howard, Mrs. J. Connors, and many others. The drafting was supervised by Mr. J. Getsko and Mr. M. Bowman; the reproductions were under Messers. K. Moelk, H. Payne, and J. MacKenzie.

To all of the above, we wish to give a sincere thank you.

REFERENCES

1. C. H. Church and R. G. Schlecht, "Arc Discharge Sources, Semiannual Report on Contract Nonr 4647(00)", 15 May 1965, AD 462 792.
2. C. H. Church, R. G. Schlecht, I. Liberman, B. W. Swanson, E. G. F. Arnott and E. Geil, "Arc Discharge Sources, Final (Actually Semiannual) Report on Contract Nonr 4647(00)", 15 November 1965, AD 473 996.
3. C. H. Church, R. G. Schlecht, I. Liberman, B. W. Swanson and E. Geil, "Arc Discharge Sources, Semiannual Report on Contract Nonr 4647(00), 15 May 1966, AD 632 892.
4. C. H. Church, B. W. Swanson, P. Buchhave, G. Basi, R. Liebermann, E. Geil and L. A. C. Weaver, "Arc Discharge Sources, Semiannual Report on Contract Nonr 4647(00), 15 November 1966, AD 803 542.
5. J. J. Lowke and E. R. Capriotti, Westinghouse Research Labs, Scientific Report 66-1E2-GASES-R1 (1966).
6. I. Liberman, C. H. Church and J. Asars, Appl. Optics 6, 279 (1967).
7. C. H. Church and L. Gampel, Appl. Optics 5, 241 (1966).
8. J. B. Gerardo and J. T. Verdeyen, Proc. IEEE 52, 690 (1964).
J. B. Gerardo, J. T. Verdeyen and M. A. Gusinow, J. Appl. Phys. 36, 2 146 (1965).
J. B. Gerardo and R. A. Hill, Phys. Rev. Letters 17, 623 (1966).
9. R. S. de Voto, Physics of Fluids 9, 1230 (1966).
10. R. S. de Voto, "Simplified Expressions for the Transport Properties of Ionized Monatomic bases", Stanford University, Report No. SUDAAR No. 283 (July 1966).
11. L. Frost and A. Phelps, Phys. Rev. 136, 1538 (1964).
12. H. Griem, Plasma Spectroscopy, McGraw Hill Book Co., New York (1964).
See also J. Cooper "Plasma Spectroscopy" in Reports of Progress in Physics 29, pt. 1, 35 (1966).
13. E. Corinaldesi, private communication.
14. R. Garstang and J. Van Blerkom, J. Opt. Soc. Am. 55, 1054 (1965).
15. D. Schlüter, Z. Astrophys. 61, 67 (1965) and private communication.

16. M. Seaton, Mon. Not. Roy. Astron. Soc. 118, 504 (1958).
17. A. Burgess and M. Seaton, Mon. Not. Roy. Astron. Soc. 120, 121 (1960).
18. G. Peach, Mon. Not. Roy. Astron. Soc. 130, 361 (1965).
19. G. Peach, to be published in Memoirs Roy. Astron. Soc.
20. See for example L. M. Biberman and G. Norman, J. Quant. Spect. Rad. Transfer 3, 221 (1963). Translated in General Atomics - San Diego. Translation GA tr 4943, there are many other papers by this group, primarily published in Optics and Spectroscopy.
21. J. C. Stewart and M. Rotenberg, Phys. Rev. 140, A 1508 (1965).
22. E. McGuire, Thesis, Cornell University, (1965).
23. M. Abramowitz and I. Stegun, Editors, "Handbook of Mathematical Functions with Formula, Graphs and Mathematical Tables". National Bureau of Standards, Applied Mathematical Series 55, U.S. Government Printing Office, Washington D.C., 20402 (1964).
24. E. McGuire, private communication.
25. C. H. Church, R. G. Schlecht, I. Liberman, and B. W. Swanson., A.I.A.A. Journal 4, 1947 (1966).
26. D. Sampson, J. Quant. Spect. Rad. Transfer 5, 211 (1965).
27. J. L. Emmett and A. L. Schawlow, Appl. Phys. Letters 2, 204 (1963).
28. C. H. Church and I. Liberman, "The Spherical Reflector for Use in the Optical Pumping of Lasers", Westinghouse Scientific Paper 66-9C1-LHICW-P1 (1966).
29. J. Whittle and D. R. Skinner, Appl. Optics 5, 1179 (1966).

BLANK PAGE

APPENDIX A

A PROGRAM FOR THE CALCULATION OF THE ELECTRICAL AND THERMAL CONDUCTIVITY OF XENON AS A FUNCTION OF TEMPERATURE AND PRESSURE

by

R. S. deVoto
Stanford University

This program, ELEC/THERM, calculates the various components of the electrical and the thermal conductivities of xenon as a function of pressure and temperature under local thermal equilibrium conditions.

The program will calculate these quantities for argon also.

The input data for argon is:

1. "ARGON", number of species - 1 (we used 2)
2. initial temperature, temperature step size, maximum temperature desired
3. number of pressures; the pressures in atmospheres
4. PHIOA (3.23 @ 4), RHOA (.224), PHIOI (5.38 @ 6), RHOI (.1965), AC (25.615), BC (1.1960), HIER (must be 0).
5. electron mass (9.1091 at -28), molec. wt. of atom (39.944), molec. wt. of first ion (39.944), molec. wt. of any other ions used.

For xenon the data required is similar to the ARGON program.

1. "XENON", 2,
2. initial temperature, step size, maximum temperature desired
3. number of pressures, the pressures (in atmospheres)
4. 3.11 @ 6, .208,0,0, 25.639, .99752,0, 9.109 @ -28, 131.3,131.3.

20122107 FRIDAY, NOVEMBER 4, 1966

HRL ALGOL VERSION OF 10/20/66

BEGIN

COMMENT THIS PROGRAM PUNCHES THE FOLLOWING CARDS:
INITIAL TEMPERATURE, STEP SIZE, FINAL TEMPERATURE
FOR EACH PRESSURE
PRESSURE (IN ATMOSPHERES)
ELECTRICAL CONDUCTIVITIES FOR ALL TEMPERATURES FOR THIS PRESSURE
THERMAL CONDUCTIVITIES FOR ALL TEMPERATURES FOR THIS PRESSURE
)

COMMENT CLOSED FCKI

FILE IN READER(2,10)

FILE OUT OFIL 4(2,15)

FILE OUT PUNCH DISK SERIAL (201650) (2,10,30,SAVE 1)

INTEGER NP,IP,IT

REAL T1,OT,TMAX

ARRAY P(10,30)

ARRAY TEMP,THEAVY,TELEC,TREACT,TTOT,SIGMA(01100)

REAL DEBYE,ELEC,PSI,LAMBDA ; REAL ARRAY Q(013,015,015,015) ;

REAL T,P, LNRDA,NTOT,ALF ; ALPHA NAN ;

INTEGER MAX,I,J ;

REAL ARRAY N(015) ;

FORMAT PFC "TRANSPORT PROPERTIES OF "A6," AT P="FA,2," ATMOS,").

CLOCK(=PROCESSOR TIME USED (5,"R0,2," SECONDS",

"I/O TIME (5,"R0,2," SECONDS"),

PUNCH6(E12,3,""),

PUNCHSTAR("=,"),

F1(=T="F",0,X1,3("N("I,"="E10,3,X1),"ALPHA="F10,3,)

"DEBYE="E10,3,X1,

"ELEC="F10,3,X1,"LAMBDA="E10,3,X1, "SIGMA="E10,3,X1,

"LMBDA="E10,3) ;

PROCEDURE SAMA (T,P,ALFA) ; COMMENT XFNON ;

VALUE T,P ; REAL T,P,ALFA ;

BEGIN REAL X,ZA,ZI ;

X = 97R34,2 / T ;

IF X > 110 THEN ALFA = 0

ELSE BEGIN

ZA = 1 ;

ZI = 4 + 2 * EXP(-15160,96 / T) ;

ALFA = 1 / SORT(1 + 1000,6 * P * X * (EXP(X) / (T * 2,5 * ZI))) ; FNDI

END SAMA ;

PROCEDURE DEBE (T,I,J) ; COMMENT VERSION 2/24/66 THIS INCLUDES THE

CRSS SECTIONS AS COMPUTED FROM FROST & PHELPS DATA-TO 5% ONLY ;

VALUE T,I,J ; REAL T ; INTEGER I,J ;

BEGIN

OWN INTEGER K ; OWN REAL ARRAY I(010,0130) ;

INTEGER S=1,ND ; REAL P1,02,03,THEYA ; LARFL LI,L2 ;

FORMAT F1(10,""),T="FA,0," IS OUT OF RANGE OF GARRISON ;)

IF K = 0 THEN BEGIN

FILL I(0,0) WITH

21,627, 0,617, 5,544, 3,940, 3,332, 3,241, 3,440, 3,443,

4,410, 5,055, 4,773, 4,544, 7,352, 4,143, 0,027, 0,874,

10,714, 11,542, 12,371, 13,170, 13,952, 14,702, 15,414, 16,142,

16,810, 17,449, 18,092, 18,647, 19,254, 19,798, 20,314, 20,849,

21,271, 21,714, 22,134, 22,532, 22,900, 23,265, 23,601, 23,910 ;

FILL I(1,0) WITH

14,247, 5,401, 3,105, 2,615, 2,633, 3,411, 4,200, 5,154,

4,213, 7,341, 4,515, 0,711, 10,910, 12,090, 13,242, 14,390,

15,474, 16,514, 17,545, 18,442, 19,327, 20,190, 20,930, 21,440,

22,340, 22,943, 23,572, 24,117, 24,622, 25,084, 25,517, 25,911,

26,272, 26,643, 26,984, 27,177, 27,425, 27,484, 27,840, 28,027 ;

FILL I(2,0) WITH

0,912, 3,243, 2,240, 2,349, 3,373, 4,444, 5,743, 7,174,

4,640, 10,229, 11,744, 13,315, 14,790, 16,210, 17,543, 18,823,

19,904, 21,042, 22,041, 22,997, 23,819, 24,501, 25,274, 25,804,

26,444, 26,944, 27,397, 27,791, 28,117, 28,341, 28,744, 28,941,

29,121, 29,274, 29,414, 29,521, 29,601, 29,654, 29,690, 29,711 ;

FILL I(3,0) WITH

7,170, 2,344, 2,194, 3,052, 4,343, 5,908, 7,640, 9,527,

11,441, 13,340, 15,140, 16,942, 18,541, 20,092, 21,471, 22,714,

23,277, 24,844, 25,717, 26,494, 27,177, 27,770, 28,241, 28,710,

29,090, 29,440, 29,655, 29,860, 30,010, 30,138, 30,220, 30,244,

30,244, 30,277, 30,242, 30,144, 30,107, 30,011, 29,909, 29,771 ;

[illegible]

```

0025 15 0048 LONG, NFKT SEG 0002
PROCEDURE DETERMINR(NC,N,DET,POW) COMMENT VERSION 10/19/65 I VALUE NR
NC,N,INTEGER NC,N,P,REAL DET,REAL ARRAY F10,011BEGIN COMMENT NC AN
N NR ARE INDICES OF FIRST ROW AND FIRST COLUMN IN ARRAY OF WHICH THE DET
ERMINANT IS TO BE EVALUATED, N+1 IS RANK INTEGER J,K,P,Q,INDICIAL ARRAY
START OF SEGMENT ..... 0026
D10IN,011LABEL L1,L2,REAL FAC,ARSPAC,COLMAX,TEMPOR FOR J=0STER UNTIL N
DO FOR K=0STER UNTIL N DO O(J,*)=E(J,NR,K*NC)/P(0,N,FAC,1)FOR J=0STER
UNTIL N=100 BEGIN COLMAX=ARSPAC(O(J,1))INO,J1FOR K=J+1STEP UNTIL N DO RE
GIN TEMP=ARSPAC(O(J,1))IF COLMAX<TEMP THEN BGIN INO,K1COLMAX=TEMPINOJNO
IFAC=O(JNO,J1)FACIF FAC<O(JNO,J1)FAC=O(JNO,J1)FOR POW=POW+100WH
ILE ARSPAC<1000 BEGIN FAC=100FACIARSPAC=ARSPAC(FAC)FENOJFOR POW=POW+100WH
ILE ARSPAC<1000 BEGIN FAC=100FACIARSPAC=ARSPAC(FAC)FENOJIF INO,K1 THEN GO
TO L1 ELSE FOR P=1 STEP UNTIL N DO BEGIN TEMP=O(J,P1)O(J,P1)O(JNO,P1)O
JNO,P1=TEMPINOJFAC=O(J1IARSPAC=1/O(J1J1)FOR Q=J+1STEP UNTIL N DO O
(J,Q1)O(J1Q1)ARSPAC=O(J1J1)FOR P=J+1STEP UNTIL N DO BEGIN TEMP=O(J,J1
)FOR Q=J STEP UNTIL N DO O(P,Q1)O(J,Q1)O(J,J1)TEMP=O(JNO,J1)O(J1O(J,Q1)O
JNO,J1)FENOJFENOJ
0026 15 0105 LONG, NFKT SEG 0002
PROCEDURE TRANS( T,P,N, MAX, SIGMA,LNROA )
COMMENT T IN DEGREES K P IN TORR N IS ARRAY OF NUMBER OF SPECIES: 0 =
SILECTRON, 1 = ATOM, 2 AND HIGHER = IONS, MAX IS INTEGER NUMBER OF SPECI
ES = 1, SIGMA AND LNROA ARE ELECT AND THERMAL CONDUCTIVITIES
VALUE T,P,MAX
REAL T,P,SIGMA,LNROA
INTEGER MAX
REAL ARRAY A101,9,015,DEF(015)
START OF SEGMENT ..... 0027
INTEGER I,J,L,K,M2,ENN,END,N
LABEL L1
REAL INM COMMENT IONIZATION POTENTIAL IN DEGREES K
REAL TROD,TSG,NTOT,RHO,LNROA,LNROE,ML2,NIM,OFNOM,NMAY, TM1,M12,
MLA, LNROA,OFM1
OWN REAL AC,RC,RMOA,RMOI,RMIOA,RMIOI,MN,MNSOP,TM3
OWN REAL ARRAY M1N13,WRTE(015,015)
OWN BOOLEAN MIFR
OFFNE F1M = FOR I = 1 STEP 1 UNTIL MAX DO #
F1M = FOR J = 1 STEP 1 UNTIL MAX DO #
F1M = FOR L = 1 STEP 1 UNTIL MAX DO #
F1M = FOR J = 1+1 STEP 1 UNTIL MAX DO #
F1M = FOR I = 0 STEP 1 UNTIL MAX DO #
F1M = FOR J = 0 STEP 1 UNTIL MAX DO #
LIST T1 RMIOA,RMOA,RMIOI,RMIOI,AC,RC, MIFR, F1OM M11 )
FORMAT PCROSS ( /PCROSS SECTIONS...// (O(F1,0,11)))
START OF SEGMENT ..... 0028
FTHRM( / "THERMAL CONDUCTIVITY CONTRIBUTIONS AT T = "F,T,0, " ARE"
WEST0002 SC 271 2012
WEST0003 SC 271 2012
WEST0004 SC 271 2012
WEST0005 SC 271 2012
WEST0006 SC 271 2012
WEST0007 SC 271 2012
WEST0008 SC 271 2012
WEST0009 SC 271 2012
WEST0010 SC 271 2012
WEST0011 SC 271 2012
WEST0012 SC 271 2012
WEST0013 SC 271 2012
WEST0014 SC 271 2012
WEST0015 SC 271 2012
WEST0016 SC 271 2012
WEST0017 SC 271 2012
WEST0018 SC 271 2012
WEST0019 SC 271 2012
WEST0020 SC 271 2012
WEST0021 SC 271 2012
WEST0022 SC 271 2012
WEST0023 SC 271 2012
WEST0024 SC 271 2012
WEST0025 SC 271 2012
WEST0026 SC 271 2012
WEST0027 SC 271 2012
WEST0028 SC 271 2012
WEST0029 SC 271 2012
WEST0030 SC 271 2012
WEST0031 SC 271 2012
WEST0032 SC 271 2012
WEST0033 SC 271 2012
WEST0034 SC 271 2012
WEST0035 SC 271 2012
WEST0036 SC 271 2012
WEST0037 SC 271 2012
WEST0038 SC 271 2012
WEST0039 SC 271 2012
WEST0040 SC 271 2012
WEST0041 SC 271 2012
WEST0042 SC 271 2012
WEST0043 SC 271 2012
WEST0044 SC 271 2012
WEST0045 SC 271 2012
WEST0046 SC 271 2012
WEST0047 SC 271 2012
WEST0048 SC 271 2012
WEST0049 SC 271 2012
WEST0050 SC 271 2012
WEST0051 SC 271 2012
WEST0052 SC 271 2012
WEST0053 SC 271 2012
WEST0054 SC 271 2012
WEST0055 SC 271 2012
WEST0056 SC 271 2012
WEST0057 SC 271 2012
WEST0058 SC 271 2012
WEST0059 SC 271 2012
WEST0060 SC 271 2012
WEST0061 SC 271 2012
WEST0062 SC 271 2012
WEST0063 SC 271 2012
WEST0064 SC 271 2012
WEST0065 SC 271 2012
WEST0066 SC 271 2012
WEST0067 SC 271 2012
WEST0068 SC 271 2012
WEST0069 SC 271 2012
WEST0070 SC 271 2012
WEST0071 SC 271 2012
WEST0072 SC 271 2012
WEST0073 SC 271 2012
WEST0074 SC 271 2012
WEST0075 SC 271 2012
WEST0076 SC 271 2012
WEST0077 SC 271 2012
WEST0078 SC 271 2012
WEST0079 SC 271 2012
WEST0080 SC 271 2012
WEST0081 SC 271 2012
WEST0082 SC 271 2012
WEST0083 SC 271 2012
WEST0084 SC 271 2012
WEST0085 SC 271 2012
WEST0086 SC 271 2012
WEST0087 SC 271 2012
WEST0088 SC 271 2012
WEST0089 SC 271 2012
WEST0090 SC 271 2012
WEST0091 SC 271 2012
WEST0092 SC 271 2012
WEST0093 SC 271 2012
WEST0094 SC 271 2012
WEST0095 SC 271 2012
WEST0096 SC 271 2012
WEST0097 SC 271 2012
WEST0098 SC 271 2012
WEST0099 SC 271 2012
WEST0100 SC 271 2012
WEST0101 SC 271 2012
WEST0102 SC 271 2012
WEST0103 SC 271 2012
WEST0104 SC 271 2012
WEST0105 SC 271 2012
WEST0106 SC 271 2012
WEST0107 SC 271 2012
WEST0108 SC 271 2012
WEST0109 SC 271 2012
WEST0110 SC 271 2012
WEST0111 SC 271 2012
WEST0112 SC 271 2012
WEST0113 SC 271 2012
WEST0114 SC 271 2012
WEST0115 SC 271 2012
WEST0116 SC 271 2012
WEST0117 SC 271 2012
WEST0118 SC 271 2012
WEST0119 SC 271 2012
WEST0120 SC 271 2012
WEST0121 SC 271 2012
WEST0122 SC 271 2012
WEST0123 SC 271 2012
WEST0124 SC 271 2012
WEST0125 SC 271 2012
WEST0126 SC 271 2012
WEST0127 SC 271 2012
WEST0128 SC 271 2012
WEST0129 SC 271 2012
WEST0130 SC 271 2012
WEST0131 SC 271 2012
WEST0132 SC 271 2012
WEST0133 SC 271 2012
WEST0134 SC 271 2012
WEST0135 SC 271 2012
WEST0136 SC 271 2012
WEST0137 SC 271 2012
WEST0138 SC 271 2012
WEST0139 SC 271 2012
WEST0140 SC 271 2012
WEST0141 SC 271 2012
WEST0142 SC 271 2012
WEST0143 SC 271 2012
WEST0144 SC 271 2012
WEST0145 SC 271 2012
WEST0146 SC 271 2012
WEST0147 SC 271 2012
WEST0148 SC 271 2012
WEST0149 SC 271 2012
WEST0150 SC 271 2012
WEST0151 SC 271 2012
WEST0152 SC 271 2012
WEST0153 SC 271 2012
WEST0154 SC 271 2012
WEST0155 SC 271 2012
WEST0156 SC 271 2012
WEST0157 SC 271 2012
WEST0158 SC 271 2012
WEST0159 SC 271 2012
WEST0160 SC 271 2012
WEST0161 SC 271 2012
WEST0162 SC 271 2012
WEST0163 SC 271 2012
WEST0164 SC 271 2012
WEST0165 SC 271 2012
WEST0166 SC 271 2012
WEST0167 SC 271 2012
WEST0168 SC 271 2012
WEST0169 SC 271 2012
WEST0170 SC 271 2012
WEST0171 SC 271 2012
WEST0172 SC 271 2012
WEST0173 SC 271 2012
WEST0174 SC 271 2012
WEST0175 SC 271 2012
WEST0176 SC 271 2012
WEST0177 SC 271 2012
WEST0178 SC 271 2012
WEST0179 SC 271 2012
WEST0180 SC 271 2012
WEST0181 SC 271 2012
WEST0182 SC 271 2012
WEST0183 SC 271 2012
WEST0184 SC 271 2012
WEST0185 SC 271 2012
WEST0186 SC 271 2012
WEST0187 SC 271 2012
WEST0188 SC 271 2012
WEST0189 SC 271 2012
WEST0190 SC
```



```

      NTOT = 0.657301A * P / T
      N(0) = N(2) * ALF * NTOT / (1 + ALF)
      Y(1) = NTOT * (1 - ALF) / (1 + ALF)
      TRANS( T, P, N, MAX, SIGMA(1), LAMDA )
      WRITE(SFIL,FI,1, FOR I = 0 STEP 1 UNTIL 2 DO (1,N(1),NTOT/(N(0)+
      N(1)),DERIV,FLTC(LAMDA,SIGMA(1),LAMDA) )
      IT=IT+1
      ENDO
      WRITE(GETL)
      WRITE(GETL,CLOCK,TIME(2)/60,TIME(3)/60)
      IT=IT+1
      ENDO
      CLASEOFCKPUNCH,GETL)
      END

```

0002 IS 0177 (ONG. NEXT SEG 000)

END	IS SEGMENT NUMBER 0030.	PRY ADDRESS IS 011A
LN	0031	0117
ROUT	0032	0121
OUTPUT#	0033	0052
BLOCK CONTROL	0034	0005
INPUT#	0035	0160
X TO TIME 1	0036	0120
ALGOL WRITE	0037	001A
ALGOL READ	0038	001A
ALGOL SELECT	0039	001A

NUMBER OF ERRORS DETECTED = 000 LAST CARD WITH ERROR WAS SFQ P
 PRY STP#0141 TOTAL SEGMENT SIZE=02A12 WORDS DISK STORAGE #FG,00101A WORDS NO. SFGS,00020.
 ESTIMATED CORE STORAGE REQUIREMENT = 0A97A WORDS.
 2012310A FRIDAY, NOVEMBER 4, 1966 PROCESSOR TIME = 37.47 SECONDS I/O TIME = 51.42 SECONDS

LABEL 000000000LINE 0016A30A2 COMPILE FLECYTHERM LIBRARY

15042000 ALGOL

APPENDIX B

CALCULATION OF BOUND-BOUND TRANSITION PROBABILITIES

by D. Sun

The overall purpose of the system or programs being developed is to represent the spectrum of an atomic species in a plasma, including all lines and portions of the continuum which carry a significant portion of the energy. Hence it will be necessary to calculate large numbers of transition probabilities for bound-bound, bound-free, and free-free transitions.

Calculation of the bound-bound case to be discussed here is fairly complete; the other two types of transitions have not been added yet. The program to be described, presently called GIANT/FIASCO, consists of four sub-programs, (following the format of E. Corinaldesi) between which information is transferred by three disc files, READF1, READF2, and READF3. Programs 1 and 2 are run together, and accepting as their input the quantum numbers and energies of the various energy levels of a species as they are given in Moore's tables.¹ Program 2 prints out transition probabilities for all transitions allowed by the selection rules within the range considered. These are also placed on the disc READF2 where they may be tapped by Program 2 or by an auxiliary program FIASCO/RESULTS, which merely prints out the results in a number of convenient forms. Program 3 calculates the Stark shift and broadening of each level, while Program 4 combines these into the shift and broadening of each spectral line. However, this paper is concerned primarily with Programs 1 and 2, the calculation of bound-bound transition probabilities.

The heart of the matter is the calculation of $|\langle \psi_n | z | \psi_m \rangle|^2$ where ψ_n , and ψ_m are the two states between which a transition may occur

¹C. Moore, Atomic Energy Levels, National Bureau of Standards, Circular 467, U.S. Government Printing Office, Washington, D.C.

²E. Corinaldesi, to be published.

and $z=r \cos \theta$ is the electric dipole operator. (Quadrupole and magnetic dipole transitions are ignored.) Although ψ_n , ψ_m , and z actually involve all the electrons in the atom, in practice, it is possible to use the one-electron wave functions of the outer electron which makes the transition (Condon and Shortley, Section 6³). Now each energy level consists of $2J+1$ states with different z -components of angular momentum. For transitions from n to m , it is necessary to sum the square of the matrix element for all of the m -states, and average it over all of the initial n -states. The oscillator strength f_{nm} is $\frac{4\pi mc\bar{\nu}}{f_n}$ times this quantity, and the following relations hold:

$$(2 J_n + 1)f_{nm} = gf = (2 J_m + 1)f_{mn}$$

$$A_{nm} = 0.667 \times \bar{\nu}^2 \quad \text{where } \bar{\nu} \text{ is in cm}^{-1}$$

$$(2 J_n + 1)A_{nm} = (2 J_m + 1)A_{mn}$$

The solutions to Schroedinger's equation separate into two parts, giving the form $\frac{R(r)}{r} Y(\theta, \phi)$. $R(r)$ is known as the radial wave function while $Y(\theta, \phi)$ is the angular part. Hence the problem separates into a radial integral $\int_0^\infty R_n R_m r dr$, and an averaging and summing process which is carried out using Racah coefficients of the quantum numbers of the initial and final states.

THE ANGULAR PART (COUPLING SCHEMES)

When an atom with more than one electron is being considered, there are several ways to add the multiple orbital and spin angular momentums. For example, one might add all the orbital angular momentum

³E. Condon and G. Shortley, Theory of Atomic Spectra, Cambridge University Press, London (1935) hereafter referred to as Condon and Shortley and the Section.

operators to get a total orbital angular momentum operator, and do the same with the spin operators. Then the total orbital angular momentum operator and the total spin angular momentum operator might be added to give a total angular momentum. If the actual states of the atom closely approximate the eigenstates of the total orbital and spin angular momentum operators, then the atom is said to be LS coupled, the L and S representing good quantum numbers of the operators. One way to express the states is to put the quantum numbers of two operators in brackets to the left of the quantum number for the sum of the two operators. An LS state is written $|[S, (L_{\text{core}}, \ell)L]J\rangle$, where L_{core} is the total L of the inner electrons, ℓ is the orbital quantum number of the outer electron, and J is the total angular momentum. A form of coupling commonly found in the rare gases is j ℓ coupling, given by $|[(J_{\text{core}}, \ell)K, S]J\rangle$, where J_{core} is the total angular momentum of the core, s is the spin of the outer electron, and K is the intermediate quantum number.

The average and sum over the initial and final states for $|\langle \psi_n | z | \psi_m \rangle|^2$ is easily seen to be equal to one third of the same average and sum for $|\langle \psi_n | \vec{r} | \psi_m \rangle|^2$. \vec{r} turns out to be a class T operator with respect to J (See Condon and Shortley, 8³). Here it is convenient to introduce a quantity $\langle j; T; j' \rangle$ which can be related to the components of the matrix element $\langle jm | \vec{r} | j'm' \rangle$ but is itself independent of m and m', the z-components. (See Condon and Shortley, 9³). Now if $[P, J_1] = 0$ and P is class T with to $J = J_1 + J_2$, then the ratio

$$\frac{|\langle j_1 j_2 j; P; j_1 j_2' j' \rangle|^2}{|\langle j_1 j_2 j; P; j_1 j_2' \rangle|^2}$$

is given by Equation 11³⁸ of Condon and Shortley, or by $(2j' + 1)j_2(2j_2 + 1)(2j_2' + L)W^2(j_2, j, j_2', j'; j_1) / \Xi(j, j')$ where $j_2' = \max(j_2, j_2')$, $W(j_2, j, j_2', j'; j_1)$ is the Racah coefficient, and $\Xi(j, j')$ is defined by:

$$\Xi(j, j+1) = (j+1)(2j+3)$$

$$\Xi(j, j) = j(j+1)$$

$$\Xi(j, j-1) = j(2j-1) \quad \text{See Condon and Shortley, 7}^4_5$$

In the program there are two procedures, XI and W2MOD, with $\text{XI}(j, j') = \Xi(j, j')$ and with $\text{W2MOD}(j_2, j, j_2', j', j_1) / \text{XI}(j, j')$ equal to the above ratio.

Returning to LS and j_1 coupling, we have:

$$|\langle [S, (L_{\text{core}}, l)L] \ddot{r} [S, (L_{\text{core}}, l')L'] J' \rangle|^2 =$$

$$\frac{\text{W2MOD}(L, J, L', J', S)}{\text{XI}(J, J')} |\langle (L_{\text{core}}, l)L \ddot{r} (L_{\text{core}}, l')L' \rangle|^2 =$$

$$\frac{\text{W2MOD}(L, J, L', J', S) \text{W2MOD}(l, l, l', L', L_{\text{core}})}{\text{XI}(J, J') \text{XI}(L, L')} |\langle l \ddot{r} l' \rangle|^2$$

for LS coupling, and

$$|\langle [(J_{\text{core}}, l)K, s] \ddot{r} [(J_{\text{core}}, l')K', s] J' \rangle|^2 =$$

$$\frac{\text{W2MOD}(K, J, K', J', s)}{\text{XI}(J, J')} |\langle (J_{\text{core}}, l)K \ddot{r} (J_{\text{core}}, l')K' \rangle|^2 =$$

$$\frac{\text{W2MOD}(K, J, K', J', s) \text{W2MOD}(l, K, l', K', J_{\text{core}})}{\text{XI}(J, J') \text{XI}(K, K')} |\langle l \ddot{r} l' \rangle|^2$$

for j_2 coupling.

Summing over all z-components of \vec{J} for both initial states and final states and dividing by $(2J+1)$ is equivalent to multiplying by $\text{XI}(J, J')$. (See Condon and Shortley, Equations 7⁴₅ and 9³₁₁)

$$|\ell \rightarrow r, \ell' \rangle|^2 = \frac{1}{4\ell_s^2 - 1} \left[\int_0^\infty R R' r dr \right]^2$$

(R and R' are radial functions although the quantum numbers pertaining to the radial part have not been written in the above equations.) The final result for $3|\langle n|z|m \rangle|^2$ summed over final states and averaged over initial states is:

$$\frac{W2MOD(L, J, L', J', S) W2MOD(\ell, L, \ell', L', L_{core}) \left[\int_0^\infty R R' r dr \right]^2}{XI(L, L') (2\ell+1)(2\ell'+1)}$$

for LS coupling, and

$$\frac{W2MOD(L, J, K', J', s) W2MOD(\ell, K, \ell', K', J_{core}) \left[\int_0^\infty R R' r dr \right]^2}{XI(K, K') (2\ell+1)(2\ell'+1)}$$

When these quantities are multiplied by $(2J+1)$ and summed over all possible J and J' in the initial and final multiplets, the result is $G(m)$ in the notation used by Rohrlich⁴ and Griem,⁵ the m standing for "multiplet". $G(L)G(m)$ is then $(2J+1)$ times the above quantities, the L standing for "line". $G(L)$ obviously was defined to satisfy the rule $\sum_{J, J'} G(L) = 1$.

A sum rule derived from first principles states that $\bar{\nu} |\langle n|z|m \rangle|^2$ summed over all discrete final states and integrated over continuum final states should equal the Rydberg constant in the same units as $\bar{\nu}$. In the program print out the quantity S3 or SUM3 is the sum over discrete states of $3 \bar{\nu} |\langle n|z|m \rangle|^2$ with $\bar{\nu}$ in cm^{-1} . It should approach 329,212.

⁴F. Rohrlich, Ap. J. 129, 441,449 (1959).

⁵H. Griem, Plasma Spectroscopy, McGraw Hill Book Company, New York (1964).

Intermediate Coupling

Most elements do not fit a well-defined coupling scheme as nicely as might be desired. In other words, their states are mixtures of pure states. No matter what basis is chosen--LS, j_1 , j_j , etc.--the actual states are linear combinations of the basis states, and a transformation matrix between the actual states and the pure states exists.

For the intermediate coupling (IC) program, an LS basis was used, and the elements of the transformation matrix between states of different configurations were assumed to be zero. For each type of configuration involved, a theoretical matrix expression for the electrostatic and spin-orbit perturbations to the Hamiltonian was generated in terms of F_0 , G_0 , F_2 , G_2 , ζ , and ζ' . The electrostatic parameters, F_0 , G_0 , F_2 , and G_2 , appeared only on the diagonal for the LS basis (See Condon and Shortley, 1¹³), while the two spin-orbit parameters ζ and ζ' appeared in many off-diagonal positions (Condon and Shortley, 1¹¹). However, no cross terms exist between states of different J , implying that J is a good quantum number in all coupling schemes.

If the theoretical expression is correct and if it is valid to ignore configuration interaction, then it should be possible to choose values for the parameters such that the diagonalized matrix corresponds closely to the observed energies, in spite of the fact that the number of energies in a configuration (the number of conditions that can be imposed on the parameters) is larger than the number of parameters. In practice, the parameters are adjusted to give a least squares fit between the energies calculated by diagonalization and the observed energies. This is done by using trace conditions from the blocks of different J within a configuration (There are no interaction terms between states of different J .) to set several of the parameters initially. As a first guess, the less significant parameters are set equal to zero. The matrix is then diagonalized and partial derivatives of the eigenvalues with respect to the parameters are calculated. A multiple-dimensional Newton's method is applied to readjust the parameters. The process is repeated until the sum of the squares of the energy differences changes by less than 0.1% from its previous value.

The matrix elements for z between various LS states are easy to calculate, although phases are somewhat of a problem. (See Condon and Shortley, ⁴11). Using the transformation matrices, calculation of oscillator strengths is straightforward.

THE RADIAL INTEGRAL

Schroedinger's equation for the radial wave function is:

$$R = R/nl = P_{nl}/r \frac{\partial^2 R}{\partial r^2} + [-2V(r) - \frac{l(l+1)}{r^2} + \epsilon]R = 0$$

where r is in Bohr radii

and ϵ is in Rydbergs

Both of the methods used in these programs for solving this equation, the Bates-Damgaard approximation⁶ and the scaled Thomas-Fermi method,⁷ are semi-empirical--that is, ϵ is set equal to the observed energy of a known level. The difference between the two approaches lies in the potential $V(r)$ that is chosen.

The Bates-Damgaard or Coulomb Approximation

As a first approximation one guesses that the potential in which the outer electron moves is simply a Coulomb field due to a nucleus of charge $+Z$ shielded by $NEL-1$ electrons very close to the nucleus. Thus $V(r) = -\frac{C}{r}$ where $C = Z-NEL+1$ is the effective core charge. ($C = 1$ for neutral atoms.) Letting $\epsilon = -\frac{C^2}{n^2}$ the differential equation is now:

$$\frac{\partial^2 R}{\partial r^2} + \left[\frac{2C}{r} - \frac{l(l+1)}{r^2} - \frac{C^2}{n^2} \right] R = 0$$

⁶L. Bates and A. Damgaard, Phil. Trans. Roy. Soc. (London) 242A, 101 (1949).

⁷J. Stewart and M. Rotenburg, Phys. Rev. 140, A1508 (1965).

There are two boundary conditions, that $R \rightarrow 0$ at the origin and infinity. They can both be met only when n is an integer. In complex atoms n is generally non-integral, and one condition must be dropped. Since the major contribution to $\int_0^\infty R_n R_m r dr$ comes from large r for most transitions, it is reasonable to forget the condition at the origin. The wave function then blows up at zero and is not normalizable.

A mathematical trick is applied at this point. An asymptotic expansion for large r is generated by making the substitution $R = u e^{-\frac{cr}{n}}$ and finding a recursion relation for u .

$$R = e^{-\frac{cr}{n}} \left(\frac{2cr}{n} \right)^n \left[1 + \sum_{t=1} \frac{a_t}{r^t} \right]$$

a_t is given by a recursion relation in reference 6.

As long as the \sum contains a finite number of terms, the condition at infinity holds and the one at zero does not. But, a quick check shows that the differential equation has an irregular singularity at infinity. Therefore, a power series expansion in $(1/r)$ does not necessarily converge to a solution. In fact, the sum diverges here. In spite of this, if the series is terminated at the proper term, it gives very good fit to the actual solution for $r > 2$ or 3 (depending upon n and l , of course).

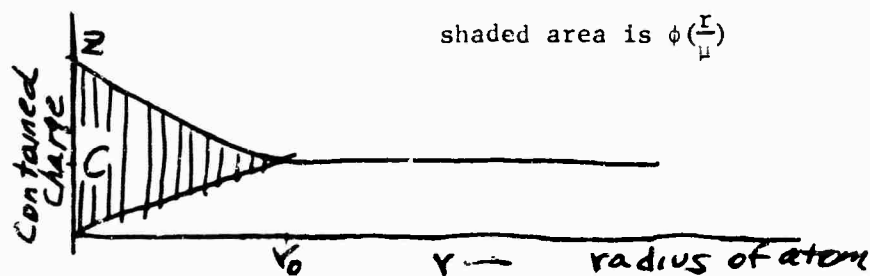
$\int_0^\infty R_n R_m r dr$ is now an integral of an exponential term times a power series in r , and may be expressed as a sum of gamma functions. Because the function does not have to be evaluated numerically at a number of points, very rapid computer calculations are possible. (The normalization is also given analytically.⁶) To overcome the problems of the singularity of the origin and of the diverging series, all powers of r less than 2 in the quantity $R_n R_m r$ are removed. These terms do not exist physically since the actual potential is not a Coulomb field near the origin. For the details of the theory and calculation, see References 6 and 8.

⁸ E. Corinaldesi and E. Geil, Computer Program for Bates-Damgaard Integrals, Westinghouse Research Laboratories Scientific Paper 66-1C1-EPLAS-P4 (1966).

The Thomas-Fermi Method

The Thomas-Fermi approach utilizes a somewhat more realistic potential. Instead of assuming that the $N_{el}-1$ shielding electrons are clustered within an infinitesimal distance of the nucleus, it predicts a distribution of the shielding electrons based on Fermi-Dirac statistics. The fact that the potentials formed in the above manner bring the wave functions much closer to fitting the boundary condition at the origin justifies the use of the method. Moreover, the fit can be made perfect by linearly expanding or contracting the potential in space by a scaling factor close to one. The latter is the scaled Thomas-Fermi method.

The easiest way to understand the method is to look at the net charge contained within a sphere of radius r as a function of r .



The contained charge must obviously go to Z as $r \rightarrow 0$, while for $r > r_0$ -- that is, for r outside of the core -- the contained charge is exactly C , as in the Bates-Damgaard method.

$$\text{contained charge} = \begin{cases} Z[\phi(\frac{r}{\mu}) + \frac{Cr}{r_0}] & r < r_0 \\ C & r > r_0 \end{cases}; \quad V(r) = \begin{cases} \frac{-Z[\phi(\frac{r}{\mu}) + \frac{Cr}{r_0}]}{r} & r < r_0 \\ -C/r & r > r_0 \end{cases}$$

$$\text{where } \phi(0) = 1, \phi(x_0) = 0, \phi'(x_0) = -\frac{C}{x_0 Z}$$

$$\text{with } x = \frac{r}{\mu}, \quad x_0 = \frac{r_0}{\mu}$$

According to Fermi-Dirac theory:

$$\mu = 0.8853 Z^{-1/3}$$

$$\frac{d^2 \phi}{dx^2} = \phi^{3/2} x^{-1/2}$$

At first glance there appears to be one extra boundary condition on the differential equation for ϕ . However, x_0 has not been specified, and all three conditions are needed to uniquely determine ϕ . The equation must be solved numerically, but without x_0 the calculations are quite extensive. Luckily, the work has already been done, and a polynomial fit for the value of x_0 as a function of (C/Z) has been made.⁵ The present j1 and IC programs merely solve for x_0 using the polynomial and then generate ϕ by starting at x_0 with $\phi(x_0) = 0$ and $\phi'(x_0) = -\frac{C}{x_0 Z}$. ϕ automatically becomes one at zero. This calculation need only be performed once for each atomic species, for ϕ is completely determined by C and Z .

The solution to Schroedinger's equation must also be done numeric. No analytical solution is possible because $V(r)$, which depends on ϕ , is only known numerically. Two transformations are made:⁵

$$R(r) = p(y^2), \quad r = y^2, \quad R(r) = R(y^2)$$

$$\text{and } p(y) = y^{1/2} q(y), \quad dr = 2y dy$$

giving:

$$\frac{\partial^2 q}{\partial y^2} = \left\{ \frac{16 \ell(\ell+1) + 3}{4y^2} + 4y^2 [2V(y^2) - \epsilon] \right\} q$$

This is solved by Numerov's method which has an error in each step on the order of h^6 (h = step size). In the program h was $y_0/32$ where $y_0 = r_0^{1/2}$.

The integration was started at a y quite a bit larger than y_0 by evaluating the asymptotic expansion of the Bates and Damgaard (BD) function at two points separated by h . Care must be taken that y is large enough for the asymptotic expansion to be sufficiently accurate and for the tail of the wave function to be negligible beyond y . Still, the starting point must not be so far out that Numerov's method drifts from the actual solution. The first term of the asymptotic expansion is of the form e^{-y^2} , and such functions do exhibit considerable drift when Numerov's method is started too far out. (The higher derivatives of

e^{-y^2} are very large compared to the function itself when y is large.) In this program the integration was started at the point where the first term of the Bates and Damgaard expansion has dropped to about 1/3000 of its maximum value.

If the scaled Thomas-Fermi method is being done, the integration is stopped at one step from the origin and the number of nodes in the wave function is checked to see if it is equal to $n_{int} - l - 1$. n_{int} is the given principal quantum number, not the effective n calculated from $\epsilon = -\frac{C^2}{n^2}$. n_{int} is always an integer. If the number of nodes is not correct, then the direction in which the scaling factor must be changed is immediately determined. On the other hand, if it is correct, then the ratio of the two points closest to the origin is checked against the ratio predicted by a special asymptotic expansion for small y , obtained from a recursion relation for the approximate equation:

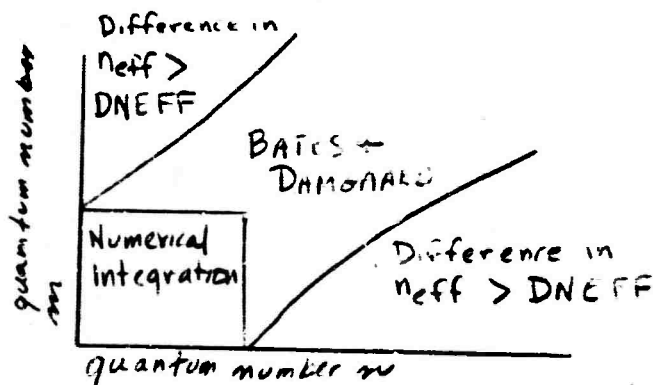
$$\frac{\partial^2 q}{\partial y^2} = \frac{16 l (l + 1) + 3}{4y^2} - 8Z^2 q$$

From this the direction of the next change is found. The scaling factor steps in the proper direction by 0.05, to either 1.05 or 0.95, and the diff. eqn. is resolved with the appropriately changed potential. The scaling factor continues to move in one direction until the value which gives a boundary fit is overstepped. Then the step size is cut in half each time a new step is made. In this manner, the interval in which the correct value falls is bisected with each step. The iteration goes on until the step size is less than 1/2000 or until the ratio of the two points next to the origin is within one percent of its predicted value.

In the rare gases the ground state has too small an n_{eff} to be put into the Bates and Damgaard (BD) method. Instead the wave function of the ground state is calculated numerically by the scaled Thomas-Fermi method. Therefore, when the ground state is involved the $\int_0^\infty R_n R_m r dr$ is done numerically, implying that the wave functions of all upper states that make transitions to the ground state must be known numerically. One way of getting the upper state wave function would be to sum BD

asymptotic expansion at each point desired. However, it is quicker to simply solve Schroedinger's equation numerically since Numerov's method requires only a small number of operations at each point, whereas summing the asymptotic expansion is somewhat involved. As long as the differential equation is being solved numerically, it is just as easy--and certainly more accurate--to use the Thomas-Fermi potential in place of a pure Coulomb potential. This constitutes the unscaled Thomas-Fermi method and has roughly a factor of ten advantage in computer time over the scaled TF method. In general, wave functions generated this way will blow up at the origin and must be chopped off near $r = 0$. The program imposes the form r^{l+1} , the first term of the expansion of the wave function for small r , when the centrifugal potential term $\frac{16 l(l+1) - 13}{4y^2}$ begins to dominate.

GIANT/FIASCO first solves for ϕ and then generates a scaled Thomas-Fermi wave function for the ground state and unscaled Thomas-Fermi wave functions for all other states up to the point where n_{eff} is greater than the n_{eff} of the ground state by more than DNEFF an arbitrary limit fed into the program. (Transitions with a difference in n_{eff} greater than DNEFF are not considered. This is true of non-ground state transitions as well.) All generation of any kind of TF wave functions is performed by an internal procedure called THOMASFERMI. The integration of $\int_0^\infty R_n R_m r dr$ is carried out numerically when both wave functions are known numerically and is done by the Bates and Damgaard method in other cases. Of course, it is not done at all if the difference in the n_{eff} 's is larger than DNEFF.



There are several arbitrary conditions dealing with the Thomas-Fermi method specifically that are built into the program and may require modification in the future. They are:

- 1) the step size h for solving differential equations--it is $x \times x_0/4096$ for ϕ , and $y_0/32$ for the wave functions
- 2) the conditions for stopping the iteration in the scaled TF method
- 3) the method of chopping off the singularity at the origin in the unscaled TF process
- 4) choosing the y outside of y_0 at which to start solving Schroedinger's equation
- 5) deciding which transitions should be done by the BD method and which should be done numerically
- 6) deciding which levels should be scaled TF and which should be unscaled TF.

SYMBOL TABLE

Program I

- Z: the atomic number
NEL: the number of electrons
C: the core charge seen by the outer electron $C=Z-NEL+1$
R: the Rydberg constant in reciprocal centimeters $R=109737.31$
N: an index running over the energy levels
L: orbital angular momentum of the outer electron
J: total angular momentum of the atom
T: energy of the level in cm^{-1}
TINF: energy limit of the level in cm^{-1}
In the LS program only
MULT: multiplicity $=2S+1$ where S is the total spin of the atom
LT: total orbital angular momentum of the atom
P: parity of the state
In the j1 and IC programs only
CORE: total angular momentum of the core
K: intermediate quantum number
TINFO: the value of TINF if $\text{CORE}=1.5$ or 0.5
TINF1: the value of TINF if $\text{CORE}=1.5$
TINF2: the value of TINF if $\text{CORE}=0.5$
NEFF: the effective principal quantum number of the outer electron

Program II

- L, J, T, MULT, LT, P, CORE, K, and NEFF have the same meaning as in Program I but are now arrays. Z, NEL, and C also have the same meaning.
N: an index running over the states. In particular, it is the index of the initial state when dealing with a transition. In PROCEDURE THOMASFERMI, however, it has the value of NEFF.
M: an index running over the final states.
K: in the LS program only, means the same thing as M does in the j1 and IC programs

DNEFF: the largest difference in NEFF for which the program will consider a transition between two levels. Also, in the j1 and IC programs, Thomas-Fermi wave functions are calculated for all levels whose NEFF is less than DNEFF & greater than NEFF of the ground state.

NMAX: the highest energy level index to be considered.

NNMAX: the highest energy level index to be considered for the initial state.

OS: the square of the matrix element of \vec{r} summed over the M_j in the final level and averaged over the M_j in the initial level.

LAMBDA: the wavelength in angstroms

TT: the energy of a transition in cm^{-1}

C1: a constant = 0.587234

YY: C1 x TT

SUM1: the sum of the OS's for all transitions to a given level

SUM2: the sum of the quantity OS/TT for all transitions to a given level

SUM3: the sum of the quantity OSxTT for all transitions to a given level

S1, S2, and S3 have the same meaning in the LS program.

A: the transition rate in sec^{-1}

I1, I2, and I3 are indices used in the Thomas-Fermi and intermediate coupling sections of the j1 and IC programs.

Variables Associated with the Thomas-Fermi Method

QQ: the independent variable in the polynomials used to initialize the ionic radius. See Stewart and Rotenberg, ⁷Appendix A.

QQSUM: the sum of the QQ polynomial

XO: the ionic radius times $Z^{1/3} / 0.8853$

AA, BB, and CC: the coefficients in the initialization polynomials

PHIM1, PHIO, and PHIP1 are ϕ_{i+1} , ϕ_i , and ϕ_{i-1} respectively. The ϕ -function is found by solving the differential equation $\phi''(x) = [\phi(x)/x]^{1/2}$ from x_0 inward.

H: the step size used in this iteration. It is = to XO/4096.

H32: a variable = to $H^{3/2}$

HSTAN: the step size used in solving for the actual wave functions. It is = to $\sqrt{r_0}/32$. The independent variable in the wave function is $y = \sqrt{r}$.

VMOD: $8y^2$ times the Thomas-Fermi potential in Rydbergs. It is given as a function of y , at points separated by $HSTAN/2$.

WF: a 2-dimensional array giving $R(y^2)/\sqrt{y}$ as a function of the index of the energy level and y , at points separated by $HSTAN$.

NORM: the normalization factor by which WF for a given level must be multiplied.

NTF: the index of the highest energy level for which a Thomas-Fermi wave function is calculated

NPOINTS: for each level, the number of points at which WF is given. It is = to the maximum y considered divided by $HSTAN$.

NINT: the principal quantum number of the outer electron for a given state. (NINT stands for N integral, as opposed to N effective.) The number of nodes expected in the wave function is $NINT-L-1$.

The following variables are declared inside PROCEDURE THOMASFERMI.

WFP1, WFO, and WFM1: values of WF around a given y

KSP1, KSO, and KSM1: values of K_s where the differential equation is

$$-\frac{d^2}{dy^2} WF(y) = K_s(y).$$

FACTORP1, FACTORO, and FACTORM1: values of the quantity $(1 - H^2 K_s / 12)$

Note: P1 and M1 stand for +1 and -1. P1 means that the value is given for a y one step closer to the origin, while M1 corresponds to a y one step farther from the origin. (The integration proceeds inward)

EPSILON: the energy eigenvalue in Rydbergs.

H (already declared outside the procedure): the step size used in solving for WF. It is readjusted as the scale factor α is varied.

H2: a variable set equal to H^2

H2T4: $4H^2$

H2012: $H^2/12$

H2T506: $5H^2/6$

Y2T4: $4y^2$

RMAX: the largest value of r considered. Outside of RMAX the wave function is assumed to be too small to make any significant contribution.

INVR: $1/RMAX$

SCALE: the scale factor α in the scaled Thomas-Fermi method

JUMP: the amount by which SCALE is varied between successive trials.

DIRECTION: the direction in which SCALE is varied. It is +1 for an increase and -1 for a decrease.

OLDDIRECTION: the previous value of DIRECTION

BEFORE: a Boolean variable which is true as long as SCALE continues to jump in one direction by steps of 0.05. When the proper value of SCALE has been overstepped, BEFORE becomes false, SCALE converges by a bisection procedure.

LASTTIME: a Boolean variable which becomes true when SCALE has converged sufficiently. It activates the normalization and cut-off procedures.

VARYSCALE: a Boolean variable which determines whether a scaled or unscaled Thomas-Fermi method is to be used. In the present program VARYSCALE is true only for the ground state.

NEWI2: the number of points at which WF is known after it has been interpolated so that the spacing between points is HSTAN

LPOLY: a function of L which is used a large number of times. It is $= 16L(L+1)+3$.

NODES: the number of times that the wave function crosses the axis each time the differential equation is solved.

RATIO: the ratio of the values of the wave function between the two points closest to the origin.

DRATIO: the change in RATIO between two successive iterations.

INSIDE: a variable which--on the last iteration--goes to true as soon as y moves from the exponential region into the oscillatory region.

NORMOD: a non-array quantity which is summed to form the array NORM, the normalization factor.

Variables Associated with Intermediate Coupling

(Not all of the variables declared are described here, but most of the important ones are mentioned.)

SPORBMATRIX (4D or 3D): the coefficients of the first spin-orbit parameter in the theoretical Hamiltonian matrix. In the 4D case, the first index is the ℓ of the configuration, the second index is the J , and the last two are the row and the column within a J -block.

The 3D (i.e. 3-dimensional) array is missing the first index.

SPORBMATRIXP (4D or 3D): the coefficients of the second spin-orbit parameter in the Hamiltonian.

ELECMATRIX (4D or 3D): the theoretical Hamiltonian for the electrostatic parameters. In the 4D array, the first three indices are the same as in **SPORBMATRIX4D** while the last index identifies the electrostatic parameter under consideration. No column index is necessary since the electrostatic interaction is diagonal in the LS basis.

IELEC and **NELEC**: the index and total number of the electrostatic parameters.

IPARAM and **NPARAM**: the index and total number of parameters.

ELECPARAM: an array containing the values of the electrostatic parameters as they are adjusted by **PROCEDURE DIAG**.

SPORBPARAM and **SPORBPARAMP**: the values of the two spin-orbit parameters.

IGREATER: the greater of the two ℓ 's of two states under consideration.

STLS3D: the matrix elements of $\cos\theta$ between pairs of LS states. The first index is **LGREATER** and the other two are the rows and columns.

J2, **J3**, **S2**, **S3**, **L2**, and **L3**: the variables used to represent quantum numbers in generating the Hamiltonian matrices and the LS strengths.

HOLD: the variable that holds on to the value of L as the energy levels are read in. When the end of a configuration is reached, the next L is no longer = to **HOLD** and **PROCEDURE DIAG** is called.

T2D and **N2D**: arrays holding the values of T and N for the levels of a given configuration. The first index is the J of the level and the second puts the states of a given J -block in order of increasing energy.

IJ, IJMIN, and IJMAX: the index and limits for the J-blocks of a given configuration.

INDEX and BLOCK: arrays over N giving the J-block and the position in that block of every level fed into the program. The number BLOCK is distinct from one configuration to the next.

LOWERBLOCK: the lowest BLOCK in a given configuration.

SIZE2 and SIZE3: the sizes of the J-blocks as predicted by the sections which generate the theoretical Hamiltonian matrices and the LS strengths.

SIZE: the size of the J-blocks in the observed levels which are read by the program.

I2LOWER and I3LOWER: integer arrays which indicate what position in the STLS3D matrix to look for a given pair of L's and J's.

TRACE and TRACES: the traces of the J-blocks. Since the traces of the undiagonalized theoretical Hamiltonian and the traces of the observed energy matrix should be the same, enough information is present to initialize the values of the parameters for a given configuration.

H: a matrix for the Hamiltonian formed from the theoretical expressions for the Hamiltonian and the values which the parameters happen to have at the moment.

TCALC: an array containing the energies calculated by diagonalizing the H-matrix.

V3D, V2D, and VTEMP: various forms of the matrix which diagonalizes the Hamiltonian.

DERIV: a matrix of the derivatives of the calculated energy eigenvalues with respect to the parameters.

ALPHS: the coefficients of the set of simultaneous equations which are solved for the corrections to the parameters. They are calculated from the DERIV's and the differences between the observed and calculated T's.

IT: the number of times that the parameters for a configuration have been readjusted for a better least-squares fit to the observed energies.

SUMSQUARES: the sum of the squares of the differences of the observed and calculated energies.

HOLD SUM: the value of SUMSQUARES from the previous iteration. If SUMSQUARES has changed by less than 0.1%, the iteration is terminated.

REAL PROCEDURE XI is the same as $-(J, J')$

$$\begin{aligned}
 & (J+1)(2J+3) & \text{if } J' = J+1 \\
 = & J(J+1) & J' = J \\
 & J(2J-1) & J' = J-1
 \end{aligned}$$

REAL PROCEDURE W2MOD is a modified Racah coefficient squared.

$$W2MOD(L, J, L', J', S) = (2J' + 1) L (2L + 1)(2L' + 1) W^2(L, J, L', J'; S)$$

Moreover,

$$\frac{W2MOD(L, J, L', J', S)}{XI(J, J')} = \frac{|\langle SLJ \ P \ SL'J' \rangle|^2}{|\langle L \ P \ L' \rangle|^2}$$

where \vec{P} is class \vec{T} with respect to \vec{J} and $[\vec{S}, \vec{P}] = 0$

REAL PROCEDURE I calculates the radial integral $\int R_n(r)R_m(r) \, r dr$ by numerical integration if both N and M are less than the index of the highest state for which a Thomas-Fermi wave function has been calculated. For all other pairs the Bates-Damgaard method of integration is called through REAL PROCEDURE BD.

PROCEDURE THOMASFERMI takes NEFF, NINT, and L for the Kth level and produces a wave function.

PHI/GENERATOR produces the Thomas-Fermi potential by numerically solving a differential equation derived from the theory. All quantities calculated in this section pertain to all levels for which PROCEDURE THOMASFERMI is applied.

Section in the program which sets NINT[N] for all the energy levels for which Thomas-Fermi wave functions are calculated must be changed for every different atomic or ionic species.

The IC Program

MATRIX/GENERATOR - the part of program which generates the theoretical expressions for electrostatic and spin-orbit perturbations to the Hamiltonian. The LS basis is used and matrices similar to those on pages 268-269 of Condon and Shortley¹¹ are produced for each parameter. Section 1¹³ page 299 gives the actual coefficients generated, since the program is at present designed to do the rare gases.

LS/STRENGTHS - produces a matrix for the angular part of the dipole operator. All possible pairs of LS states are considered. When **PROCEDURE DIAG** has expressed each energy level as a linear combination of LS states, it is then easy to calculate the angular matrix element between any two of the actual states.

A section in the program takes the energy levels in each configuration as a group, places them in blocks of different J, and then re-orders each J-block in order of increasing energy, which are then fed into **PROCEDURE DIAG**, one configuration at a time.

PROCEDURE DIAG takes each configuration fed into it and compares the actual observed energies with the theoretical expressions for the Hamiltonian which have been generated by **MATRIX/GENERATOR**. **DIAG** then adjusts the theoretical parameters so that the diagonalization of the theoretical Hamiltonian gives a least-squares fit to the observed energy eigenvalues. Once this is done, the matrix which diagonalizes the Hamiltonian is merely an expansion of the observed levels in terms of LS basis states. This matrix saved for the final computation of the oscillator strengths.

INPUTS TO PROGRAMS 1 AND 2 OF GIANT/FIASCO (LS PP GRAM)

under "FIASCO" (input to Program 1):

a card with Z, the atomic number and N_{el} , the number of electrons

a card with the value of T_{inf}

for each level of Moore's tables a card giving:

L (orbital angular momentum of the outer electron)

MULT (multiplicity = $2S + 1$)

LT (total orbital angular momentum)

P (parity + +1 even, = -1 odd)

J (total angular momentum)

T (energy of the level in cm^{-1})

under "READER2" (input to Program 2):

a card with NMAX (the maximum N to be read) and NNMAX (max on the index of the initial state)

a card with DNEFF (the limitation on interacting levels)

INPUTS TO PROGRAMS 1 AND 2 OF GIANT/FIASCO (j1 and IC PROGRAM)

under "FIASCO" (input to Program 1):

a card with Z, the atomic number and N_{el} , the number of electrons

a card with the value of T_{inf} for CORE = 0, the value of

T_{inf} for CORE = 1.5, the value of T_{inf} for CORE = 0.5

for each level of Moore's tables a card giving:

CORE (total angular momentum of the core)

L (orbital angular momentum of the outer electron)

K (intermediate quantum number)

J (total angular momentum)

T (energy of the level in cm^{-1})

under "READER2" (input to Program 2):

a card with NMAX (the maximum N to be read)

a card with DNEFF (the limitation on interacting levels)

15 cards giving the coefficients of the three initialization polynomials for the Thomas-Fermi function. Each card has four numbers:

the index of the coefficient,
 A(index),
 B(index),
 C(index),

(See Stewart and Rotenberg⁵, Appendix A)

and, for the IC program only, for each possible L (L = 0, 1, 2, 3) a card with:

LMI (coeff of F_2 if $L_{\text{total}} = L - 1$),
 LSAME (coeff of F_2 if $L_{\text{total}} = L$),
 LPI (coeff of F_2 if $L_{\text{total}} = L + 1$),
 LMISC (coeff of G_0 if $L_{\text{total}} = L - 1$ and $S = 0$),
 LPI50 (coeff of G_2 if $L_{\text{total}} = L + 1$ and $S = 0$),
 (See Condon and Shortley, pp 285-299).

ON EXTENDING PROGRAMS 1 AND 2

1S Program: For elements in which the L of the parent term is non-zero, the expression for OS must be changed from $W2MOD(1, J, L', J', S)\sigma^2$ to

$$W2MOD(L, J, L', J, S) \frac{W2MOD(1, L, 1', L', L_{\text{parent}})}{XI(L, L')} \sigma^2$$

In more complex elements, coefficients of fractional parentage must also be added.

jl and IC Programs: To do other rare gases, the only change necessary is the setting of NINT (the principal quantum number) for all of the levels to be done by Thomas-Fermi method.

To do other elements the cards which define the ground state as a $'S_0$ state and multiply the strengths of ground state transitions by six, must be altered.

IC Program: NMAX must be set low enough that no configuration with fewer than the predicted number of levels gets read by Program 2. NMAX should be one greater than the last level in the highest configuration to be done. Although this greatly limits the IC Program, it would be possible to do many more transitions if PROCEDURE DIAG expanded the actual states in terms of jl basis states instead of LS states. Higher states in incomplete configurations could then be approximated as pure jl states. Therefore, a matrix which transforms the LS basis to the jl basis would be a useful addition. For elements with more complex configurations, the variables which identify the states and the J-blocks must be changed, along with the generator of the theoretical Hamiltonian and the LS strengths. This involves rewriting most of the procedures.

OUTPUT FROM PROGRAM 2 OF GIANT/FIASCO

Following the listing of the energy levels from Program 1, Program 2 will print out varying quantities of fairly self-explanatory information, depending upon the coupling scheme--that is, LS, j1, or IC.

The j1 and IC programs will first list all the Thomas-Fermi wave functions as a function of the number of steps from the origin in y. (The function printed is actually $q(y)$; see the section describing GIANT/FIASCO.) Note that the first ten steps are given, and then jumps of five steps are taken to save space. Immediately below each wave function is printed the expected number of nodes, which is simply $n_{int}-1$, and the actual number of nodes in the wave function shown. The two numbers are always the same for levels done by the scaled TF method, but in the unscaled cases (These can be identified by the fact that SCALE = 1.000.) there is no guarantee that this is so. When the two are the same, it is an indication that the Thomas-Fermi method is valid.

The IC program will now print out the transformation matrices from LS states to the observed states. Double lines separate different configurations, while single lines separate the iterations approaching a leastsquares fit for a given configuration. For each block of a different J, the observed energies and the energies calculated by diagonalizing the theoretical Hamiltonian appear next to the corresponding rows of the transformation matrix. (Note that some of the matrices are rectangular although all of them should be square. Extra columns on the right should be ignored.) Directly below, and within the same J block, are the derivatives of the calculated energy eigenvalues with respect to the various adjustable parameters. The rows are in order of increasing energy eigenvalues, and the columns are in the same order as the list of parameters, which appears once for each iteration. (Derivatives for parameters which are not involved--that is, parameters which are zero after the first iteration--should be ignored.)

Finally, the LS, j1, and IC programs all print out the transition probabilities in the form $3|<n|z|m>|^2$, which had already been summed

over final states for m and averaged over initial states for n. At the far right is Einstein's spontaneous emission coefficient in the form $A_{nm} \times 10^{-8}$. However, at present the j1 and IC programs have a card near the end of Program 2 which reads:

$$A \leftarrow 4x(2xJ(N)+1/(2xJ(M)+1);$$

This reverses the indexes n and m so that $A_{mn} \times 10^{-8}$ is printed out instead of $A_{nm} \times 10^{-8}$ as the comment cards in Program 2 claim.

AUXILIARY PROGRAM FIASCO/RESULTS

This program merely reads the stored output of Program 2 from the disc READF2 and prints out the transition probabilities in several forms. GF is gf, FNM is f_{nm} , ANM is A_{nm} , and AMN is A_{mn} . Input is just the levels of Moore's tables with the same cards that go into Program 1.

NRL ALGOL VERSION OF 5/01/67

[illegible][illegible]


```

PROCEDURE 7148)
BEGIN
  REAL JUNR, SPORPARAM, SPORPARAMP, MOLOSUN, SUNSQUARES)
  SC 51 4010
  SC 51 4010
  SC 51 4010
  START OF SEGMENT ..... 16
  ARRAY SPORBNATX30, SPORBNATXP30(015,014,0141,TRACE,TRACE1015,017),
  TCALC(019),ELEC(010),N(010,014))
  INTEGER NELEC,NPARAM,IPARAM,SIZE,10)
  INTEGER ARRAY ELECMATRIX30(015,014,016))
  REAL OUR(VON)
  ARRAY ALPHS(016,017),VTEMP,V20(016,014),DEIV(014,016))
  INTEGER IPARAMV,IPARAMH)
  INTEGER IT)
  REAL BU,TH,CT)
  LABEL ITVMEZ,ERRON,SKIN)
  WRITE (PRINTER,FL1)
  IF MOLOMO THEN BEGIN NELEC=2) NPARAM=3)
  END ELSE BEGIN NELEC=4) NPARAM=4) END)
  FOR IJ=IJMIN STEP 1 UNTIL IJMAX DO BEGIN
    SIZE=I2MAX(MOLO,IJ)
    I6=IJ-IJMIN+1)
    FOR IPARAM=1 STEP 1 UNTIL NPARAM=1 DO TRACE(I4,IPARAM)=0)
    FOR I1=1 STEP 1 UNTIL I2MAX(IJ) DO
      TRACE(I6,NPARAM=I1)+TRACE(I6,NPARAM=I1)+T20(IJ,I1))
    FOR I3=1 STEP 1 UNTIL SIZE DO BEGIN
      FOR IELEC=1 STEP 1 UNTIL NELEC DO BEGIN
        ELECMATRIX30(IJ,I2,IELEC)=ELECMATRIX30(MOLO,IJ,I2,IELEC)
        TRACE(I6,IELEC)+TRACE(I6,IELEC)+ELECMATRIX30(IJ,I2,IELEC)
      END)
      FOR I3=1 STEP 1 UNTIL SIZE DO BEGIN
        SPORBNATX30(IJ,I2,I3)+SPORBNATX30(MOLO,IJ,I2,I3)
        SPORBNATX30(IJ,I2,I3)+SPORBNATX30(MOLO,IJ,I2,I3)
      END)
      TRACE(I6,NELEC=1)+TRACE(I4,NELEC=1)+SPORBNATX30(IJ,I2,I2)
      IF MOLOMO THEN
        TRACE(I6,NELEC=2)+TRACE(I4,NELEC=2)+SPORBNATX30(IJ,I2,I2)
      END)
    END)
  END)
  IT=0)
  TCALC(010)=P20)
  IF MOLOMO THEN BEGIN
    SNEB(TRACE,5,JUNK,6))
    IF JUNK=0 THEN WRITE (PRINTER(PAGE),PERROR)
    FOR IELEC=1,2 DO ELEC(010)=TRACE(IELEC,6))
    SPORPARAM=TRACE(5,4))
  END ELSE IF MOLO=1 THEN BEGIN
    FOR IJ=IJMIN STEP 1 UNTIL IJMAX DO BEGIN
      I6=IJ-IJMIN+1)
      FOR IELEC=1,2,3 DO TRACE(I4,IELEC)+TRACE(I4,IELEC)
      TRACE(I4,4)+TRACE(I4,5))
      TRACE(I4,5)+TRACE(I6,7))
    END)
    SNEB(TRACE,5,JUNK,6))
    IF JUNK=0 THEN WRITE (PRINTER(PAGE),PERROR)
    FOR IELEC=1 STEP 1 UNTIL 4 DO ELEC(010)=TRACE(IELEC,4))
    SPORPARAM=TRACE(5,4))
  END)
  IT=TYPE)
  TIMEIT(PRINTER)
  WRITE (PRINTER(OBL),PPARAM,FOR IELEC=1,2,3,4 DO ELEC(010)=TRACE(IELEC,5)
  SPORPARAM,SPORPARAMP)
  MOLOSUN=SUNSQUARES)
  SUNSQUARES=0)
  FOR IPARAMV=1 STEP 1 UNTIL NPARAM DO
    FOR IPARAMH=1 STEP 1 UNTIL NPARAM=1 DO
      ALPHS(IPARAMV,IPARAMH)=0)
  FOR IJ=IJMIN STEP 1 UNTIL IJMAX DO BEGIN
    SIZE=I2MAX(MOLO,IJ)
    FOR I2=1 STEP 1 UNTIL SIZE DO
      FOR I3=1 STEP 1 UNTIL SIZE DO
        N(12,I3)=0)
      FOR I2=1 STEP 1 UNTIL SIZE DO BEGIN
        FOR IELEC=1 STEP 1 UNTIL NELEC DO
          N(12,I2)+N(12,I2)+ELECMATRIX30(IJ,I2,IELEC)+ELEC(010)=TRACE(IELEC)
        FOR I3=1 STEP 1 UNTIL SIZE DO
          N(12,I3)+N(12,I3)+SPORBNATX30(IJ,I2,I3)+SPORBNATX30(MOLO,IJ,I2,I3)+SPORBNATX30(IJ,I2,I3)+SPORBNATX30(MOLO,IJ,I2,I3)
        END)
      END)
  END)

```

3C	1A1	2A410
3C	1A1	2A711
3C	1A1	2A912
3C	1A1	2P112
3C	1A1	2P210
3C	1A1	2P211
3C	1A1	2P310
3C	1A1	2P411
3C	1A1	2P412
3C	1A1	2P413
3C	1A1	2P414
3C	1A1	2P415
3C	1A1	2P416
3C	1A1	2P417
3C	1A1	2P418
3C	1A1	2P419
3C	1A1	2P420
3C	1A1	2P421
3C	1A1	2P422
3C	1A1	2P423
3C	1A1	2P424
3C	1A1	2P425
3C	1A1	2P426
3C	1A1	2P427
3C	1A1	2P428
3C	1A1	2P429
3C	1A1	2P430
3C	1A1	2P431
3C	1A1	2P432
3C	1A1	2P433
3C	1A1	2P434
3C	1A1	2P435
3C	1A1	2P436
3C	1A1	2P437
3C	1A1	2P438
3C	1A1	2P439
3C	1A1	2P440
3C	1A1	2P441
3C	1A1	2P442
3C	1A1	2P443
3C	1A1	2P444
3C	1A1	2P445
3C	1A1	2P446
3C	1A1	2P447
3C	1A1	2P448
3C	1A1	2P449
3C	1A1	2P450
3C	1A1	2P451
3C	1A1	2P452
3C	1A1	2P453
3C	1A1	2P454
3C	1A1	2P455
3C	1A1	2P456
3C	1A1	2P457
3C	1A1	2P458
3C	1A1	2P459
3C	1A1	2P460
3C	1A1	2P461
3C	1A1	2P462
3C	1A1	2P463
3C	1A1	2P464
3C	1A1	2P465
3C	1A1	2P466
3C	1A1	2P467
3C	1A1	2P468
3C	1A1	2P469
3C	1A1	2P470
3C	1A1	2P471
3C	1A1	2P472
3C	1A1	2P473
3C	1A1	2P474
3C	1A1	2P475
3C	1A1	2P476
3C	1A1	2P477
3C	1A1	2P478
3C	1A1	2P479
3C	1A1	2P480
3C	1A1	2P481
3C	1A1	2P482
3C	1A1	2P483
3C	1A1	2P484
3C	1A1	2P485
3C	1A1	2P486
3C	1A1	2P487
3C	1A1	2P488
3C	1A1	2P489
3C	1A1	2P490
3C	1A1	2P491
3C	1A1	2P492
3C	1A1	2P493
3C	1A1	2P494
3C	1A1	2P495
3C	1A1	2P496
3C	1A1	2P497
3C	1A1	2P498
3C	1A1	2P499
3C	1A1	2P500
3C	1A1	2P501
3C	1A1	2P502
3C	1A1	2P503
3C	1A1	2P504
3C	1A1	2P505
3C	1A1	2P506
3C	1A1	2P507
3C	1A1	2P508
3C	1A1	2P509
3C	1A1	2P510
3C	1A1	2P511
3C	1A1	2P512
3C	1A1	2P513
3C	1A1	2P514
3C	1A1	2P515
3C	1A1	2P516
3C	1A1	2P517
3C	1A1	2P518
3C	1A1	2P519
3C	1A1	2P520
3C	1A1	2P521
3C	1A1	2P522
3C	1A1	2P523
3C	1A1	2P524
3C	1A1	2P525
3C	1A1	2P526
3C	1A1	2P527
3C	1A1	2P528
3C	1A1	2P529
3C	1A1	2P530
3C	1A1	2P531
3C	1A1	2P532
3C	1A1	2P533
3C	1A1	2P534
3C	1A1	2P535
3C	1A1	2P536
3C	1A1	2P537
3C	1A1	2P538
3C	1A1	2P539
3C	1A1	2P540
3C	1A1	2P541
3C	1A1	2P542
3C	1A1	2P543
3C	1A1	2P544
3		

9C	1A1	40012
9C	1A1	41110
9C	1A1	41110
9C	1A1	41112
9C	1A1	41310
9C	1A1	45P12
9C	1A1	4A011
9C	1A1	4A011
9C	1A1	4A111
9C	1A1	4A010
9C	1A1	4A011
9C	1A1	47312
9C	1A1	47310
9C	1A1	47711
9C	1A1	49311
9C	1A1	4S512
9C	1A1	4RA10
9C	1A1	4A011
9C	1A1	4R113
9C	1A1	4R010
9C	1A1	4R010
9C	1A1	50213
9C	1A1	50410
9C	1A1	50A11
9C	1A1	51012
9C	1A1	71113
9C	1A1	92211
9C	1A1	95811
9C	1A1	97713
9C	1A1	99A10
NFY1 9FG 4C		
9C	91	40110
9C	91	41110
9C	91	71113
9C	91	70111
9C	91	67113
9C	91	14711
9C	91	17211
9C	91	12310
9C	91	12410
9C	91	14710
9C	91	15115
9C	91	14012
9C	91	15112

3C	31	13311
3C	31	13810
3C	31	14910
3C	31	17610
3C	31	17715
3C	31	17912
3C	31	18011
3C	31	18210
3C	31	18611
3C	31	18712
3C	31	18913
3C	31	19112
3C	31	19211
3C	31	19410
3C	31	19811
3C	31	19910
3C	31	20312
3C	31	20313
3C	31	20412
3C	31	20610
3C	31	21011
3C	31	21110
3C	31	21110
3C	31	21211
3C	31	21510
3C	31	21513
3C	31	21512
3C	31	21812
3C	31	22210
3C	31	22213
3C	31	22312
3C	31	22711
3C	31	22910
3C	31	23310
3C	31	23411
3C	31	23411
3C	31	23612
3C	31	24211
3C	31	24715
3C	31	24813
3C	31	25513
3C	31	24710
3C	31	26110
3C	31	26211
3C	31	26310

SC	51	27713
SC	51	28410
SC	51	28413
SC	51	28913
SC	51	29510
SC	51	29812
SC	51	29913
SC	51	30311
SC	51	30911
SC	51	31013
SC	51	31212
SC	51	31610
SC	51	32112
SC	51	32510
SC	51	32613
SC	51	33011
SC	51	33313
SC	51	33711
SC	51	33713
SC	51	34111
SC	51	34413
SC	51	35C11
SC	51	35J11
SC	51	34110
SC	51	34610
SC	51	34111
SC	51	34A13
SC	51	34610
SC	51	34912
SC	51	35113
SC	51	35410
SC	51	35712
SC	51	36210
SC	51	36610
SC	51	36911
SC	51	39112
SC	51	39313
SC	51	39612
SC	51	39911
SC	51	40412
SC	51	1011
SC	51	1610
SC	51	A2211
SC	51	42413
SC	51	42613

```

SPONHMATRIXPAU(MOLO,J2,I2,I3)+SPPJ
END01
END01
I2MAX(M*LU,J2)+I2J
END01
END01
FOR LGREATER=1 STEP 1 UNTIL 3 DO BEGIN
  I2=01
  FOR J2=LGREATER=3 STEP 1 UNTIL LGREATER+1 DO
    IF J2=0 THEN BEGIN
      I2L=ERILGREATER=1,J2)+I2J
      FOR S2=01 DO
        FOR L2=ABS(J2-S2) STEP 1 UNTIL J2+ S2 DO
          IF L2>ABS(LGREATER=2) AND L2SLGREATER THEN BEGIN
            I2=01 I2+I2+I2
          FOR J3=LGREATER=2 STEP 1 UNTIL LGRFATER=2 DO
            IF J3=0 THEN BEGIN
              I3LOWERILGREATER,J3)+I3J
            FOR S3=01 DO
              FOR L3=ABS(J3-S3) STEP 1 UNTIL J3+ S3 DO
                IF L3>ABS(LGREATER=1) AND L3SLGREATER+1 THEN BEGIN
                  I3=I3+11
                  IF ABS(J2-J3)+1 AND ABS(L2-L3)+1 AND (J2+J3)=0 AND S2=S3 THEN BEGIN
                    STL5=SQRT((2HJ2+1)*
                      H2H00(L2,J2,L3,J3,S2)+H2H00(LGREATER=1,L2,LGREATER,L3,1)/
                      X(L2,L3))
                    IF J2+J3=J3+1 THEN STL5=STL5
                    IF L3=L2 THEN STL5=STL5
                    END ELSE STL5=01
                    STL5=STL5(LGREATER,I2,I3)+STL5
                  END01 END01 END01 END01 END01
                WRITE(PRINTER,FLJ)
                LOWERBLOCK=0, MOLO=11 IJMAX=01 IJMIN=101
                FOR IJ=0 STEP 1 UNTIL 10 DO T20(IJ,0)+11
                FOR N=2 STEP 1 UNTIL NMAX+1 DO BEGIN
                  IF H0LO=1 THEN BEGIN
                    FOR IJ=IJMIN STEP 1 UNTIL IJMAX DO
                      FOR I1=1 STEP 1 UNTIL IMAX(IJ) DO
                        INOEX(N20(IJ,I1))+I1J
                      IF H0LO=1 THEN DIAGI
                        LOWERBLOCK=LOWERBLOCK+(IJMAX+1)
                        IJMAX=01 IJMIN=101
                      FOR IJ=0 STEP 1 UNTIL 10 DO IMAX(IJ)+01
                    END01
                    IJ=ENTIER(IJN))
                IF IJ=IJMAX THEN IJMAX=IJ
                IF IJ=IJMIN THEN IJMIN=IJ
                HLOCK(N)=LOWERBLOCK+I1J
                IMAX(IJ)=IMAX(IJ)+11
                FOR I1=1 IJMAX(IJ) STEP 1 WHILE TEN>STP(IJ,I1)=1 DO BEGIN
                  T20(IJ,I1)+T20(IJ,I1-1)
                  T20(IJ,I1)+420(IJ,I1-1)
                END01
                T20(IJ,I1)+TINJ
                T20(IJ,I1)+N1
                H0LO=LENJ
              END01
              WRITE (PRINTER,FLJ)
              BLOCK(IJ)=01 INOEX(I1)=1
              V30(IJ,I1)=SQRT(A) V30(IJ,I2)=01
              FOR N=1 STEP 1 UNTIL NMAX
                DO BEGIN SUM1=01SUM2=01SUM3=01 WRITE (PRINTER|OHL,FAJ)
                  SIZE2=I2MAX(LI)+ENTIER(IJN))
                  I2LO=H00+I2LOWER(LI,N,IJN))
                  FOR I2=1 STEP 1 UNTIL SIZE2 DO
                    V10(I2)=V30(BLOCK(IJ),INOEX(N),I2J)
                  FOR N=1 STEP 1 UNTIL NMAX DO
                    IF ABS(LI)=L(N)+1 AND ABS(JI)=J(N)+1 AND (JI)=J(N)+J(N)+0
                      AND ABS(NEFF(IJ)=NEFF(N))=0NEFF
                    THEN BEGIN
                      LGREATER=MAX(LI)+L(N))
                      SIZE3=I2MAX(LI)+ENTIER(J(N))
                      I3LO=H00+I3LOWER(LI,N,IJN))
                      I3=01
                      IF LI=JALGREATER THEN
                        FOR I3=1 STEP 1 UNTIL SIZE2 DO
                          FOR I1=1 STEP 1 UNTIL SIZE3 DO
                            OS=OS+V10(I2)+STL5(IJ,LGREATER,I2+I2LO=H00,I3+I3LO=H00)+
                              V30(BLOCK(IJ),INOEX(N),I3J)
                          ELSE
                            FOR I3=1 STEP 1 UNTIL SIZE3 DO
                              FOR I2=1 STEP 1 UNTIL SIZE2 DO
                                OS=OS+V10(I2)+STL5(IJ,LGREATER,I3+I3LO=H00,I2+I2LO=H00)+
                                  V30(BLOCK(IJ),INOEX(N),I3J)
                              JS=(OS+1)+2/((CAR(LGREATER=2-1)*(2HJ(N)+1)))
                              TT=TI+TINJ TT=CI+TTJ SUM1=SUM1+OS1 SUM2=SUM2+OS/TTJ
                              LAMBOA=OB, IJ SUM3=SUM3+OS+TTJ
                              A=2.0200001+ANDSTT+3J
                              A=AN(2HJ(N)+1)/(2HJ(N)+1)
                              WRITE (PRINTER,FS,N,N+OS+TT,LAMBOA,AJ)

```

```

WRITE (READF2,F0,N,M,OS,YY))
END)
WRITE (PRINTERIOBL,F3,N,SUM1,SUM2,SUM3))
WRITE (READF2,F4,N,M,SUM1,SUM2))
TIMEIT(PRINTER))
WRITE (READF2,F7,N,COREIN,LIN,KIN,JLIN,TIN))
END) READIN(READF2) ) END)

LOCK (READF2))
END,

EXP      IS SEGMENT NUMBER 0017, PRT ADDRESS IS 0207
LN        0018      0208
SBRT      0019      0076
OUTPUT(=  0020      0062
BLOCK CONTROL 0021      0009
INPUT(=)  0022      0096
X TO THE I  0023      0216
GO TO SOLVER 0024      0079
ALGOL WRITE 0025      001A
ALGOL READ  0026      0019
ALGOL SELECT 0027      0016

NUMBER OF ERRORS DETECTED = 0
LAST CARD WITH ERROR WAS SEG #
PRT SIZE = 200; TOTAL PGM SEGM SIZE = 2600 WORDS; DISK SIZE = 160 SEGS; NO. PGM. SEGS = 28
ESTIMATED CORE STORAGE REQUIREMENT = 7029 WORDS.
13:19:37 MONDAY, MAY 10, 1967 PROCESSOR TIME = 55.42 SECONDS I/O TIME = 59.87 SECONDS

```

LABEL 00000000LINE 001671NOT COMPILE GIANT/FIASC0 SYNTAX

OR079ACC ALGOL

APPENDIX C

CALCULATION OF THE OPTICAL RADIATION EMITTED BY A CYLINDRICAL ARC OF KNOWN TEMPERATURE PROFILE

by. R. Liebermann

INTRODUCTION

In order to compare measurable physical properties of an emitting plasma with theory, a computer program has been written to calculate at the surface of a cylindrical arc discharge:

- (1) the spectral radiance (normal to the surface) due to radiant contribution from along the line of sight of the diameter which has a spatial temperature gradient, and
- (2) the spectral radiant emittance due to contributions from all radiating volume elements of a homogeneous temperature arc column.

The above calculations involve self-absorption processes within the arc column and therefore are solutions of a radiant heat transfer equation.

A. Radiant Heat Transfer Equation

With the assumption that the plasma is in local thermal equilibrium (LTE) the spectral radiance is related to the properties of the medium through the radiant heat transfer equation

$$-\frac{d I_v}{d \tau_v} = I_v - B_v \quad (1)$$

which describes the spatial gradient of intensity along the line of sight at some point x where I_v is the spectral radiant intensity at frequency v in the proper direction, B_v is the corresponding black body intensity and τ_v is the optical depth as measured from $x = -\infty$ to x . We define the optical depth as

$$\tau_v(T) \equiv \int_{-\infty}^x \kappa'_v(T) ds \quad (2)$$

where $\kappa'_v(T)$ is the spectral absorptivity coefficient (including stimulated emission) due to free-free, bound-free, and bound-bound radiative processes. The solution of 1 is given as

$$I_v(\bar{\tau}_v) = \int_0^{\bar{\tau}_v} B_v(\tau_v) \exp \{ -\bar{\tau}_v + \tau_v \} d\tau_v \quad (3)$$

where

$$\bar{\tau}_v \equiv \int_{-\infty}^L \kappa'_v(T) ds \quad (4)$$

with L corresponding to that location along the line of sight (at the surface of the arc column) having spectral radiance $I_v(\bar{\tau}_v)$. In 3 it was assumed for $x \leq 0$ that no contribution to $I_v(\bar{\tau}_v)$ is made (i.e., no external radiation field is present).

1. Spectral Radiance

If our interest is radiance at the arc column's surface due to contributions from along the line of sight of the diameter, equation 3 by an assumption of radial symmetry can be placed in the following form.

$$I_v(\bar{\tau}_v) = I_v(r=R) = \int_0^{\bar{Z}} B_v(Z) \left[\exp \{ Z \} + \exp \{ -Z \} \right] \exp \{ -\bar{Z} \} dZ \quad (5)$$

where Z is an optical depth measured from the center of the arc column to some radial point r along the radius which has a maximum dimension R . The correspondence is $Z = 0$ at $r = 0$ and $Z = \bar{Z}$ at $r = R$ thus

$$\bar{Z} = \int_0^R \kappa'_v(T(r)) dr ; Z = \int_0^r \kappa'_v(T(r)) dr \quad (6)$$

For programming purposes Equation 5 is the better form of 3. In order to solve 5 it is first necessary to have prior knowledge of the temperature profile $T(r)$ and for a given gas vapor pressure a method by which κ'_v can be determined such that solutions of 6 are obtainable. Part D of this section describes the general theory involved for determining $\kappa'_v(T)$.

Utilizing the theory of Part D we are then prepared to numerically integrate Equations 6 and thus 5. The method of approach was as follows. For a specified temperature profile and frequency the integrand of 6 was determined at division points in r and interpolated in r^2 between division points. Using a linear expansion of κ'_v in r^2 a closed form integration was performed between division points and a summation yielded $Z(r)$. In similar fashion the black body term in the integrand of 5 was calculated at division points in r and linearly expanded in Z^2 . A closed form integration of 5 was then possible between division points of $Z(r)$ and was summed to yield $I_v(\bar{\tau}_v)$. Although the latter integration can be performed for all values of the parameters serious errors (due to cancellation effects) may develop when ΔZ is small between end points of the intervals. Hence for $\Delta Z < .01$ the solution was expanded in terms of ΔZ whereas for $\Delta Z > .01$ the closed form was used. Solution of 5 was then repeated for other selected v values of the specified band pass to yield a representative spectrum.

2. Spectral Radiant Emittance

If our interest is spectral emittance at the arc column's surface due to contributions from all radiating volume elements with the

discharge assumed homogeneous in temperature then Equation 3 which yields the spectral radiance along a particular line of sight reduces to

$$I_v(T, S) = B_v(T) \left[1 - \exp \{ - \bar{\tau}_v \} \right] \quad (7)$$

where now from Equation 4

$$\bar{\tau}_v = K'_v(T) S \quad (8)$$

S being the distance through which radiation travels along a particular line of sight and is a function of arc geometry.

The spectral radiant emittance at the surface of the arc column can be calculated using 7 by applying the cosine law and integrating over solid angle. Using the geometry shown in Reference 1 the spectral radiant emittance is given as

$$F_v(T) = B_v(T) \left[\pi - 4 \int_0^{\pi/2} \int_0^1 \exp \left\{ \frac{-K'_v(T) D u}{u^2 + (1-u^2) \sin^2 \phi} \right\} u du d\phi \right] \quad (9)$$

where D is the column diameter

The radiant emittance is then determined by

$$F(T) = \int_0^\infty F_v(T) dv \quad (10)$$

Equations (9) and (10) were solved using straightforward numerical techniques.

B. Input to Arc Intensity Program

The input required for the above calculations is fully described within the program itself which is shown in Part E of this Section. In brief the basic required input is as follows:

- (1) Spectroscopic data involving bound-bound transitions such as
 - (a) oscillator strengths
 - (b) electron impact line shifts and widths
 - (c) excitation energies
 - (d) statistical weights
- (2) thermodynamic properties such as tables of
 - (a) electron number densities
 - (b) neutral particle number densities
 - (c) internal partition functions
 - (d) ionization lowering values
- (3) temperature profile
- (4) specified wavelength band pass.

C. Output of Arc Intensity Program

The output of the program provides plots as well as printouts of the spectral radiance and spectral radiant emittance. In addition plots of spectral absorptivities are obtainable. Samples of these plots are shown in Figures 3, 4, and 5. For particulars on how to obtain these plots see program Part E.

D. Spectral Absorptivities

The net absorption coefficient κ' which is the difference between true absorption and induced emission coefficients is in a spectral line for a given frequency ν and temperature T (assuming LTE)

$$\kappa'_{\nu}(T) = \pi r_o c f_{mn} N_n \left[1 - \exp \left\{ \frac{-h\nu}{kT} \right\} \right] L(\nu) \quad (11)$$

where π , r_0 , c , h and k are the usual constants, f_{mn} is the absorption oscillator strength for transitions from state n to m (n being the lower energy level state), N_n is the population density of the initial state, and $L(\nu)$ is the line profile normalized such that

$$\int_{-\infty}^{\infty} L(\nu) d\nu = 1 \quad (12)$$

where $L(\nu)$ is a function of the lines, shifts, widths etc. all a function of temperature and pressure.

For conditions of LTE the population density N_n can be expressed in terms of N_0 (the total number of atoms or ions in question) by use of the Boltzmann relation

$$N_n = \frac{g_n N_0}{U_0} \exp \left\{ \frac{-E_n}{kT} \right\} \quad (13)$$

where g_n is the statistical weight of the initial level, E_n is the excitation energy of the initial level, U_0 is the atomic (or ionic) internal partition function and T is the absolute electron temperature.

The line profile $L(\nu)$ is course dependent on the mechanisms of line broadening. The stark effect due to electron impact has the Lorentz dispersion profile given as

$$L(\nu) = \frac{1}{\pi\omega} \left[\frac{1}{\left[\frac{\nu - (\nu_0 + d)}{\omega} \right]^2 + 1} \right] \quad (14)$$

where ω is the half width of the line at half intensity and d is the electron impact shift. ν_0 is the observed frequency of the line in an unperturbed condition.

When resonance broadening mechanisms are of importance, one must add to the electron impact half width ω the resonance half width ω_R which from first order approximation can be expressed for resonance lines as

$$\omega_R = \frac{3r_o c}{4\pi} \left(\frac{g_1}{g_2} \right)^{1/2} \frac{f N_g}{v_o} \quad (15)$$

where g_1 and g_2 are respectively the lower and upper states' statistical weight factors of the resonance line, N_g is the ground state population density and f is the absorption oscillator strength of the transition (actually f as defined here is the average value for the resonance multiplet transition obtained by a sum of the multiplet's individual f 's over final states which are then averaged over initial states). In equation 15, N_g are neutral perturbers of the same kind (radiating atoms). For the case when perturbers of unlike kind are of such abundance (e.g. a strong concentration of another gas specie is present) then Van der Waals broadening may be of some importance and should be included in the dispersion profile.

Besides line broadening due to charge perturbers (Stark effect) or neutral atoms (Resonance and Van der Waals effects) there exists other broadening mechanisms which must also be considered, namely Doppler broadening, which results in a Gaussian line shape profile. This type of profile is dominant when collisions are negligible and the velocities of the radiating systems have a thermal distribution. The Gaussian line shape is given as

$$L_D(\Delta\nu) = \left(\frac{\ell n 2}{\pi} \right)^{1/2} \frac{1}{\omega_o} \exp \left[-\frac{\ell n 2}{\omega_D^2} (\Delta\nu)^2 \right] \quad (16)$$

with $\Delta\nu = \nu - \nu_o$ and where ω_D is the Doppler half (half) width

$$\omega_D = \left[\frac{2kT \ell n 2}{Mc^2} \right]^{1/2} \nu_o \quad (17)$$

M being the mass of the radiating system. When collision effects cannot be neglected (e.g. when ω , ω_R etc. are of the same order of magnitude as ω_D) then joint effects of Doppler and the more important pressure

broadening mechanisms should be considered. The observed line shape is then the so called Voigt profile provided the broadening processes are statistically independent. From 17 it is obvious that lines occurring in the UV regions will tend to be more of a Voigt profile type.

The net absorption coefficient κ'_V as expressed in 6 is not only due to bound-bound transitions but also includes bound-free and free-free processes as well. Therefore, one must add to a sum of Equation 11 these other processes to obtain representative values of 5 in the spectral regions where bound-bound transitions are not dominant. For conditions of LTE the bound free absorptivity $\kappa_{bf}(\nu, T)$ can be expressed in terms of a sum over excited states designated by quantum numbers n and l having corresponding photoionization cross-sections σ_{nl} and population density $N_{n,l}$ whose edge frequencies ν_{nl} are less than or equal to ν

$$\kappa_{bf}(\nu, T) = \sum_{n,l} \sigma_{nl} N_{nl} \left\} \nu_{nl} \leq \nu \quad (18)$$

The net bound-free absorptivity is then expressed as

$$\kappa'_{bf}(\nu, T) = \kappa_{bf}(\nu, T) \left[1 - \exp \left\{ \frac{-h\nu}{kT} \right\} \right] \quad (19)$$

Solution of 18 is a formidable task since σ_{nl} for each level requires numerical solutions of the Schrodinger equation.* A simplified approach is to separate 18 into two distinctive regions i.e., into levels which are hydrogen like and into levels which are non hydrogen like thus

$$\kappa_{bf}(\nu, T) = \sum_{n,l} \sigma_{nl} N_{nl} + \sum_{n,l} \sigma_{nl}^H N_{nl}^H \quad (20)$$

* See for example Ref. 1.

where in general for the hydrogen like terms $n \gg 1$. The sum over the hydrogenic levels can be simplified further as follows. Starting with a sum rule analogous to that for bound-bound transitions

$$\int_{\nu_{nl}}^{\infty} \sigma_{nl}^H d\nu = \pi r_o c f_{nl} \quad (21)$$

and using the proportionality $\sigma_{nl}^H \sim \nu^{-3}$ the hydrogenic photoionization cross section σ_{nl}^H is

$$\sigma_{nl}^H = 2\pi r_o c \frac{\nu_{nl}^2}{\nu^3} f_{nl} \quad (22)$$

where f_{nl} corresponds to the excited n, l state's continuum oscillator strength. Using the Rydberg formula for hydrogenic energy levels, the binding energy E_B of the excited level is ($E_{nl} \approx E_n$)

$$E_B = h\nu_{nl} = E_{\infty} - E_{nl} = \frac{E_H Z^2}{n^2} \quad (23)$$

where Z refers to the ionization stage, n is the principal quantum number, E_{∞} is the ionization potential, E_{nl} is the excitation energy of the excited level and E_H is the Rydberg constant. From 23 we see that the rate at which the binding energy changes with respect to unit change in principal quantum number for $n \gg 1$ is

$$\Delta E_B \approx \frac{-2E_H Z^2}{n^3} \quad (24)$$

We now define an average hydrogenic cross section σ_n for all l states with same quantum number n as

$$\sigma_n \equiv \sum_l (2l+1) \sigma_{nl}^H / \sum_l (2l+1) \quad (25)$$

where l is the orbital-angular momentum quantum number. Thus using the hydrogenic relations

$$\left. \begin{aligned} \sum_l (2l+1) f_{nl} &\approx .5n \\ \text{and} \quad \sum_l (2l+1) \left| \begin{array}{c} \\ n=\text{constant} \end{array} \right| &= n^2 \end{aligned} \right\} \quad (26)$$

Equation 25 takes the form of

$$\sigma_n = 4\pi^2 \frac{\alpha a_0^2}{n^5} \left(\frac{h}{h\nu} \right)^2 Z^4 \quad (27)$$

where α and a_0 are the usual constants. Equation 25 is the familiar hydrogenic cross section less the Gaunt factor G_{bf} . Using Equation 13, and noting for atomic gases, whose higher levels are hydrogen like but degenerate in J (total angular momentum quantum number) that

$$g_n = \sum (2J+1)_n = 2n^2 g_1 \quad (28)$$

where g_1 is the statistical weight factor of the ground state of the parent term; and using the relationship of Equation 24 the hydrogenic sum term of 20 becomes

$$\sum_{n,l} \sigma_{nl}^H \frac{N_{nl}^H}{N_o E_u} = \frac{-4\pi^2 \alpha a_0^2 g_1}{U_o E_u} \left(\frac{h}{h\nu} \right)^3 Z^2 N_o \sum \exp \left\{ \frac{-E_n}{kT} \right\} \Delta E_B \cdot G_{bf} \quad (29)$$

For hydrogen the excitation energy E_n is approximately equivalent to $E_{n\ell}$. However, for other gases whose higher levels are hydrogen like but degenerate in J then E_n should be averaged over these J, ℓ states which have $E_{J\ell}$ excitation energies such as

$$E_n = \sum_J (2J+1) E_{J\ell} / 2n^2 g_1 \quad (30)$$

Thus with E_n as defined in 30 obeying Equation 23 wherein $E_{n\ell}$ is replaced by E_n then 29 takes the form of

$$\sum_{n\ell} \sigma_{n\ell}^H N_{n\ell}^H = \frac{-4\pi^2 \alpha a_o^2 g_1}{U_o E_F} \left(\frac{E_H}{h\nu} \right)^3 Z^2 N_o G_{bf} \exp \left\{ \frac{-E_\infty}{kT} \right\} \cdot \sum \exp \left\{ \frac{E_B}{kT} \right\} \Delta E_B \quad (31)$$

with the assumption that $G_{bf} \approx \text{constant}$ for $n \gg 1$.

The sum on the right of 31 may for practical purposes be taken as an integral with lower limit $E_B = h\bar{\nu}_n$ and upper limit $E_B = 0$. Hence for $\bar{\nu}_n$ representing the maximum edge frequency of the merged levels where $n \gg 1$ with $\bar{\nu}_n \leq \nu$ then

$$\begin{aligned} \sum_{n\ell} \sigma_{n\ell}^H N_{n\ell}^H &= \frac{4\pi^2 \alpha a_o^2 g_1}{U_o} \left(\frac{kT}{E_H} \right) Z^2 N_o \left(\frac{E_H}{h\nu} \right)^3 \exp \left\{ \frac{-E_\infty}{kT} \right\} \left[\exp \left\{ \frac{h\bar{\nu}_n}{kT} \right\} - 1 \right] G_{bf} \\ &= 1.82 \times 10^{24} \frac{g_1 T}{U_o} Z^2 \frac{N_o}{\nu^3} \exp \left\{ \frac{-E_\infty}{kT} \right\} \left[\exp \left\{ \frac{h\bar{\nu}_n}{kT} \right\} - 1 \right] G_{bf} \end{aligned} \quad (32)$$

or for the case when ν is less than the maximum edge frequency of the merged levels ($\nu < \bar{\nu}_n$) then

$$\sum_{n\ell} \sigma_{n\ell}^H N_{n\ell} = 1.82 \times 10^{24} \frac{g_1 T}{U} Z^2 \frac{N_0}{v^3} \exp \left\{ \frac{-E_\infty}{kT} \right\} \left[\exp \left\{ \frac{h\nu}{kT} \right\} - 1 \right] G_{bf} \quad (33)$$

Equations 32 and 33 are equivalent to those presented by Biberman, Norman and Ulyanov⁽²⁾ less their correction factor which for our high n levels is approximately one and equivalent to the Gaunt factor. It is of interest to note that in the form of 31 if the right hand sum is taken as an integral with lower limit set to $E_B=0$ and upper limit $E_B = -\infty$ representing unbound electrons we obtain at once the familiar free-free absorptivity expression

$$\kappa_{ff} = 1.82 \times 10^{24} \frac{g_1 T N_0 Z^2}{U_0 v^3} \exp \left\{ \frac{-E_\infty}{kT} \right\} \cdot G_{ff} \quad (34)$$

where the G_{ff} term has been introduced and is the free-free Gaunt factor. Thus equation 20 takes the form (including the f-f absorption)

$$\kappa_{bf+ff} = \sum \sigma_{n\ell} N_{n\ell} + 1.82 \times 10^{24} \frac{g_1 T N_0 Z^2}{U_0 v^3} \exp \left\{ \frac{-E_\infty}{kT} \right\} \cdot \left[G_{ff} + G_{bf} \left(\exp \left\{ \frac{h\nu'}{kT} \right\} - 1 \right) \right] \quad (35)$$

whereby previous definitions $\nu' = \bar{\nu}_n$ if $\nu \geq \bar{\nu}_n$ and $\nu' = \nu$ if $\nu < \bar{\nu}_n$. In equation 35 the non-hydrogenic sum term then only includes such levels having edge frequencies ν_E which meet the requirement that $\bar{\nu}_n < \nu_E \leq \nu$. In the above derivations the assumption that G_{ff} is constant independent on temperature and frequency is valid provided $T < 2$ ev (see Ref. 3) however when T is of greater value than G_{ff} increases and varies somewhat with frequency. Likewise when n is of some lower value then G_{bf} is no longer a constant but varies with

quantum number and frequency. The accuracy of 35 is thus better enhanced when the sum term includes the majority of the excited levels. Such calculations involving the sum term have been made by Ref. 2 and 4 who have utilized the techniques proposed by Ref. 1 for determining photoionization cross sections for ionized gases other than hydrogens. However their results differ somewhat in that they have chosen different normalization factors. In essence (using their results) Equation 35 remains the same with the exception of replacing the factor $Z^2 G_{bf}$ with a ζ (Zeta) factor, and in addition when using the ζ factor of Ref. 4. ν' is to be replaced by ν for all values. Their sum term then only includes a limited number of lower excited levels (including the ground state).

Since several b-b transitions usually occur for a given lower excited state near the frequency of its continuum photoionization edge (the upper excited state being near the ionization limit) there results a pseudo continuum (i.e. the lines in question merge with the continuum causing in appearance a false photoionization edge at a slightly lower frequency). When these b-b transitions are not included in the sum of Equation 11 near such corresponding photoionization edges then serious errors may develop in solutions of radiant heat transfer problems. Therefore in order to avoid such difficulty (when all such b-b transitions are not fully resolved) one should assign a correction term to the photoionization edge ν_E to yield an apparent edge ν'_E such as

$$\nu'_E = \nu_E - \Delta E_S / h \quad (36)$$

where h is the usual constant and ΔE_S is the so called advance of the series limit (see Ref. 5), and let the photoionization edge cross-section $\sigma(\nu_E)$ for this particular level be defined at ν'_E . In addition the lowering of the ionization potential ΔE_∞ should be included in the calculation of ν_E such as

$$h\nu_E = E_\infty - \Delta E_\infty - E_{nl} \quad (37)$$

where E_∞ is the ionization potential and E_{nl} is the excitation energy of the level in question.

REFERENCES

1. C. H. Church, et.al., "Final Report on Contract Nonr 4647(00)", 15 November 1965, AD 473 996. See also A. Burgess and M. Seaton, Mon. Not Roy. Astron. Soc. 120, 121 (1960).
2. L. M. Biberman, G. Norman and K. Ulyanov, Optics and Spectroscopy 10, 297 (1961).
3. J. M. Berger, Ap. J. 124, 550 (1956).
4. D. Schluter, Z. Astrophys. 61, 67 (1965) and private communication.
5. H. Griem, Plasma Spectroscopy, McGraw Hill Book Co., New York (1964).

14407132 THURSDAY, MAY 11, 1967
BEGIN

MRL ALGOL VERSION OF 5/01/67

	SC	LI	010
START OF SEGMENT	SC	21	010
2	SC	21	010
COMMENT	SC	21	010
THIS PROGRAM HAS BEEN WRITTEN TO CALCULATE THE SPECTRAL RADIANCE	SC	21	010
OF AN ARC DISCHARGE AT ITS SURFACE (NORMAL) DUE ONLY TO RADIANT	SC	21	010
CONTRIBUTIONS FROM ALONG THE LINE OF SIGHT ON THE DIAMETER WHICH MAY	SC	21	010
OR MAY NOT HAVE A SPATIAL TEMPERATURE GRADIENT. THIS PROGRAM	SC	21	010
INITIATES BY FIRST READING FROM DISK FILES SPECTROSCOPIC DATA	SC	21	010
INVOLVING BOUND-BOUND TRANSITIONS FOR THE PARTICULAR GAS IN QUESTION	SC	21	010
-- SUCH AS UNPERTURBED LINE FREQUENCIES AND THEIR CORRESPONDING	SC	21	010
OSCILLATOR STRENGTHS, ELECTRON IMPACT SHIFTS AND WIDTHS, EXCITATION	SC	21	010
ENERGIES, AND STATISTICAL WEIGHT PARAMETERS. WITH THIS INFORMATION (SC	21	010
IN ADDITION TO THE ABOVE INPUT, THE PROGRAM READS IN PARTICLE	SC	21	010
NUMBER DENSITIES AND INTERNAL ATOMIC PARTITION FUNCTIONS.)	SC	21	010
THE PROGRAM THEN TAKES THE INITIAL BAND PASS INPUT AND CALCULATES	SC	21	010
WAVELENGTH INCREMENTS SUCH THAT ALL LINE PEAKS FOR ALL LINES THEREIN	SC	21	010
FOR ALL TEMPERATURES ASSIGNED TO THE PROFILE ARE INCLUDED.	SC	21	010
FOR BOUND-BOUND TRANSITIONS INVOLVING GROUND STATE, A CALCULATION	SC	21	010
OF RESONANCE LINE BROADENING IS ADDED TO THE ELECTRON IMPACT WIDTH--	SC	21	010
ALL LINE PROFILES ARE ASSUMED TO BE OF THE LOMENTZ TYPE.	SC	21	010
WITH THE ABOVE INFORMATION SPECTRAL ABSORPTIVITIES DUE TO THE	SC	21	010
BOUND-BOUND TRANSITIONS ARE CALCULATED AND ADDED TO A BARE CONTINUUM	SC	21	010
VALUE WHICH IS SPECIFIED BY INPUT. FOR XENON GAS THE CONTINUUM SPECTRAL	SC	21	010
ABSORPTIVITIES ARE CALCULATED DIRECTLY USING SCHLUTENS BOUND - FREE	SC	21	010
ZETA TABLES CONNECTING A HYDROGENIC B-F EXPRESSION WHICH IS THEN SUMMED	SC	21	010
TO AN ADJUSTED HYDROGENIC FREE-FREE EXPRESSION--THE SUM BEING ADDED TO	SC	21	010
THE BOUND-BOUND VALUES.	SC	21	010
ONCE THE SPECTRAL ABSORPTIVITIES HAVE BEEN CALCULATED THE	SC	21	010
PROGRAM SOLVES THE RADIANT HEAT TRANSFER EQUATION ALONG THE ARC DIAMETER	SC	21	010
. THE SPECTRAL RADIANCE IS THEN PRINTED OUT AND PLOTTED AS A FUNCTION	SC	21	010
OF WAVELENGTH. IN ADDITION TO THIS OUTPUT THE PROGRAM WILL IF CALLED	SC	21	010
UPON CALCULATE AND PLOT AS A FUNCTION OF WAVELENGTH THE SPECTRAL	SC	21	010
RADIANT EMITTANCE (PRINTING OUT THE RADIANT EMITTANCE FOR THE BAND PASS)	SC	21	010
AT THE SURFACE OF A HOMOGENEOUS CYLINDRICAL ARC FOR ANY OR ALL	SC	21	010
TEMPERATURES ASSIGNED TO THE PREVIOUS TEMPERATURE PROFILE FOR ANY NUMBER	SC	21	010
OF DIFFERENT ARC DIAMETERS. FOR THE ABOVE TEMPERATURES THE PROGRAM WILL	SC	21	010
PLOT THE SPECTRAL ABSORPTIVITIES AS A FUNCTION OF WAVELENGTH.	SC	21	010
THIS PROGRAM HAS BEEN WRITTEN FOR THE FOLLOWING ATOMIC GASES--	SC	21	010
SODIUM (ATOMIC NUMBER 11)	SC	21	010
POTASSIUM (ATOMIC NUMBER 19)	SC	21	010
XENON (ATOMIC NUMBER 54)	SC	21	010
COMMENT	SC	21	010
THIS PROGRAM CONTAINS TEN HEAD STATEMENTS FOR INPUT CARDS WHICH ARE	SC	21	010
LISTED BELOW IN ORDER OF CALL AND VARIABLE CONCERNED----	SC	21	010

1) NMAX (INTEGER) MAXIMUM NUMBER OF ATOMIC LEVELS LISTED ON DISK FILES	SC	21	010
2) SCHUTEMPH (REAL) WAVELENGTH (INCHES)	SC	21	010
3) BOUNDONE (INTEGER)	SC	21	010
4) T (REAL)	SC	21	010
5) M (REAL)	SC	21	010
6) PRESS (REAL)	SC	21	010
7) KONT (REAL)	SC	21	010
8) WAVE (REAL)	SC	21	010
9) PLOT (REAL)	SC	21	010
10) DIT (REAL)	SC	21	010
-----	SC	21	010
THE ABOVE VARIABLES ARE DEFINED BELOW	SC	21	010
-----	SC	21	010
NMAX (INTEGER) MAXIMUM NUMBER OF ATOMIC LEVELS LISTED ON DISK FILES	SC	21	010
HEAD1 AND HEAD2	SC	21	010
NT (INTEGER) NUMBER OF TEMPERATURES ON DISK FILE HEAD3 FOR WHICH	SC	21	010
THE ELECTRON IMPACT SHIFTS AND WIDTHS HAVE BEEN	SC	21	010
CALCULATED	SC	21	010
LAMIN (REAL) MINIMUM WAVELENGTH (ANGSTROM UNITS) OF THE	SC	21	010
DESIRED BAND PASS	SC	21	010
LAMMAX (REAL) MAXIMUM WAVELENGTH (ANGSTROM UNITS) OF THE	SC	21	010
DESIRED BAND PASS	SC	21	010
QMAX (INTEGER) TOTAL NUMBER OF RADIAL TEMPERATURES OF THE ARC	SC	21	010
TEMPERATURE PROFILE	SC	21	010
LAM (REAL) ATOMIC NUMBER INCREMENT OF THE WAVELENGTH BAND PASS (SC	21	010
ANGSTROM UNITS)---THIS VALUE CAN BE ZERO IF THE ATOMIC	SC	21	010
LEVELS ARE MORE THAN A FEW ANGSTROMS APART	SC	21	010
NLAP (INTEGER) TOTAL NUMBER OF INCREMENTS DESIRED IN THE BAND	SC	21	010
PASS (AND T EXCEEDS 1.22)	SC	21	010
IMP (REAL) AN INCREMENT OF BAND PASS (ANGSTROM UNITS) BEYOND	SC	21	010
THE BAND PASS WHICH ALLOWS LINES IN THIS INCREMENT	SC	21	010
TO CONTRIBUTE TO THE INPUT BAND PASS SPECTRUM	SC	21	010
LY (REAL) LENGTH (INCHES) OF X AXIS FOR PLOTS	SC	21	010
LX (REAL) LENGTH (INCHES) OF X AXIS FOR PLOTS	SC	21	010
ATNU (REAL) ATOMIC NUMBER OF GAS	SC	21	010
-----	SC	21	010
SCH ((THE JENKINS LAMMA) SCHLUTENS ZETA FACTORS FOR XENON	SC	21	010
MUST BE INPUT IN SPECIAL FORM	SC	21	010
-----	SC	21	010
FO (LAPLACE) ATOMIC INTERNAL PARTITION FUNCTION	SC	21	010
NU (LAPLACE) NEUTRAL PARTICLE DENSITY (1/CM ³)	SC	21	010
NE (LAPLACE) ELECTRON NUMBER DENSITY (1/CM ³)	SC	21	010
OEL (LAPLACE) IONIZATION POTENTIAL (ELECTRON VOLTS)	SC	21	010
-----	SC	21	010
T (ARRAY) DESIRED TEMPERATURE PROFILE DEG. KELVIN	SC	21	010

READ(HEADF1,/,A,B,C)	SC 271 1911
IF ATNUM=0 THEN	SC 271 1113
READ(HEADF1,/,FOR 1=1	SC 271 1212
E(1))	SC 271 4613
ELSE	SC 271 4811
READ(HEADF1,/,FOR 1=1 STEP 1 UNTIL NMAX DO (N,A,B,A,A,J(1),	SC 271 5313
E(1)))	SC 271 4910
HEWIND (READ(1)) LOCK(HEADF1)	SC 271 7913
FOR 1=1 STEP 1 UNTIL NMAX DO J(1)=J(1) +	SC 271 7911
READ(HEADF2,/,A,B,C,F,G)	SC 271 8313
I=0	SC 271 9813
LAMMIN=LAMPMIN+1	SC 271 9912
LAMMAX=LAMMAX+1	SC 271 10013
NUMIN=1/LAMMIN	SC 271 10210
NMAX=1/LAMMIN	SC 271 10311
DUP=USP+1	SC 271 10412
C=.5872344*NUMIN/(1+NUMIN*DUP) + F*NMAX*DUP	SC 271 10513
IF F=1 THEN H=.5872344*7 ELSE H=.5172344*NMAX/(1+F)	SC 271 10913
START1	SC 271 11811
READ(HEADF2,/,A,B,C,F,G,LAMBDA) (EXIT)	SC 271 11910
IF H=1 THEN	SC 271 13513
IF YTR THEN IF YTSR THEN	SC 271 13710
BEGIN	SC 271 14912
HEAL A	SC 271 14010
IF ATNUM=0 THEN IF N=	SC 281 010
1=1	SC 281 610
A=YY/.5872344	SC 281 711
LAMBDA=1/A	SC 281 812
GFMN(1)=OS*H*(2*J(1)+1)/329211.93	SC 281 913
NUC(1)=A	SC 281 1313
N(1)=N + (1+1)*H + E(1)*E(1)	SC 281 1510
WRITE (PRINTENF,/,	SC 281 1910
END OF IF STATEMENT	SC 281 1911
GO TO START 1	SC 271 14110
EXIT 1 HEWIND(HEADF2) LOCK(HEADF2)	SC 271 14112
ZZ=IMAX+1	SC 271 14512
READ(HEADF3,/,A,B,C,F,G)	SC 271 14613
START1	SC 271 14113
IT=0	SC 271 14710
START2	SC 271 14213
READ(HEADF3,/,A,B,C,F,G) (EXIT)	SC 271 14310
IF B=0 THEN GO TO START2	SC 271 17413
IF B=1 THEN	SC 271 18010
BEGIN	SC 271 14013
IT=IT+1 + (FMP(1)+C) + (1+1)*F + (1+1)*G	SC 271 14111
WRITE (PRINTENF,/,A,B,C,F,G)	SC 271 14113
END	SC 271 20111
XIX=CMP(1)/100	SC 271 20111
READ(HEADF3,/,A,B,C,F,G)	SC 271 20713
IF IT=NT THEN GO TO START2 ELSE GO TO START1	SC 271 21713
EXIT 1 HEWIND(HEADF3) LOCK(HEADF3)	SC 271 21912
READ(HEADF4,/,FOR 1=1 STEP 1 UNTIL NT DO (UD(1)+ND(1), NE(1),	SC 271 22312
J(1))	SC 271 23313
READ(HEADF4,/,FOR 1=1 STEP 1 UNTIL NMAX DO (1))	SC 271 24113
BEGIN	SC 271 24613
COMMENT DETERMINE FREQUENCY AND WAVELENGTH ARRAYS WHICH INCLUDE ALL	SC 271 24613
PEAK LINE VALUES FOR ALL TEMPERATURES LISTED IN PROFILE	SC 271 25413
REAL NU(1) HEAL ARRAY SIZE(101000)	SC 271 25413
REAL NMAX (INTEGER N1)	SC 291 113
LABEL EXIT2 REAL DELN(1) INTEGER NMAX + 1	SC 291 113
REAL DELLA(1)	SC 291 113
REAL J(1)2=0	SC 291 113
J=0	SC 291 113
FOR 1=1 STEP 1 UNTIL NMAX DO	SC 291 212
BEGIN	SC 291 410
IT=ENTIER(.3+XIX+1*(G)/1000)	SC 291 410
IF IT=NT THEN IT=NT+1	SC 291 410
U3=U3+IT	SC 291 1112
H=NE(1)	SC 291 1113
NMAX=(NE(1)+1)/H+.3)*H+1	SC 291 213
FOR 1=1 STEP 1 UNTIL ZZ DO	SC 291 1713
READ(NU(1)+1,/,A,B,C,F,G)	SC 291 2110
UD(1)=UD(1)+((1+G3)+((1+1)+1)*U3+1)*H	SC 291 2310
UD=NU(1)+1	SC 291 1113
A=UD(1)+0.3	SC 291 1311
IF A=H THEN	SC 291 1413
IF A=H THEN	SC 291 1512
BEGIN	SC 291 141
J(1)=1	SC 291 1711
S(1)=A	SC 291 1812
END	SC 291 1913
END OF J LOOP	SC 291 1913
END OF G LOOP	SC 291 4210
NMAX=J	SC 291 4411
NU(1)=1/(LAMB(1)+LAMMIN)	SC 291 4510
DELLA=(LAMMAX-LAMMIN)/LAM	SC 291 4713
FOR 1=1 STEP 1 WHILE LAMB(1)<LAMMAX DO	SC 291 4912

```

      BEGIN
      IF K2TU20 THEN GO TO EXIT2 J
      MOLA(M(K)) J
      A=M*DELLAM J
      M=M*LAMBDA**4 J
      A=A*LAMBDA**5 J
      FOR J=1 STEP 1 UNTIL JMAX DO
      BEGIN
      C=1/5N(J) J
      IF CPH THEN IF CKA THEN C=C
      ENDO J
      LAMB(M+1)=A J
      NU(M+1)=1/A J
      ENDO OF K LOOP J
EXIT2: KMAX=K+1 J NCMAX=NU(K+1) J Z=KMAX J
LAMBDA=LAMB(M+1) J
END OF FREQUENCY AND WAVELENGTH ARRAYS J
      29 IS R3 LONG, NEXT SFG 27
      BEGIN COMMENT RADIANT INTENSITY CALCULATION AT SURFACE OF CYLINDRICAL
      ARC COLUMN FROM ALONG LINE OF SIGHT OF DIAMETER HAVING
      SPATIAL TEMPERATURE GRADIENT J
      REAL AA, BH, CC, LL, XX, GG, FF J
      START OF SEGMENT ***** 30
      REAL KK J
      INTEGER ARRAY PLOT(KTIOQMAX) J
      ARRAY KTIOQMAX(0:Z-1) J
      ARRAY KP, LN, PNUO, BEXP, HXNU, MINNU(0:QMAX, 0:ZZ) J
      INTEGER MAXN J
      LOGICAL PLOTTEST J
      REAL C1, C2, INTERP, A, H, C, C3, G J
      REAL NI J
      REAL YIN, Y, XMIN, XJ J
      INTEGER I, J, K, IMAX, JMAX, KMAX, N, NMAX J
      NMAX=Z-1 J
      JMAX=QMAX-1 J
      IMAX=Z+JMAX J
      KMAX=AX+JMAX J
      BEGIN
      REAL ARRAY FINU(0:NMAX) J
      START OF SEGMENT ***** 31
      REAL ARRAY LAMB(0:IOZU) J
      REAL UN J
      REAL PRESS J
      REAL ARRAY R (0:JMAX) J
      REAL ARRAY NT, NR, KAPPA, IB(0:IMAX) J
      REAL ARRAY DELTAU, TAU, VIB, DELINU, FINU(0:KMAX) J
      LABEL STARTA, EXITA J
      LABEL STARTSI
      REAL Q3, H J INTEGER IT J
      REAL Z J
      REAL T, TT, ZETA J
      REAL KUNT, H, J9 J
      REAL (HEADER, FARMAY, " FOR J=0 STEP 1 UNTIL JMAX DO NI(J) (EXITA) J
      FOR J=0 STEP 1 UNTIL JMAX DO T(J)=T(J+1) J
      WRITE (PRINT, FARMAY, " T= FOR J=0 STEP 1 UNTIL JMAX DO T(J)) J
      WRITE (PRINT, FARMAY, " RH= FOR J=0 STEP 1 UNTIL JMAX DO R(J)) J
      FOR J=0 STEP 1 UNTIL JMAX DO
      BEGIN COMMENT GENERATE NEW TEMP AND RADIUS TABLES J
      NT(2*J)=T(J) J
      NR(2*J)=R(J) J
      IF (2*J+1<IMAX THEN
      BEGIN
      A=R(J+1) J
      B=R(J) J
      C=A+B J
      INTERP=(.35KA+.75HR)/C J
      NT(2*J+1)=T(J)+(T(J+1)-T(J))*INTERP J
      NM(2*J+1)=.5NC J
      ENDO J
      ENDO OF GENERATING NEW TEMPERATURE AND RADIUS TABLES J
      WRITE (PRINT, FARMAY, " A=, FOR I=0 STEP 1 UNTIL IMAX DO NR(I)) J
      WRITE (PRINT, FARMAY, " A=, FOR I=0 STEP 1 UNTIL IMAX DO NT(I)) J
      C1= 1.470200E-24 J
      C2= 4.700320E-11 J
      PLOTTEST=FALSE J
      REAL (HEADER, FARMAY, " PRESS) J
      WRITE (PRINT, FARMAY, " PRESS=, PRESS) J
      REAL (HEADER, FARMAY, " T) J
      REAL (HEADER, FARMAY, " STARTA) J
      REAL (HEADER, FARMAY, " FOR I=0 STEP 1 UNTIL MAXN DO PLOT(KTIOQ(I))(STARTA) J
      PLOTTEST=TRUE J
      STARTA:
      BEGIN COMMENT DETERMINE KAPPA ARRAY FOR A GIVEN FREQUENCY THEN
      TAKE THIS ARRAY AND CALCULATE THE ARC RADIANT TRANSFER J
      REAL D1, C2, Q3 J
      START OF SEGMENT ***** 32
      REAL ARRAY Q1(0:100) J
      REAL Q4, Q5, Q6 J
      LABEL A10, CONTINUE J
      LABEL ASA J

```

APPENDIX D

WHITTAKER AND GAMMA FUNCTIONS - DESCRIPTION OF TWO ALGOL PROCEDURES

By G. Basi
Computer Sciences R & D

ABSTRACT

This report describes the development and testing of two computer algorithms WOG and GAMMAC required in connection with computation of spectral properties of plasma arcs being carried out for Dr. C. H. Church of Quantum Electronics R & D. The algorithm WOG computes the irregular Whittaker function $W_{\eta, \ell+1/2}$ for real positive non-integral η , and for ℓ a non-negative integer. GAMMAC computes the function $\Gamma(z)$ for z real or complex. A very good accuracy has been obtained from both of these algorithms. GAMMAC is used in WOG, which calculates one of the four confluent hypergeometric functions needed in the calculation of transitions between eigenstates described by the Coulomb wave functions.

```

SCHLUTEN(TT,50A)*(EXP(50A/C)-1)/EXP(BB/C)-1) ELSE
SCHLUTEN(TT,50B) )
KONT = (4.04*EXP(7*HNT(U)/(RB+1)*EXP(-(97834.4+66)/C)*
(1.4 + EXP(141/C) + ZETAN(EXP(BB/C)-1) ) + BB
( IF BB2 2.03495/3 THEN QB=17 + (2.59*2.93)*QB=17+
7.77*QB=22 ELSE 0 ) )*Q7 )
END OF KONT )
IF 345.001<KONT THEN BEGIN
Q0=50H(1000*U5/KONT-1) )
MAXNU(0,1)=95+AAAQ0 )
MINNU(0,1)=R3+AAAQ0 )
END ELSE BEGIN
MAXNU(0,1)=0 )
MINNU(0,1)=020 )
END )
END OF I LOOP )
END OF Q LOOP )
END )

32 IS 208 LONG. NEXT SEG 31

N=0 )
STANT91
FF=NUIN+1 )
FOR J=0 STEP 1 UNTIL Q=AR-1 OF
BEGIN
IT=ENTIER(J+X1+1)*T(Q/1000) )
IF IT 2222 THEN IT=222-1 )
Q3=Q3-1 )
M=ND(IT)/U(1) )
M=MM(INU(IT+1)/U(1)+1)/M+Q3 )
M=DEL(IT) )
GG=MM(DEL(IT+1)/M+Q3 )
C=AP5H1 )
QB=1-EXP(-FF/C) )
KK=7 )
FOR I=1 STEP 1 UNTIL 24 00
IF FF<MINNU(0,1) THEN
IF FF<MAXNU(0,1) THEN
BEGIN
QB=MINNU(0,1) )
LL=1/(FF+RB)/LW(U,1)=2+1 )
KK =KK +QB/8EXP(6.1)*KKP(6.1)=LL )
END OF I LOOP )
IF ATNUM=9A THEN
BEGIN
Q7=QB )
HU=FF )
TTQ= IF TQ>T(Q)5000 THEN 5000 ELSE IF TQ21600 THEN 14000 ELSE TQ )
ZETA = IF H515A THEN 1.1 ELSE IF RB2 50A THEN
SCHLUTEN(TT,50A)*(EXP(50A/C)-1)/(EXP(BB/C)-1) ELSE
SCHLUTEN(TT,50B) )
KONT = (4.04*EXP(7*HNT(U)/(RB+1)*EXP(-(97834.4+66)/C)*
(1.4 + EXP(141/C) + ZETAN(EXP(BB/C)-1) ) + BB
( IF BB2 2.03495/3 THEN QB=17 + (2.59*2.93)*QB=17+
7.77*QB=22 ELSE 0 ) )*Q7 )
END OF KONT )
KAPPA(0,1)=KONT )
END OF J LOOP )
IF PLOTTEST THEN FOR I=1 STEP 1 UNTIL MAXN 00
BEGIN
Q=PLTHT(I)=1 )
KT(J,N)=KAPPA(J) )
END )
FOR J=0 STEP 1 UNTIL J=AR 00
BEGIN COMMENT GENERATE NEW KAPPA TABLE )
NKAPPA(2HJ)=KAPPA(J) )
IF (2HJ+1)<IMAX THEN
BEGIN
INTERP=(.25*P(J+1)+.75*P(J))/(P(J+1)+P(J)) )
NKAPPA(2HJ+1)=KAPPA(J)+KAPPA(J+1)-KAPPA(J)*INTERP )
END )
END OF CALCULATING NEW KAPPA TABLE )
TAU(0)=0.01
FOR I=1 STEP 1 UNTIL I=AX 00
BEGIN COMMENT CALCULATION OF OPTICAL DEPTH )
A=TH(I) )
A=AP(I)=1 )
DELTAU(I)=NKAPPA(I-1)*(A+8)+(NKAPPA(I)-NKAPPA(I-1))*
(A+3/3-(A+2+4/3)*H+23/(A+8))*(A+R) )
TAU(I)=TAU(I-1)+DELTAU(I) )
END OF CALCULATING OPTICAL DEPTH )
IN=NUIN+1 )
LAMB(I)=A+LAMB(I-1) )
LAMB(I)=A+R*(1-B)=A*(6+.32R+20A/R,1/(1+A-B/8/(A+2))+255,A/(41+B/(A+2)
)) )
FOR J=0 STEP 1 UNTIL J=AX 00
BEGIN COMMENT CALCULATE BLACK BODY )
C3=(NUIN+3)*I=30 )
IB(2HJ)= C3*G1/(EXP(C2*NU(I)/T(J))-1) )
IF (2HJ+1)<IMAX THEN
BEGIN

```



```

REAL
PROCEDURE SIMPSON(A,H,X,Y,N)
COMMENT N MUST BE EVEN
VALUE A,H,X,Y
REAL A,H,X,Y
BEGIN
REAL U1,DX2,SUM2,SUM4,SUM6,SUM8
IF N MOD 2 = 0 THEN BEGIN
SUM2+S=SUM4;
X1=(H+1)/N;
DX2=(X2-X1)*H;
FOR X=X1 STEP DX2 UNTIL X2 DO
SUM2+S=SUM4;
FOR X=X1 STEP DX2 UNTIL X2 DO
SUM4+S=SUM6;
FOR X=X1 DO
SUM6+S=SUM8;
SIMPSON=(S+2*SUM2+4*SUM4+6*SUM6+8*SUM8)*H/3;
END ELSE
WRITE(PRINTER,"N IS NOT AN INTEGER  ",N);
END OF PROCEDURE SIMPSON;
REAL VOIV,OV,V,DTAU,UDIV,DU,U2,FF;
INTEGER I; HIDDEN TRY; LABEL EXIT6;
SAVE ARRAY SINV(0:4);
ALPHA ARRAY YALF(0:4),XALF(0:3),BC01(0:4),BC02(0:3);
ALPHA ARRAY BC03,BC04(0:3);
FILL YALF(0) WITH "SPECTRUMAL RADIANCY EMITTANCE",CE (AA);
"ITS/CM",P/CM;
FILL XALF(0) WITH "WAVELENGTH (", "ANGSTROMS ";
FILL BC01(0) WITH "TEMPERATURE (", " OF ", " K ";
FILL BC02(0) WITH
"MODIANT EXITANCE (", " WATTS/CM",P/CM;
FILL BC03(0) WITH "ARC DIAMETER (", " CM ";
FILL BC04(0) WITH "PRESSURE (", " ATM ";
VOIV=1;
OV=1.570795369/VOIV; V=OV*OV*OV*OV;
FOR I=0 STEP 1 UNTIL V-IV DO
SINV(I)=SINV(V+OV)*2;
TRY=TRUE;
IF PLOTTEST THEN FOR I=1 STEP 1 UNTIL NMAX DO
BEGIN
READ(READER,UDIV)EXIT6;
P=PLOTT(I)=1;
FOR N=0 STEP 1 UNTIL NMAX DO
BEGIN
TAU=AT(0,N)*U;
UDIV=ENTER(TAU),S;
IF UDIV MOD 2=0 THEN UDIV=UDIV+1;
IF UDIV<2 THEN UDIV=2;
FF=U(N);
C3=(FF+1)*10+30;
FINU(N)=C3/C1/(EXP(C2*FF/TAU))-1*(3.1415926530*H
* ( IF UDIV > 100 THEN 0 ELSE
SIMPSON(0,1,UDIV,SIMPSON(0,VOIV,V,FF*(TAU+U/(UDIV+U))
(1+2*SINV(V)),VOIV)=VOIV*1.570795369/VOIV)
*(FF+2)*H+1/2,99793;
END;
A=0;
FOR N=0 STEP 1 UNTIL NMAX DO
A=A+(FINU(N)+FINU(N+1))*LLAMR(N)/2;
WRITE(PRINTER,ARRAY,LLAMR(0),FOR N=0 STEP 1 UNTIL NMAX DO FINU(N));
WRITE(PRINTER,ARRAY," END OF FOR N=0 STEP 1 UNTIL NMAX DO FINU(N));
WRITE(PRINTER,"FLUX DUE TO THIS BAND PASS",E18,A,2,A);
A=ENTER(,A,20,LC(4));
A=A/(1+A);
X1S(0)=XALF(2)+LX+0,THIN+DX;
SCALE(FINU,NMAX+1,1,LY,THIN+DY);
X1S(0)=25+0,YALF(2)+LY+0,THIN+DY;
SYMBOL(1,LY,3,1,BC01(0,30);
NUMBER(2,6,LY,3,1,BC02(0,30);
SYMBOL(1,LY,3,1,BC02(0,45);
NUMBER(2,80,LY,3,1,BC03(0,4);
NUMBER(4,00,LY,3,1,BC04(0,0);

```

```

SC 311 45310
START OF SEGMENT ..... 38
SC 381 010
SC 381 010
SC 381 010
SC 381 010
SC 381 010
SC 381 010
START OF SEGMENT ..... 39
SC 391 010
SC 391 113
SC 391 312
SC 391 511
SC 391 813
SC 391 1413
SC 391 1612
SC 391 2212
SC 391 2811
SC 391 2911
SC 391 3110
SC 391 3413
SC 391 3813
40 IS 8 LONG, NEXT SEG 39
SC 391 3811
39 IS 42 LONG, NEXT SEG 38
SC 381 010
SC 381 010
SC 381 010
SC 381 113
SC 381 813
SC 381 1013
START OF SEGMENT ..... 41
SC 381 1212
41 IS 7 LONG, NEXT SEG 38
SC 381 1212
START OF SEGMENT ..... 42
42 IS 4 LONG, NEXT SEG 38
SC 381 1811
START OF SEGMENT ..... 43
43 IS 5 LONG, NEXT SEG 38
SC 381 1610
"J SC 381 1412
START OF SEGMENT ..... 44
SC 381 1713
44 IS 8 LONG, NEXT SEG 38

START OF SEGMENT ..... 45
45 IS 4 LONG, NEXT SEG 38
SC 381 1912
START OF SEGMENT ..... 46
46 IS 4 LONG, NEXT SEG 38
SC 381 2111
SC 381 2210
SC 381 2413
SC 381 2810
SC 381 3312
SC 381 3811
SC 381 3610
SC 381 3610
SC 381 4413
SC 381 4611
SC 381 4710
SC 381 4710
SC 381 4911
SC 381 4912
SC 381 4912
SC 381 4913
SC 381 4811
SC 381 4811
SC 381 7412
SC 381 4511
SC 381 4910
SC 381 0111
SC 381 2210
SC 381 2612
SC 381 1610
SC 381 12211
SC 381 11911
47 IS 10 LONG, NEXT SEG 38
SC 381 14711
SC 381 14010
SC 381 15311
SC 381 15611
SC 381 15911
SC 381 14212
SC 381 14512
SC 381 14811
SC 381 17111
SC 381 17113

```

```

SC 381 17811
SC 381 17911
SC 381 18113
SC 381 18413
SC 381 18711
SC 381 19011
SC 381 19211
SC 381 19412
SC 381 19510
38 IS 209 LONG, NEXT SEG 31
SC 311 45410
SC 311 45411
SC 311 45413
SC 311 45413
START OF SEGMENT ..... 48
SC 481 010
SC 481 511
SC 481 513
START OF SEGMENT ..... 49
SC 481 710
49 IS 5 LONG, NEXT SEG 48
SC 481 710
START OF SEGMENT ..... 50
50 IS 4 LONG, NEXT SEG 48
SC 481 513
START OF SEGMENT ..... 51
51 IS 5 LONG, NEXT SEG 46
SC 481 1012
SC 481 1111
SC 481 1210
SC 481 1210
SC 481 1510
SC 481 1612
SC 481 1810
SC 481 2212
SC 481 2512
SC 481 2813
SC 481 3113
SC 481 3412
SC 481 3712
SC 481 3912
SC 481 4113
48 IS 49 LONG, NEXT SEG 31
SC 311 45410
51 IS 459 LONG, NEXT SEG 30

```

```

START OF SEGMENT ..... SC 311 45413 48
SC ARI 010
SC ARI 511
SC ARI 513
START OF SEGMENT ..... 49
SC ARI 710
SC ARI 710
START OF SEGMENT ..... 50
50 IS 4 LONG, NEXT SEG 48
SC ARI 513
START OF SEGMENT ..... 51
51 IS 5 LONG, NEXT SEG 46
SC ARI 1012
SC ARI 1111
SC ARI 1210
SC ARI 1210
SC ARI 1510
SC ARI 1612
SC ARI 1810
SC ARI 2212
SC ARI 2512
SC ARI 2813
SC ARI 3113
SC ARI 3412
SC ARI 3712
SC ARI 3912
SC ARI 4113
48 IS 49 LONG, NEXT SEG 31
51 IS 459 LONG, NEXT SEG 30

```

```

START OF SEGMENT ..... SC 311 45413
                                AB
                                SC AB1 010
                                SC AB1 511
                                SC AB1 513
START OF SEGMENT ..... 49
                                SC AB1 710
                                SC AB1 710
START OF SEGMENT ..... 50
50 IS 4 LONG, NEXT SEG ..... SC AB1 513
                                SC AB1 51
                                SC AB1 1012
                                SC AB1 1111
                                SC AB1 1210
                                SC AB1 1210
                                SC AB1 1510
                                SC AB1 1612
                                SC AB1 1810
                                SC AB1 2212
                                SC AB1 2512
                                SC AB1 2813
                                SC AB1 3113
                                SC AB1 3412
                                SC AB1 3712
                                SC AB1 3912
                                SC AB1 4113
48 IS 49 LONG, NEXT SEG ..... SC 311 45410
31 IS 459 LONG, NEXT SEG ..... SC 311 45410

```

START OF	SEGMENT	SC	ABI	513
		SC	ABI	49
49 IS	5 LONG	SC	ABI	710
		SC	NEXT SEG	48
START OF	SEGMENT	SC	ABI	710
50 IS	4 LONG	SC	ABI	50
		SC	NEXT SEG	48
		SC	ABI	513
START OF	SEGMENT	SC	ABI	51
51 IS	5 LONG	SC	NEXT SEG	46
		SC	ABI	1012
		SC	ABI	1111
		SC	ABI	1210
		SC	ABI	1210
		SC	ABI	1510
		SC	ABI	1612
		SC	ABI	1810
		SC	ABI	2212
		SC	ABI	2512
		SC	ABI	2813
		SC	ABI	3113
		SC	ABI	3412
		SC	ABI	3712
		SC	ABI	3912
		SC	ABI	4113
48 IS	49 LONG	SC	NEXT SEG	31
		SC	ABI	45610
31 IS	459 LONG	SC	SFG	30

```

START OF          SC  ARI  710
50 IS            4 LONG, NEXT SEG  50
                                48
START OF          SC  ARI  513
51 IS            5 LONG, NEXT SEG  51
                                46
                                SC  ARI  1012
                                SC  ARI  1111
                                SC  ARI  1210
                                SC  ARI  1210
                                SC  ARI  1510
                                SC  ARI  1612
                                SC  ARI  1810
                                SC  ARI  2212
                                SC  ARI  2512
                                SC  ARI  2813
                                SC  ARI  3113
                                SC  ARI  3412
                                SC  ARI  3712
                                SC  ARI  3912
                                SC  ARI  4113
48 IS            49 LONG, NEXT SEG  31
                                SC 311 4510
31 IS            459 LONG, NEXT SEG  30

```

```

START OF SEGMENT ..... 51
51 IS 5 LONG NEXT SEG 46
      SC 481 1012
      SC 481 1111
      SC 481 1210
      SC 481 1210
      SC 481 1510
      SC 481 1612
      SC 481 1810
      SC 481 2212
      SC 481 2512
      SC 481 2813
      SC 481 3113
      SC 481 3412
      SC 481 3712
      SC 481 3912
      SC 481 4113
48 IS 49 LONG NEXT SEG 31
      SC 311 45610
31 IS 459 LONG NEXT SEG 30

```

40 15 49 LONG. SC 411 4113
NEXT SEG 31
SC 311 45010
31 15 459 LONG. NEXT SEG 30

```

30 15 21 LONG, SC 31 1A10
27 15 260 LONG, NEXT SEG 27
SC 31 1A10
SC 31 1A11
3 15 93 LONG, NEXT SEG 2
SC 21 110
2 15 5 LONG, NEXT SEG 1

```

```

30 15 21 LONG, SC 31 1A10
27 15 260 LONG, NEXT SEG 27
SC 31 1A10
SC 31 1A11
3 15 93 LONG, NEXT SEG 2
SC 21 110
2 15 5 LONG, NEXT SEG 1

```

```

3 15 93 LONG. NEXT SEG 2
      SC 31 4011
2 15 5 LONG. NEXT SEG 1
      SC 21 110

```

```

          SC 301 1A10
30 IS    21 LONG, NEXT SEG      27
27 IS    260 LONG, NEXT SFG     3
          SC 31  A810
          SC 31  A211
3 IS     93 LONG, NEXT SEG       2
          SC 21  110
2 IS     5 LONG, NEXT SFG        1

```

```

          SC 301 1A10
30 IS    21 LONG, NEXT SEG      27
27 IS    260 LONG, NEXT SFG     3
          SC 31  A810
          SC 31  A211
3 IS     93 LONG, NEXT SEG       2
          SC 21  110
2 IS     5 LONG, NEXT SFG        1

```

APPENDIX D

WHITTAKER AND GAMMA FUNCTIONS - DESCRIPTION OF TWO ALGOL PROCEDURES

By G. Basi
Computer Sciences R & D

ABSTRACT

This report describes the development and testing of two computer algorithms WOG and GAMMAC required in connection with computation of spectral properties of plasma arcs being carried out for Dr. C. H. Church of Quantum Electronics R & D. The algorithm WOG computes the irregular Whittaker function $W_{\eta, l+1/2}$ for real positive non-integral η , and for l a non-negative integer. GAMMAC computes the function $\Gamma(z)$ for z real or complex. A very good accuracy has been obtained from both of these algorithms. GAMMAC is used in WOG, which calculates one of the four confluent hypergeometric functions needed in the calculation of transitions between eigenstates described by the Coulomb wave functions.

Summary

This report describes the development and testing of two computer algorithms WOG and GAMMAC required in connection with computation of spectral properties of plasma arcs being carried out for Dr. C. H. Church of Quantum Electronics R & D. The algorithm WOG computes the irregular Whittaker function $W_{\eta, \lambda+1/2}$ for real positive non-integral η , and for λ a non-negative integer. GAMMAC computes the function $\rho(z)$ for z real or complex. A very good accuracy has been obtained from both of these algorithms. GAMMAC is used in WOG, which calculates one of the four confluent hypergeometric functions needed in the calculation of transitions between eigenstates described by the Coulomb wave functions.

Introduction

Purpose of this study was to translate two subroutines WOG and GAMMAC from fortran into Algol and improve upon them. As received neither of the subroutines were in usable form, and considerable revision has been necessary. These algorithms will be used in a program to calculate the transitions between the eigenstates described by the Coulomb wave function.

The calculation of the transitions involves the use of confluent hypergeometric functions. Two of the four confluent hypergeometric functions are the solutions to Kummer's equation¹

$$x \frac{d^2 y}{dx^2} + (b-x) \frac{dy}{dx} - ay = 0.$$

The two solutions of the above are Kummer's functions ${}_1F_1(a; b; x)$ and $U(a; b; x)$ defined as follows:

$$y = {}_1F_1(a; b; x) = \sum_{n=0}^{\infty} \frac{(a)_n}{(b)_n} \frac{x^n}{n!}$$

Where $(a)_n = a(a+1) \dots (a+n-1)$ for $n \geq 1$ and $(a)_0 = 1$

$(b)_n$ is similarly defined.

$$y = U(a; b; x) = \frac{\pi}{\sin \pi b} \left\{ \frac{{}_1F_1(a; b; x)}{\Gamma(1+a-b)\Gamma(b)} - \frac{x^{1-b} {}_1F_1(1+a-b; 2-b; x)}{\Gamma(a)\Gamma(2-b)} \right\}.$$

The other two confluent hypergeometric functions are the solutions to Whittaker's equation²

$$\frac{d^2 y}{dz^2} + \left(-\frac{1}{4} + \frac{\eta}{z} - \frac{\ell^2 + \ell}{z^2} \right) y = 0.$$

Two solutions are Whittaker's functions $M_{\eta, \ell+1/2}(z)$ and $W_{\eta, \ell+1/2}(z)$. Whittaker's functions are defined as follows:

$$M_{\eta, \ell+1/2}(z) = z^{\ell+1} e^{-1/2z} {}_1F_1(\ell+1-\eta; 2\ell+2; z).$$

$$W_{\eta, \ell+1/2}(z) = \frac{\pi}{\sin(2\ell+1)\pi} \left[\frac{-M_{\eta, \ell+1/2}(z)}{\Gamma(-\ell-\eta)\Gamma(2\ell+2)} + \frac{M_{\eta, -(\ell+1/2)}(z)}{\Gamma(\ell+1-\eta)\Gamma(-2\ell)} \right]$$

1.1 Available programs

Two programs that calculate the generalized hypergeometric function

$${}_pF_q(a_1, a_2, \dots, a_p; b_1, b_2, \dots, b_q; z)$$
 are available in Algol B5000.

These programs were written by Hammers³. One of these two programs computes a general hypergeometric function which has a complex or real argument and any number of real parameters. The other program computes the same function for any number of real or complex parameters.

There are three programs called BEAUTY, BEAST, and CHIC in Fortran II. These programs were written by Johnson and Sangren⁴ and calculate any generalized hypergeometric functions. Program BEAUTY can be used to calculate any generalized hypergeometric function with up to ten numerator and ten denominator parameters and one argument. Program BEAST can be used to compute analytical continuation of an ordinary hypergeometric function. The program called CHIC can be used for calculating 3^4 distinct hypergeometric series in two variables.

Two other programs WOG and HLIGAM are obtained from McGuire⁵. Both these programs were obtained in Fortran. Program WOG calculates the irregular Whittaker function $W_{\eta, \ell+1/2}(z)$ for $\eta > 0$, real, and non-integral. Program HLIGAM calculates the same function where η is a pure imaginary number.

Both of these programs call for another program--GAMMAC-- which calculates the function $\Gamma(z)$ for any z real or complex. GAMMAC was obtained in Fortran from Dr. McGuire.

2. Computation of GAMMAC

Procedure GAMMAC computes the value of $\Gamma(z)$ in the following way:

Let $z = (x, y)$ {i.e. $z = x+iy$ }. The notation $z_i = (x_i, y_i)$ will be used during the discussion and shall be understood for $i = 1, 2, 3, 4$. \bar{z} will denote the complex conjugate of any complex number z .

For positive real integral values of z , $\Gamma(z)$ is computed as $(z-1)!$, for non-positive real integral values of z , the procedure does not work.

If $x < 0$, then the procedure uses the following recurrence relation to relate $\Gamma(z)$ to $\Gamma(z_1)$ where the real part of z_1 is positive.

$$\Gamma(z) = \frac{1}{z} \Gamma(z+1)$$

or

$$\Gamma(x, y) = \frac{1}{\Gamma(\bar{x}, \bar{y})} \Gamma(x+1, y).$$

Now if y_1 (which is the same as y), in z_1 is negative, the $\Gamma(z_1)$ is related to $\Gamma(z_2)$, where y_2 is positive, by the following relation

$$\Gamma(z_1) = \overline{\Gamma(\bar{z}_1)} = \overline{\Gamma(z_2)}$$

$$\text{i.e. } z_2 = \bar{z}_1, \text{ or } y_2 = -y_1 \text{ and } x_2 = x_1$$

with the use of the above relations the computation of $\Gamma(z)$ for general z reduces to the computation of $\Gamma(z_2)$ whose both real and imaginary parts are positive.

The next step is to relate $\Gamma(z_2)$ with $\Gamma(z_3)$ where $0 \leq y_3 < 1$. This is done by making use of Gauss' multiplication theorem. Gauss' multiplication theorem asserts that if $z_2 = nz_3$ where n is an integer then

$$\Gamma(z_2) = \frac{\Gamma(z_3)\Gamma(z_3+\frac{1}{n})\Gamma(z_3+\frac{2}{n}) \dots \Gamma(z_3+\frac{n-1}{n})}{(2\pi)^{\frac{1}{2}} \frac{(n-1)!}{n^{\frac{1}{2}} - z_2}}$$

In our case integer n is chosen to be the next greater integer than y_2 so that $y_2/n = y_3 < 1$. Next we relate $\Gamma(z_3)$ to $\Gamma(z_4)$ where z_4 is such that both x_4 and y_4 satisfy the inequalities $0 < x_4 \leq 1$, $0 \leq y_4 < 1$. In fact $y_4 = y_3$ and $x_4 = x_3 - [x_3]$ in case x_3 is a nonintegral real and if x_3 is an integer $x_4 = 1$, where $[x_3]$ is greatest integer contained in x_3 . The relation between $\Gamma(x_3)$ and $\Gamma(z_4)$ can conveniently be expressed as follows.

$$\Gamma(x_3) = (z_3-1)(z_3-2)(z_3-3) \dots (z_4)\Gamma(z_4)$$

Now the computation of $\Gamma(z)$ for any complex number z has been related to $\Gamma(z_4)$ where z_4 is such that $0 < x_4 \leq 1$, $0 \leq y_4 < 1$. $\Gamma(z_4)$ is determined by the Padé power approximation of $1/\Gamma(z)$.

The procedure GAMMAC was obtained in Fortran and has been translated into Algol. Some changes were made during the translation to make the program

more efficient and clear. A basic constant was defined to greater accuracy to reduce the error. At present it is as discussed above, and calculates the function $\Gamma(z)$ for z real or complex. The values were checked against the available tables and found to be accurate to eight significant figures in the region

$$x = -2.0 (.25) \quad 2.0$$

$$y = -2.0 (.25) - 2.5 \quad \text{and}$$

$$y = .25 (.25) \quad 2.0$$

3. Computation of Irregular Whittaker Function $W_{\eta, \ell+1/2}(z)$ for η real, positive and non-integral.

Program WOG calculates the irregular Whittaker function $W_{\eta, \ell+1/2}(z)$ for η real, positive and non-integral. The function is $\frac{W_{\eta, \ell+1/2}(z)}{\Gamma(\eta+\ell+1)}$ computed by two different expressions for smaller and larger values of $2R/\eta$ where $2R/\eta = z$. The expression used to compute the function for small values of z is given by Hartree⁶ and is as follows.

$$\begin{aligned}
 (-)^{\ell+1} \frac{W_{\eta, \ell+1/2}(z)}{\eta^{\ell} \Gamma(\eta-\ell)} &= \frac{\sin \pi \eta}{\pi} e^{-1/2z} (\eta z)^{-\ell} \\
 &\quad \left[- \sum_{m=0}^{2\ell} \frac{\Gamma(\eta+\ell+1)}{\Gamma(\eta+\ell+1-m)} \frac{(2\ell-m)!}{m!} z^m \right. \\
 &\quad \left. + \sum_{m=2\ell+1}^{\infty} (-)^{m-1} \frac{\Gamma(\eta+\ell+1)}{\Gamma(\eta+\ell+1-m)} \frac{z^m}{m!(m-2\ell-1)!} \right. \\
 &\quad \left. \left[\log z + \pi \cot \pi \eta + \psi(\eta+\ell+1-m) - \psi(m+1) - \psi(m-2\ell) \right] \right] \quad (1)
 \end{aligned}$$

Some important aspects of the evaluation of this expression are worth mentioning. Computation of the multiplying factor makes use of the identity

$$\frac{1}{\eta^{2\ell+1}} \frac{\Gamma(\eta+\ell+1)}{\Gamma(\eta-\ell)} = \prod_{k=1}^{\ell} \left\{ 1 - \left(\frac{k}{\eta} \right)^2 \right\} \quad (A2)$$

In computing the finite sum in Equation (1), use is made of the identity

$$\prod_{k=1}^m \left[\frac{(\eta+\ell+1-k)}{k(2\ell+1-k)} \left(\frac{2R}{\eta} \right) \right] = \frac{\Gamma(\eta+\ell+1)}{\Gamma(\eta+\ell+1-m)} \frac{(2\ell-m)!}{m!(2\ell)!} z^m \quad (A5)$$

In summing the infinite series in Equation (1) the summation parameter is transformed by $k = m - 2\ell - 1$ where k goes from 0 to ∞ . The term when $k = 0$ is obtained separately. The expression containing ψ functions is computed in three different ways depending upon the value of η . In case $\eta < \ell$ and $\eta < 60$ the identities

$$\psi(n) = -\gamma + \sum_{k=1}^{n-1} \frac{1}{k} \quad (n \geq 2) \quad (2)$$

$$\psi(1+z) = -\gamma + \sum_{k=1}^{\infty} \frac{z}{k(k+z)} \quad z \neq -1, -2, -3, \dots \quad (3)$$

$$\psi(1-z) = \psi(z) + \pi \cot \pi z \quad (4)$$

are used. If $\ell < \eta < 60$ the following additional relation is used,

$$\psi(n+z) = \frac{1}{(n-1)+z} + \frac{1}{(n-2)+z} + \dots + \frac{1}{z} + \psi(z) \quad (5)$$

In the case $\eta > 60$ the asymptotic expansion of the ψ function is used,

$$\psi(z) \sim \ln(z) - \frac{1}{2z} - \frac{1}{12z^2} + \frac{1}{120z^4} - \frac{1}{252z^6} + \dots$$

$$(z \rightarrow \infty \text{ in } |\arg z| < \pi). \quad (6)$$

When the argument z of the Whittaker function is large, the asymptotic expansion is used for the computation in place of Equation (1). This expansion is given by Whittaker and Watson⁸.

$$W_{\eta, \ell+1/2}(z) \sim e^{-\frac{1}{2}z} z^{\eta} \left\{ 1 + \sum_{n=1}^{\infty} \frac{\left\{ \frac{(\ell+1/2)^2 - (\eta-1/2)^2}{\eta!} \right\} \left\{ \frac{(\ell+1/2)^2 - (\eta-3/2)^2}{2^{\eta}} \right\} \dots}{\left\{ \frac{(\ell+1/2)^2 - (\eta-n+1/2)^2}{n!} \right\} z^n} \right\} \quad (7)$$

Some test runs with McGuire's program gave results of rather low accuracy--two or three significant figures, and some steps were taken to improve this. The major source of error appeared to be the summation for the ψ function in Equation (3), which is slowly convergent. McGuire truncated this summation at 50 terms. We have summed greater numbers of terms and also introduced a correction for the remainder term by consideration of the integral

$$\int_{x_0}^{\infty} \frac{dx}{x(x-a)} = \frac{1}{a} \ln \left(\frac{x_0}{x_0-a} \right)$$

By approximating to the integral in two different ways, we determine the error bounds for the remainder

$$\frac{1}{a} \ln \left| \frac{N-1}{N-1-a} \right| - \frac{1}{2(N-1)(N-1-a)} < \sum_{j=N}^{\infty} \frac{1}{j(j-a)} < \frac{1}{a} \ln \left| \frac{N-1/2}{N-1/2-a} \right|$$

The remainder term is approximated by the mean of the two bounds and good accuracy is obtained by taking $N = 1001$. In the case of the infinite sum involved

in (1), the series was being truncated when the term became less than 10^{-3} of the sum. In the modified version, the summation is truncated when the term becomes smaller than 10^{-8} of the sum and when at least 10 terms have been summed.

In computing the asymptotic expansion of Whittaker's function, the number of terms summed by McGuire was the greatest integer contained in $l + \eta$. The reason for this choice is not clear and it was found that improvement could be obtained by summing up to, but excluding, the smallest term (normal procedure with an asymptotic series). This method was, therefore, adopted.

With these modifications, a considerable increase in accuracy has been obtained, at the expense of some increase in computer time. Tables of the Whittaker's irregular function were not available. For checking the accuracy of the results Coulomb tables⁷ were used. Coulomb tables list the functions $P_l(\frac{1}{\eta^2}, R)$ and $Q_l(\frac{1}{\eta^2}, R)$. The relation between Whittaker's function and the functions $P_l(\frac{1}{\eta^2}, R)$ and $Q_l(\frac{1}{\eta^2}, R)$ is given by the equation

$$W_{\eta, l+\frac{1}{2}}\left(\frac{2R}{\eta}\right) = \frac{\left(\frac{-2}{i}\right)^{l+1} \Gamma(l+\eta+1)}{(2l+1)!} \left\{ Q_l\left(\frac{1}{\eta^2}, R\right) \sin \pi \eta + P_l\left(\frac{1}{\eta^2}, R\right) \cos \pi \eta \right\}$$

The results of the program have been found to agree with the results obtained by using the tabulated values to six or more significant figures for the ranges $l = 0, 1, 2, 1/\eta^2 = -2.0(.2)-.2, z = .5(.5)4.0$. From results obtained in these ranges, it appeared appropriate to switch the computation from the series (1) to the asymptotic form (7) at the value $z = 9$.

Our next step in the project of writing a computer program for the calculation of transitions between eigenstates will be to check the results for the other program called HLIGAM against the available Coulomb tables and make the possible changes if necessary to improve its accuracy. Procedure HLIGAM calculates the function

$$\frac{(i\eta)^{l+1}}{\Gamma(l+1+i\eta)} W_{i\eta, l+1/2} \left(\frac{2R}{i\eta} \right)$$

for $i\eta$ a pure imaginary number. Then both of these functions (one calculated by WOG and the other by HLIGAM) will be integrated to determine the transitions probabilities. The result of integration will be checked against the tables given by Peach⁹.

References

1. L. J. Slater, Confluent Hypergeometric Functions, Cambridge University Press P. 2. (1960).
2. L. J. Slater, Confluent Hypergeometric Functions, Cambridge University Press P. 9. (1960).
3. R. R. Hammers, "Technical Bulletin, Mathematical report series MRS-133. Burroughs Corporation, February 21, 1961.
4. M. L. Johnson and W. Sangren. Technical reports, GA-1704, GA-1543, GA-2739 General Atomic, Division of General Dynamic Corporation, September 6, 1960, October 10, 1960, and December 1, 1961.
5. Dr. E. J. McGuire. Through private communication. Radiation Phenomena Division 5242, Sandia Corp. Albuquerque, New Mexico.
6. Dr. D. R. Hartree, Proc. Camb. Phil. Soc. V. 24, P. 426 (1928).
7. M. Abramowitz and I. A. Stegun, Handbook of Mathematical Functions, AMS 55. National Bureau of Standards, June 1964.
8. E. T. Whittaker and G. N. Watson, A Course of Modern Analysis, Cambridge University, Press. Fourth Edition P. 343 (1952).
9. G. Peach "A Revised General Formula for the Calculation of Atomic Photoionization Cross-sections", Private Communication (to be published in Memoirs of the R.A.S.).

Appendix Program Usage

A1. GAMMAC (x,y,u,v); An algol procedure to compute $\Gamma(z)$ for real or complex values of the argument z.

Procedure GAMMAC (x,y,u,v) computes the function $\Gamma(z)$ for any argument z, real or complex. This procedure can be included in any main program by including the following two cards in the programme declarations

\$\$ A GAMMAC

COMMENT HIGHER SEQUENCE CARD;

Both the cards must have some sequence number in the column 73-80. and the sequence number on the comment card must be higher than that on the \$\$ A GAMMAC card. The formal parameters x and y are the input parameters. x and y are both real and respectively are the real and imaginary part of the complex number z, whose gamma function is required. u and v are the output parameters and respectively are the real and imaginary parts of the complex number $\Gamma(z)$.

For example if one wants to calculate $\Gamma(z_i)$ and store the value at z_2 where $z_i = (x_i, y_i)$ for $i = 1, 2$, are complex numbers then one would do so by including a card, at the desired place, in the main program with the following information on it.

GAMMAC (x₁,y₁,x₂,y₂);

Either one or both of the input parameters x and y can be real valued arithmetic expressions. There is no loss of efficiency caused by using the expression as an actual input parameter since it is called by value.

Limitations. The procedure has the following limitations.

For the non-positive integral values of the argument an error message of divide by zero would occur since the gamma function is singular at such points. For the rest of the negative real values of the argument procedure calculates $\Gamma(z)$ except very close to the negative integers where an exponent overflow message would occur. For positive real values of the argument procedure computes $\Gamma(z)$ for $z \leq 53.3$. For larger values of z an error message of exponent overflow occurs. For very small values of z ($z < 8.758 \times 10^{-47}$) an error message of divide by zero occurs since computer sets such numbers to zero.

For pure imaginary argument $|z| > 66$, the value of $|\Gamma(z)|$ is so small that it is set to zero by the computer.

For $z = a$ a complex number on the diagonal $x = y$ or $x = -y$ and $x > 0$. While computing $\Gamma(z)$ of z such that $x > 42.00$ an error message of maximum argument of exponent would occur. On the diagonals $x = y$ and $x = -y$ for $x < 0$ the value of $\Gamma(z)$ is so small for $x < -22.60$ that it is set to zero by the computer.

A2. WOG (L, ETA, R, W); An algol procedure to compute the irregular

Whittaker function $\frac{W_{n, \ell+1/2}(\frac{2R}{n})}{\Gamma(n+\ell+1)}$

The procedure WOG(L,ETA,R,W) calculates the function

$$\frac{W_{n, \ell+1/2}(\frac{2R}{n})}{\Gamma(n+\ell+1)}$$

A deck of cards for this procedure, to be included in the main program, may be obtained from the writer. The formal parameters L, ETA and R correspond to the variables ℓ , n and R in the Whittaker function $W_{n, \ell+1/2}(\frac{2R}{n})$. Either one or any number of these input variables L, ETA, and R can be a real valued arithmetic expression. There is no loss of efficiency caused by using an expression as an actual parameter since it is called by value. W is the output parameter, which has the value of the function $\frac{W_{n, \ell+1/2}(\frac{2R}{n})}{\Gamma(n+\ell+1)}$ as computed by the procedure.

One of the infinite series involved in computation is a function of ℓ and n but not R . This summation is the most time-consuming part of the computation. To increase efficiency when successive values of W are to be calculated with constant ℓ and n , varying R , the procedure has been written so that this particular sum is preserved between calls. It is recomputed only when either ℓ or n changes. Therefore it is recommended that the user arrange his program so that consecutive calls on the procedure WOG are made, as far as possible, with constant ℓ and n (i.e. variation of R should be the innermost loop).

Limitations. This procedure is limited to the real values of R , to n positive and nonintegral, and to ℓ integral only.

1513A107 FRIDAY, APRIL 13, 1967

HRL ALGOL VERSION OF 10/20/66

BEGIN

COMMENT THIS PROGRAM IS WRITTEN ONLY TO TEST THE ACCURACY OF THE
PROCEDURE GAMMAC. PROCEDURE GAMMAC CALCULATES THE GAMMA FUNCTION
OF A REAL OR COMPLEX ARGUMENT Z. LN (GAMMAC(Z)) IS CALCULATED IN
THE MAIN PROGRAM AND THE VALUES ARE COMPARED WITH THE VALUES OF
LN (GAMMAC(Z)) TABULATED IN HANDBOOK OF MATHEMATICAL FUNCTIONS, AMS 55
G. S. PASTI

FILE IN READER (2,100)

FILE OUT PRINTER 4(2,150)

INTEGER N, J

REAL X, Y, U, V, I

REAL FI, FII, IMAGI

REAL ARHY, YI(0:20)

FORMAT M1 (25, 'X', 15, 'Y', 15, 'X', 15, 'COMPUTED VALUES OF LN(GAMMAC(X,Y))',

X17, 'TABULATED VALUES OF LN(GAMMAC(X,Y))',

FORMAT M2 (X12, 2(X4, 'REAL', X19, 'IMAGINARY', A6))

FORMAT F1 (X2, F15.1, A23.11)

PROCEDURE GAMMA2(X,Y,U,V)

VALUE F, FI

REAL X,Y,U,V

BEGIN

COMMENT THIS PROCEDURE CALCULATES GAMMA(X+iy) WHERE X AND Y ARE

NOT GREATER THAN ONE BY PART POWER APPROXIMATION OF 1/GAMMA(Z)

LOCAL ARRAY A*(0:12) I

INTEGER I

REAL F, FII, G, GII, C, CII

FILL A(0) WITH 0.0, 1.2576302988, 6.22981244014-2,

-1.9367839704-1, 9.5294089018-3, 1.00216777428-2,

-1.74492402174-3, 7.90276356030-5)

FILL A(1) WITH 0.1, 6.76414434940-1, 3.27735074448-1,

1.02799945280-1, 2.70185045388-2, 5.10472682470-3,

8.75219954480-4, 9.51291440838-5, 7.0428024108-6)

I = A(0)*X*(8)

F = A(1)*Y*(1)

G = A(2)*X*(4)*(8)

H = A(3)*Y*(1)

FOR I=7 STEP 1 UNTIL 1 DO

BEGIN

R = EXX*FXYI

F = EXX*FXYI

E = F*(1)

G = GXY*HXYI

H = GXY*HXYI

G = G*(1)

END

H = E*(2)*F(2)

U = (GXY*HXYI)/H

V = (EHX*GXYI)/H

END

PROCEDURE GAMMA1(X,Y,U,V)

VALUE F, FI

REAL X,Y,U,V

BEGIN

COMMENT TO CALCULATE GAMMA(X+iy), WHERE X IS POSITIVE AND Y IS

LESS THAN 1

INTEGER N, J

N = 1

LABEL EXIT

IF N=1 THEN BEGIN

GAMMA2(X,Y,U,V)

GO TO EXIT END

N = ENTIER (X)

X = X-N

IF X=0 THEN BEGIN

A = 1-X*(1) END

GAMMA2(X,Y,U,V)

N = N-1

FOR J = 0 STEP 1 UNTIL N DO

BEGIN

P = (X+J)*U-V

V = (X+J)*V+Y*U

U = P

END

START OF SEGMENT 0002

SC 21 010

SC 21 010

SC 21 010

SC 21 010

SC 21 010

SC 21 010

SC 21 010

SC 21 010

SC 21 010

SC 21 010

SC 21 010

SC 21 010

SC 21 010

SC 21 010

SC 21 010

SC 21 010

SC 21 010

SC 21 010

SC 21 010

SC 21 010

SC 21 010

SC 21 010

SC 21 010

SC 21 010

SC 21 010

SC 21 010

SC 21 010

SC 21 010

SC 21 010

SC 21 010

SC 21 010

SC 21 010

SC 21 010

SC 21 010

SC 21 010

SC 21 010

SC 21 010

SC 21 010

SC 21 010

SC 21 010

SC 21 010

SC 21 010

SC 21 010

SC 21 010

SC 21 010

SC 21 010

SC 21 010

SC 21 010

SC 21 010

SC 21 010

SC 21 010

SC 21 010

SC 21 010

SC 21 010

SC 21 010

SC 21 010

SC 21 010

SC 21 010

SC 21 010

SC 21 010

SC 21 010

SC 21 010

SC 21 010

SC 21 010

SC 21 010

SC 21 010

SC 21 010

SC 21 010

SC 21 010

SC 21 010

SC 21 010

SC 21 010

SC 21 010

SC 21 010

SC 21 010

SC 21 010

SC 21 010

SC 21 010

SC 21 010

SC 21 010

SC 21 010

SC 21 010

SC 21 010

COMPUTED VALUES OF LNC GAMMA(X,Y)

REAL		IMAGINARY	
1.0	1.0	-1.159312281644+00	-1.15447042888+01
1.0	5.0	-1.15117524004+00	-1.145121177470+00
1.1	7.0	-2.2001337334+00	1.433455134030+00
1.1	9.0	-1.24435204033+00	4.74271191718+01
1.2	2.0	-2.2317558815+00	7.15112333490+01
1.2	6.0	-7.4311657023+00	2.41914117580+01
1.3	3.0	-1.1721184145+00	1.49270187588+00
1.3	4.0	-5.1637357470+00	-2.15540456748+00
1.4	1.0	-1.1373352710+00	1.44255131781+01
1.4	8.0	-0.2784.34426+00	-2.46230268416+00
1.5	2.0	-1.9542400140+00	1.084076334370+00
1.5	4.0	-1.9172003199+00	3.00207621034+00
1.6	6.0	-2.5112651048+00	2.3741306+07+00
1.7	8.0	-7.1876529449+00	4.37237944440+01
1.7	1.0	-0.72432846004+00	-1.07016177055+00
1.8	1.0	-0.1443081617+00	-2.13014031435+00
1.8	1.0	-0.7511354670+00	7.2977222530+01
1.9	7.0	-1.121700+07+00	1.405117115340+00
1.9	8.0	-7.0124455178+00	2.79942110805+00
1.9	9.0	-0.4542912301+00	-1.1571418473+01

TABULATED VALUES OF LNC GAMMA(X,Y)

REAL		IMAGINARY	
1.1	1.1	-1.159312281644+00	-1.15447042888+01
1.1	5.1	-1.15117524004+00	-1.145121177470+00
1.1	9.1	-2.2001337334+00	1.433455134030+00
1.2	2.1	-1.24435204033+00	4.74271191718+01
1.2	6.1	-7.4311657023+00	2.41914117580+01
1.3	3.1	-1.1721184145+00	1.49270187588+00
1.3	4.1	-5.1637357470+00	-2.15540456748+00
1.4	1.1	-1.1373352710+00	1.44255131781+01
1.4	8.1	-0.2784.34426+00	-2.46230268416+00
1.5	2.1	-1.9542400140+00	1.084076334370+00
1.5	4.1	-1.9172003199+00	3.00207621034+00
1.6	6.1	-2.5112651048+00	2.3741306+07+00
1.7	8.1	-7.1876529449+00	4.37237944440+01
1.7	1.1	-0.72432846004+00	-1.07016177055+00
1.8	1.1	-0.1443081617+00	-2.13014031435+00
1.8	1.1	-0.7511354670+00	7.2977222530+01
1.9	7.1	-1.121700+07+00	1.405117115340+00
1.9	8.1	-7.0124455178+00	2.79942110805+00
1.9	9.1	-0.4542912301+00	-1.1571418473+01

LABEL 000000000-115000101042 COMPILE 64-44457/4001

0010014 GAMMA

APPENDIX E

RADIATIVE TRANSPORT IN A XENON ARC

by

B. W. Swanson

I. INTRODUCTION

The problem of interest has been to determine the steady state temperature profile in a Xenon arc, which requires a solution of the energy equation

$$\frac{\partial^2 S}{\partial r^2} + \frac{1}{r} \frac{\partial S}{\partial r} - \vec{\nabla} \cdot \vec{F} + \sigma(P, S)E^2 = 0 \quad (1)$$

where $\vec{F}(r)$ is the radiative flux vector, T the plasma temperature, σ the electrical conductivity, P the pressure and E the electric field. The Schmitz function S is defined by the equation

$$S(T) = \int_{TW}^T K(T) dT \quad (2)$$

and the divergence of F is given by

$$\vec{\nabla} \cdot \vec{F} = \frac{dF}{dr} + \frac{F}{r} \quad (3)$$

where the radiative flux F is found from the equation

$$F(r) = \int_0^\infty \int_{\omega=4\pi} I_\lambda(r, \vec{\omega}) \vec{\omega} d\omega d\lambda \quad (4)$$

In equation 4, $\vec{\omega}$ is a unit direction vector and $I_\lambda(r, \vec{\omega})$ is the monochromatic intensity of radiation.

The first phase of this program consisted of writing a computer program for calculating the radiative flux¹, which can be expressed as

$$F(r) = -4 \int_{\lambda_{\min}}^{\lambda_{\max}} \int_0^{\pi} \int_0^{R_M(\phi)} K_{\lambda}(s) B_{\lambda}(s) G_1[B_{\lambda}(s)] \cos \phi \, ds d\phi d\lambda \quad (5)$$

In equation 5, $K_{\lambda}(T)$ is the spectral absorptivity, λ_{\min} and λ_{\max} the wavelength band of interest, B_{λ} is the Planck function, $B_{\lambda} \equiv \int_0^s K_{\lambda}(\zeta) d\zeta$ and the function G is given by

$$G_n(x) = \int_0^{\frac{\pi}{2}} \frac{e^{-\frac{x}{\sin \theta}}}{(\sin \theta)^n} d\theta \quad (6)$$

and accounts for the attenuation of radiation by self absorption. The geometry for the evaluation of equation 5 is shown in figure 1.

Since the numerical evaluation of the triple flux integral is expensive the second phase of the program sought a faster flux approximation method. An analysis was made which permitted an a priori integration with respect to wavelength to reduce computation time. The approximate flux integral is given² by the equation

$$\hat{F}(r) = -4 \int_0^{\pi} \int_0^{R_M(\phi)} K_a(s) B(s) G_1 \left[\int_s^{R_M(\phi)} K_a(\zeta) d\zeta \right] \cos \phi \, ds d\phi \quad (7)$$

where

$$B(s) = \int_{\lambda_1}^{\lambda_2} B_{\lambda}[T(s)] d\lambda \quad (8)$$

and the mean absorption coefficient $K_a(s)$ is defined by the equation

$$K_a(s) = \left[\frac{b}{b + \tau_p(s)} \right] \left[\frac{b + \tau_R(s)}{b + \tau_p(s)} \right] K_p(s) + \left[\frac{\tau_p(s)}{b + \tau_p(s)} \right] K_R(s) \quad (9)$$

The term b is a constant of the order of unity which can be varied to improve the approximation. The terms τ_R and τ_p are the Rosseland and Planck optical lengths along the ray from point M to point R in figure 1 and are given by

$$\tau_R(s) = \int_0^s K_R(\zeta) d\zeta \quad (10)$$

$$\tau_p(s) = \int_0^s K_p(\zeta) d\zeta$$

where the Planck and Rosseland absorption coefficients are given by

$$K_p(T) = \int_{\lambda_1}^{\lambda_2} \frac{K_\lambda(T) B_\lambda(T) d\lambda}{B(T)} \quad (11)$$

$$K_R(T) = \frac{-1}{\int_{\lambda_1}^{\lambda_2} \frac{1}{K_\lambda(T)} \frac{dB_\lambda}{dT} d\lambda} \frac{dB}{dT}$$

and

$$B(T) = \int_{\lambda_1}^{\lambda_2} B_\lambda(T) d\lambda \quad (12)$$

The form of the approximation is such that under optically thin conditions when τ_p and τ_R are much less than unity, the mean absorption coefficient K_a approaches the Planck absorptivity K_p and equation 7 is exact. Under optically thick conditions, when τ_p and τ_R are much greater than unity, K_a approaches the Rosseland mean K_R and equation 7 is a good approximation.

The subject of this report, which is the third phase of the program, consists of the numerical solution of equation 1 utilizing the exact and approximate flux programs.

II. XENON PROPERTIES

The initial data needed for a numerical solution consists of the electrical conductivity, thermal conductivity and spectral absorptivity as functions of temperature and pressure. The temperature dependence of the S integral is shown in figure 2 for a pressure of 11 atmospheres, and the electrical conductivity σ is shown as a function of S in figure 3. The variation of spectral absorptivity with temperature is shown in Table I. An inspection of the table reveals that the spectral absorptivity in the ultra violet region is orders of magnitude greater than that in the visible region. Therefore, the flux computer program consists of an exact flux program for the U. V. and an approximate flux program for the visible. The wavelength bands defining these regions are given by the equations

$$\text{U.V.} \quad \begin{cases} \lambda_{\min} = .0612 \times 10^{-4} \text{ cm} \\ \lambda_{\max} = .0952 \times 10^{-4} \text{ cm} \end{cases}$$

$$\text{Visible} \quad \begin{cases} \lambda_1 = .1034 \times 10^{-4} \text{ cm} \\ \lambda_2 = 2.0 \times 10^{-4} \text{ cm} \end{cases}$$

III. NUMERICAL ANALYSIS

A steady state solution of the energy equation can be obtained by solving the "transient" equation

$$\frac{\partial S}{\partial t} = \frac{\partial^2 S}{\partial r^2} + \frac{1}{r} \frac{\partial S}{\partial r} - \left[\frac{dF}{dr} + \frac{F}{r} \right] + \sigma(s)E^2 \quad (13)$$

until a steady state solution is achieved. The following calculation procedure was followed:

Table I - Spectral Absorptivity of Xenon (cm^{-1})

	$\lambda \times 10^4$ cm	T [$^{\circ}\text{K}$]				
		3000	6000	10000	14000	18000
VISIBLE	2.0	1.257@-14	4.909@-05	.2502	3.046	2.406
	.7500	2.616@-14	1.679@-05	.0523	.5612	.4115
	.4615	1.224@-12	1.052@-04	.1352	.9441	.5476
	.3333	8.184@-12	9.594@-05	.0768	.5461	.3027
	.2609	6.775@-11	1.076@-04	.0511	.3594	.1872
	.2143	5.557@-10	1.194@-04	.0345	.2446	.1193
	.1818	9.842@-10	9.506@-05	.0225	.1598	.0761
	.1579	6.446@-10	6.226@-05	.0147	.1049	.0501
	.1395	4.449@-10	4.297@-05	.0107	.0725	.0347
	.1250	3.198@-10	3.089@-05	.00731	.0521	.0250
	.1132	2.376@-10	2.295@-05	.00543	.0387	.0186
	.1034	1.813@-10	1.751@-05	.00414	.0295	.0142
ULTRA VIOLET	.0952	2,269.0	1,134.0	614.1	145.9	13.07
	.0882	2,094.0	1,047.0	561.0	135.7	12.07
	.0822	1,920.0	959.7	519.8	124.4	11.07
	.0769	1,746.0	872.6	472.6	113.1	10.06
	.0723	1,572.0	785.5	425.4	101.8	9.06
	.0682	1,397.0	698.4	378.3	90.51	8.05
	.0645	1,223.0	611.3	331.1	79.22	7.05
	.0612	1,049.0	524.2	283.9	67.94	6.04

- (a) specify arc radius and central core temperature.
- (b) specify an initial temperature profile
- (c) calculate a radial flux profile
- (d) define E by the equation

$$E = \frac{\sqrt{-\nabla^2 S(o) + 2 \frac{dF(o)}{dr}}}{\sigma(o)}$$

- (e) select a time step Δt and solve for a new S profile
- (f) repeat steps c,d, and e until the solution converges to a steady state

The field E is so defined as to keep the central temperature essentially constant. This procedure was adopted to avoid large central temperature variations which would greatly affect the flux and its divergence. The finite difference equation used to replace equation 13 is

$$\begin{aligned} \frac{S_i^{n+1} - S_i^n}{\Delta t} = & \frac{1}{\Delta r^2} \left[\left(1 + \frac{\Delta r}{2r_i}\right) S_{i+1}^{n+1} + \left(1 - \frac{\Delta r}{2r_i}\right) S_{i-1}^{n+1} - 2S_i^{n+1} \right] \\ & - \left[\frac{F_{i+1}^n - F_{i-1}^n}{2\Delta r} + \frac{F_i^n}{r_i} \right] + \sigma(S_i^n) (E^n)^2 \end{aligned} \quad (14)$$

where the subscript i denotes a radial position. Equation 14 is an implicit difference equation, which for linear equations, is known³ to be unconditionally stable. Now let $\theta = \frac{\Delta t}{\Delta r^2}$ and define the coefficients $C_{i,j}$ by the equations

$$\begin{aligned} C_{i,i-1} &= -\theta \left(1 - \frac{\Delta r}{2r_i}\right) \\ C_{i,i} &= (1 + 2\theta) \\ C_{i,i+1} &= -\theta \left(1 + \frac{\Delta r}{2r_i}\right) \end{aligned} \quad (15)$$

Then equation 14 can be written as

$$C_{i,i-1} S_{i-1}^{n+1} + C_{i,i} S_i^{n+1} C_{i,i+1}^{n+1} = B_i^n \quad (16)$$

where

$$B_i^n = \sigma(S_i^n) (E_i^n)^2 - \left[\frac{F_{i+1}^n - F_{i-1}^n}{2\Delta r} + \frac{F_i^n}{r_i} \right] \quad (17)$$

Let \vec{S}^n and \vec{B}^n define the vectors

$$\vec{S}^n = \begin{pmatrix} S_1^n \\ S_2^n \\ \vdots \\ S_i^n \\ \vdots \\ S_N^n \end{pmatrix}; \quad \vec{B}^n = \begin{pmatrix} B_1^n \\ B_2^n \\ \vdots \\ B_i^n \\ \vdots \\ B_N^n \end{pmatrix} \quad (18)$$

Then the finite difference equations can be written in matrix form as

$$\langle C \rangle \vec{S}^{n+1} = \vec{B}^n \quad (19)$$

The k^{th} row of $\langle C \rangle$ contains only the coefficients $C_{K,K-1}$, $C_{K,K}$, $C_{K,K+1}$ and the matrix is tri-diagonal. The matrix $\langle C \rangle$ can be "inverted" very efficiently by Gauss's⁴ elimination method. The first equation ($i=1$) is used to eliminate S_1^{n+1} from the second equation ($i=2$), the new second equation used to eliminate S_2^{n+1} from the third equation and so on until finally the new last but one equation can be used to eliminate S_{N-2}^{n+1} from the last equation, giving only one equation with only one unknown S_{N-1}^{n+1} . The unknowns S_{N-2}^{n+1} , S_{N-3}^{n+1} , ..., S_1^{n+1} can then be found in turn by back substitution. The method provides a fast computational procedure for large numbers of equations. In the numerical solution,

50 radial increments were employed. The flux program was used to evaluate the flux at 9 points and intermediate values were obtained with the use of a quadratic interpolation program.

IV. NUMERICAL SOLUTIONS

Numerical solutions were obtained for a pressure of 11 atm. and central arc temperatures of 10,000°K and 18,000°K. For the first example, several iterative S profiles are shown in figure 4. S_0 denotes the initial profile, and S_{29} denotes the final profile obtained after 29 time increments. The final solution has a maximum error ϵ of .03% where ϵ is defined as

$$\epsilon = \frac{\frac{\partial S}{\partial t}}{\sigma E^2} \quad (20)$$

In figure 5 are shown several iterative flux profiles. For the final S profile (S_{29}), the approximate flux calculations were compared with exact calculations over the range $\lambda_1 - \lambda_2$ and were found to agree to within 1%. In figure 6 is shown the final temperature profile corresponding to S_{29} . The temperature profile is very flat with a narrow conduction layer near the tube wall. The total current was evaluated from Ohm's law as

$$I = 2\pi E \int_0^R r \sigma [S(r)] dr \quad (21)$$

In figure 7 is given the variation of E with "time", showing a convergence to 20.69 volts/cm.

The iterative S profiles for the second example are shown in figure 8. A total of 80 time increments was required for convergence and the final profile S_{80} differs markedly from the initial S_0 profile. The final solution S_{80} has a maximum error of 0.2%. In figure 9 are shown the initial and final flux profiles. A comparison of approximate and exact flux calculations over the range $\lambda_1 - \lambda_2$ gave agreement to within

10%. Therefore the "final" solution S_{80} must still be considered an approximation to the exact solution. The temperature profile corresponding to S_{80} is shown in figure 10. Lowke and Capriotti⁵ have shown that the curvature of the temperature in the central core region is due to self absorption effects. Also, the thermal conduction edge is smaller than in the first example. The iterative variation of E is given in figure 11 showing convergence to a final value of 68.95 volts/cm and the corresponding current is 5795 amps. In summary, these examples indicate that the numerical method employed is stable and provides a convenient method for obtaining steady state solutions to the energy equation. Furthermore, with slight modification, the method can be used to calculate actual thermal transients in radiative plasmas, for applications where transient effects are important.

ACKNOWLEDGEMENTS

The author gratefully acknowledges the assistance of Mr. R. Lieberman who modified and consolidated existing flux programs; Mr. B. Wang who programmed the finite difference equations; and discussions with Mr. J. Vine and Dr. J. Lowke.

NOMENCLATURE

$$B_{\lambda} \quad \text{Planck function } B_{\lambda} = \frac{2c^2 h}{\lambda^5 [\exp(\frac{ch}{\lambda KT}) - 1]}$$

$$B(T) \quad B(T) = \int_{\lambda_{\min}}^{\lambda_{\max}} B_{\lambda}(T) d\lambda$$

b constant in equation 9

$$B_i^n \quad B_i^n \equiv \sigma(S_i^n)(E^n)^2 - [\frac{F_{i+1}^n - F_{i-1}^n}{2\Delta r} + \frac{F_i^n}{r_i}]$$

$$\vec{B}^n \quad \vec{B}^n = \text{col}(B_1^n, B_2^n, \dots, B_i^n, \dots, B_N^n)$$

$$C_{i,i-1} = -\Theta(1 + \frac{\Delta r}{2r_i})$$

$$C_{ij} \quad C_{i,i} = (1 + 2\Theta)$$

$$C_{i,i+1} = -\Theta(1 - \frac{\Delta r}{2r_i})$$

$$\langle C \rangle \quad \text{matrix } \langle C \rangle = (C_{ij})$$

E Electric Field (volts/cm)

E^n value of E for $n\Delta t$ (volts/cm)

\vec{F} radiative flux vector (watt/cm^2)

$$\vec{F} = \vec{r} F(r)$$

$$F(r) \quad F(r) = \int_{\lambda_{\min}}^{\lambda_{\max}} \int_{\omega=4\pi} I_{\lambda}(r, \vec{\omega}) \omega d\omega d\lambda; \text{ equation 5}$$

$\hat{F}(r)$ approximate flux; see equation 7

$$G_n(x) \quad G_n(x) = \int_0^{\frac{\pi}{2}} e^{-\frac{x}{\sin\theta}} (\sin\theta)^n d\theta$$

I current (amperes)

$I_{\lambda}(r, \vec{\omega})$ intensity of radiation at r in direction $\vec{\omega}$ (watts/cm³)

$K(T)$ thermal conductivity (watt/cm⁰K)

K_a mean absorption coefficient in equation 9 (cm⁻¹)

K_R Rosseland mean absorption coefficient (cm⁻¹)

$$K_R^{-1} = \int_{\lambda_1}^{\lambda_2} \frac{1}{K_{\lambda}} \frac{dB_{\lambda}}{dT} d_{\lambda} / \frac{dB}{dT}$$

K_P Planck mean absorption coefficient (cm⁻¹)

$$K_P = \int_{\lambda_1}^{\lambda_2} K_{\lambda}(T) B_{\lambda}(T) d\lambda / B(T)$$

N number of radial subdivisions

n number of "time" steps

P arc pressure (atm)

R	tube radius (cm)
r	radial coordinate (cm)
r_i	i^{th} radial position (cm)
Δr	$\Delta r = r_i - r_{i-1}$ (cm)
$S(T)$	$S = \int_{T_w}^T KdT$ (watt/cm)
s	position along a ray (cm)
S_i^n	value of $S(r_i)$ at the n^{th} time step
T	temperature ($^{\circ}\text{K}$)
T_w	wall temperature ($^{\circ}\text{K}$)
Δt	time step
β_λ	$\beta_\lambda = \int_0^S K_\lambda(\zeta) d\zeta$
θ	$\theta = \Delta t / \Delta r^2$
K_λ	spectral absorptivity (cm^{-1})
λ	wavelength (cm)
λ_1	$\lambda_1 = .1034 \times 10^{-4}$ cm
λ_2	$\lambda_2 = 2 \times 10^{-4}$ cm

$$\lambda_{\min} \quad \lambda_{\min} = .0612 \times 10^{-4} \text{ cm}$$

$$\lambda_{\max} \quad \lambda_{\max} = .0952 \times 10^{-4} \text{ cm}$$

σ electrical conductivity (mho/cm)

$$\tau_R \quad \text{Rosseland optical length; } \tau_R = \int_0^S K_R(\zeta) d\zeta$$

$$\tau_P \quad \text{Planck optical length; } \tau_P = \int_0^S K_P(\zeta) d\zeta$$

ϕ spherical coordinate measuring azimuth angle of a ray in figure 1.

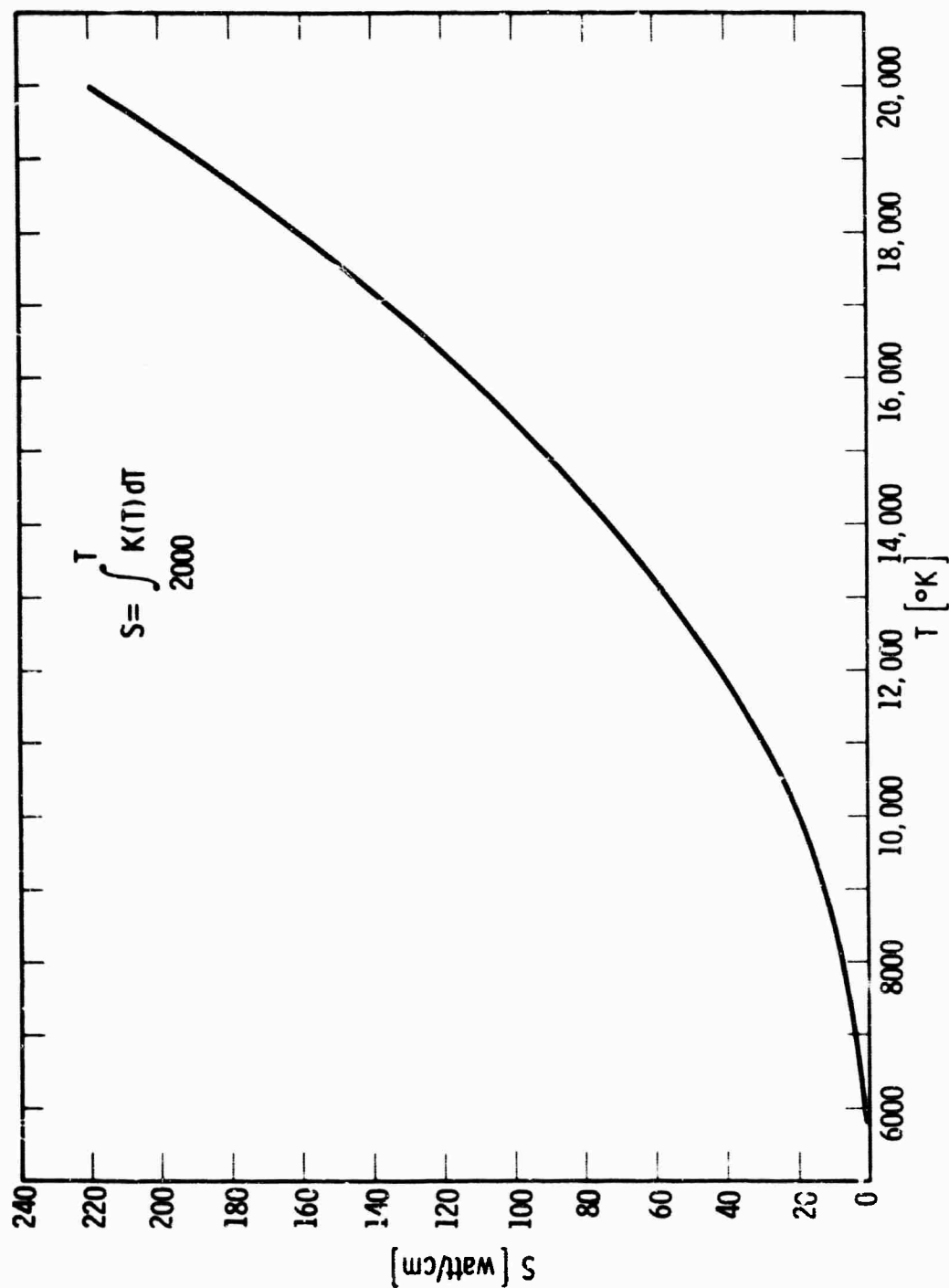
$\vec{\omega}$ unit direction vector of a ray

REFERENCES

1. B. W. Swanson, "Radiative Flux in a Non-Isothermal Non-Grey Cylindrical Arc", Westinghouse Scientific Paper 65-1D8-GASDY-P2, November 1, 1965.
2. B. W. Swanson, "Radiative Flux Approximation in a Non-Grey Cylindrical Arc", Westinghouse Research Report 65-8D8-GASDY-R1, August 16, 1965.
3. R. D. Richtmyer, Difference Methods for Initial-Value Problems Interscience Publishers Inc., 1957.
4. G. D. Smith, Numerical Solution of Partial Differential Equations Oxford University Press, 1965 (page 20).
5. J. J. Dowke, E. R. Capriotti, "The Influence of Radiation on High Pressure Arcs", Westinghouse Research Report 66-1E2-GASES-R1, October 28, 1966.

Fig. 1—Arc geometry with $\theta' = 0$

Curve 581579-A



$$S = \int_{2000}^T K(T) dT$$

Fig. 2— $S(T)$ vs T for Xenon at 11 atm pressure

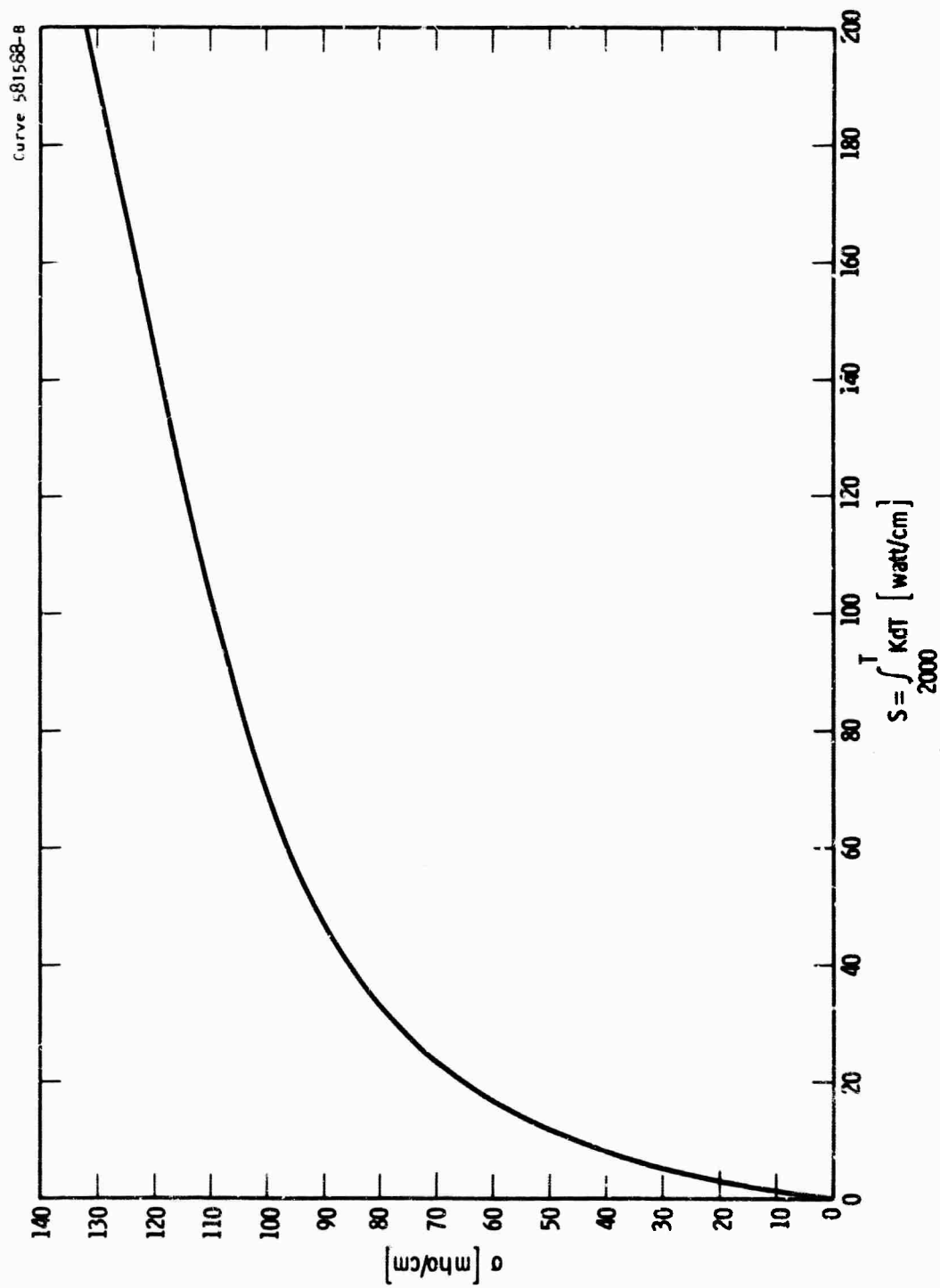


Fig. 3-- σ vs S for Xenon at 11 atm pressure

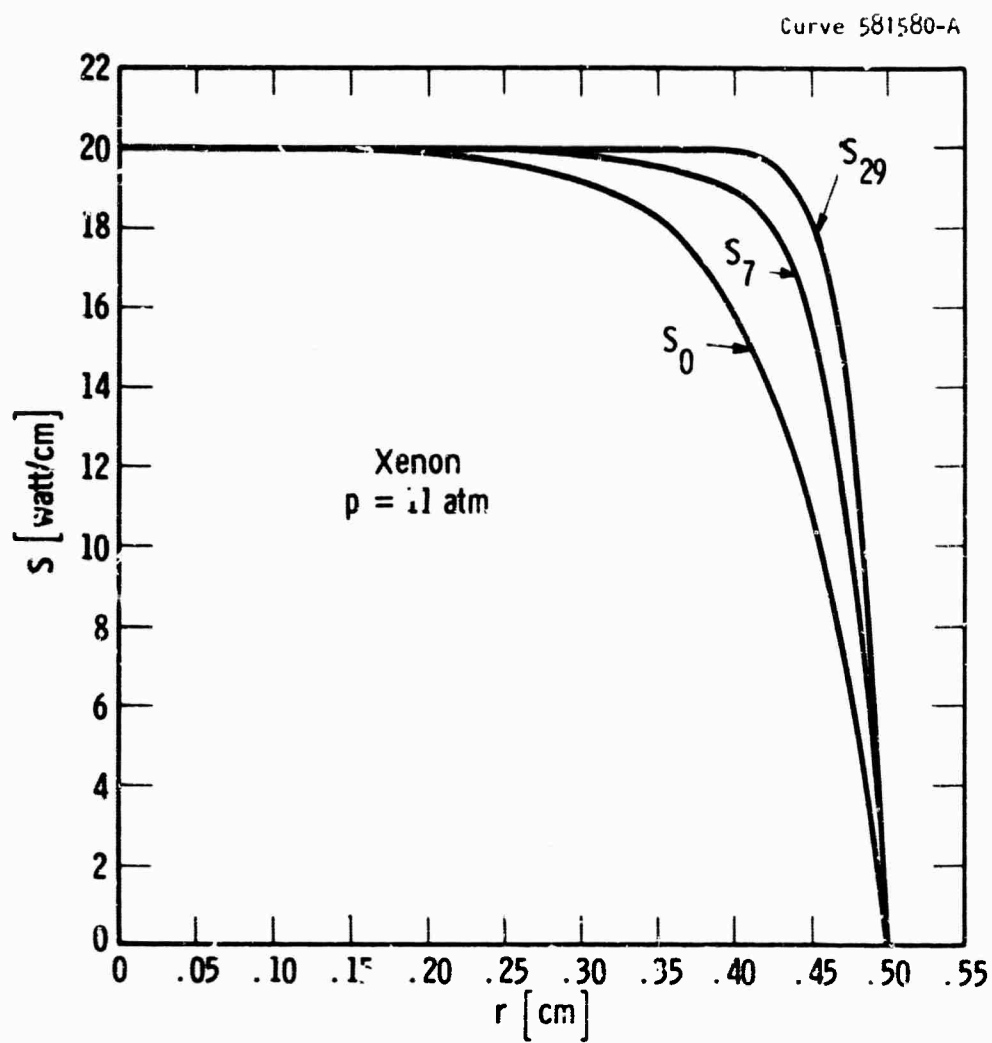


Fig. 4-Iterative S profiles

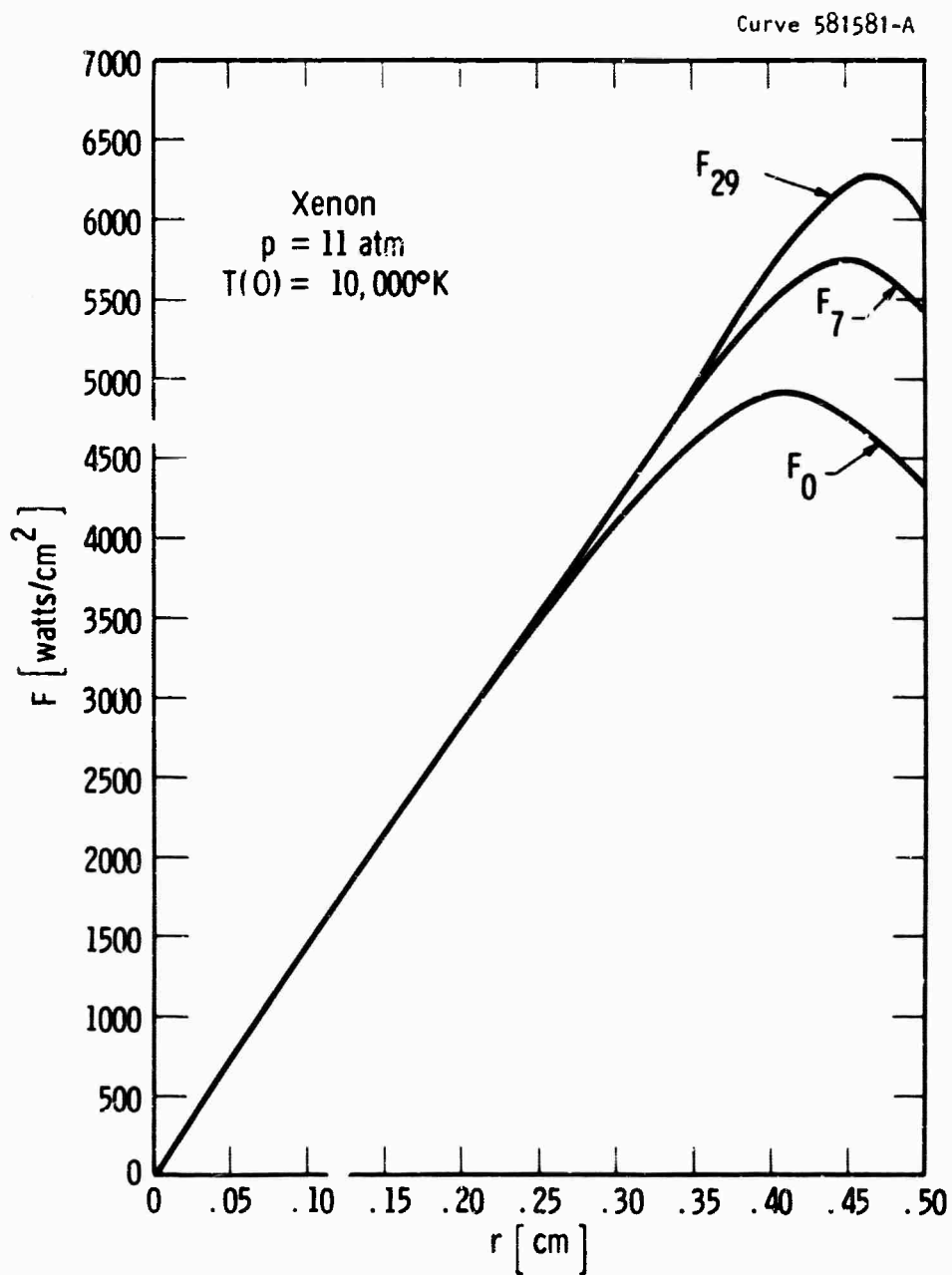


Fig. 5—Iterative flux profiles

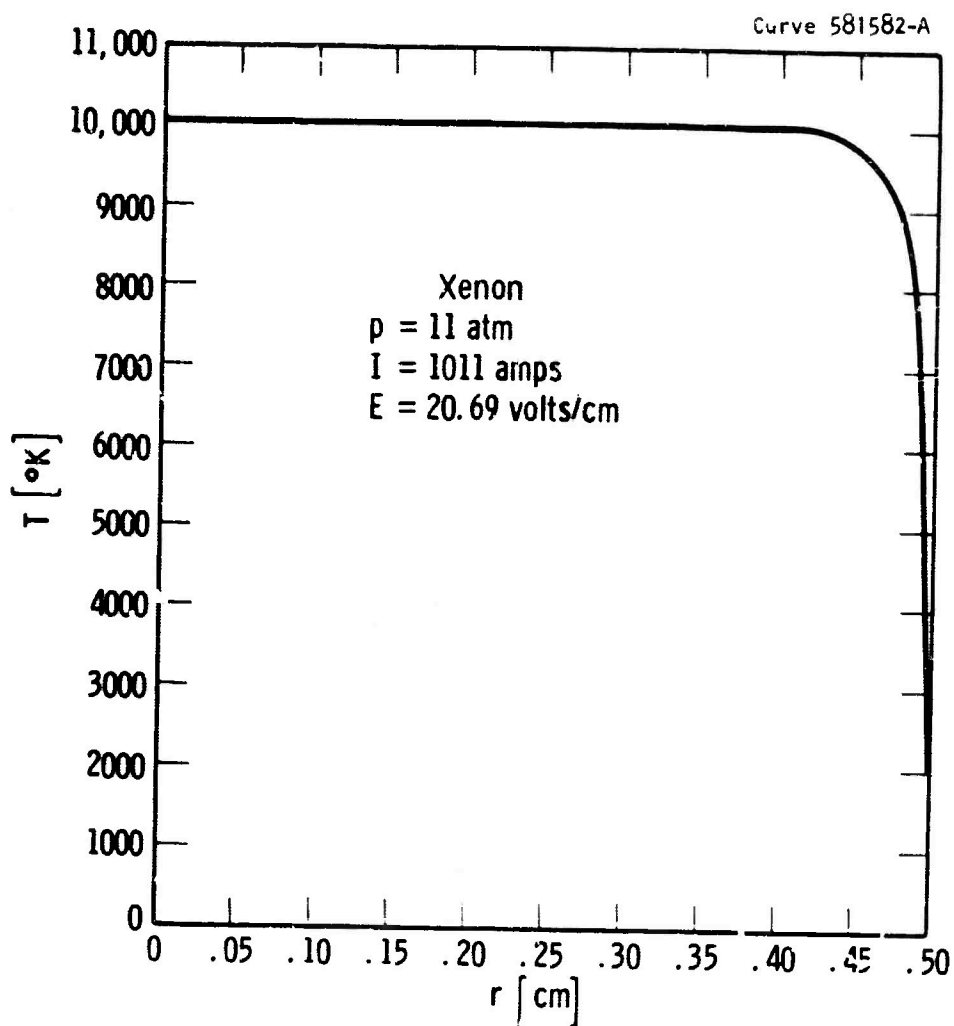


Fig. 6—Steady state temperature profile

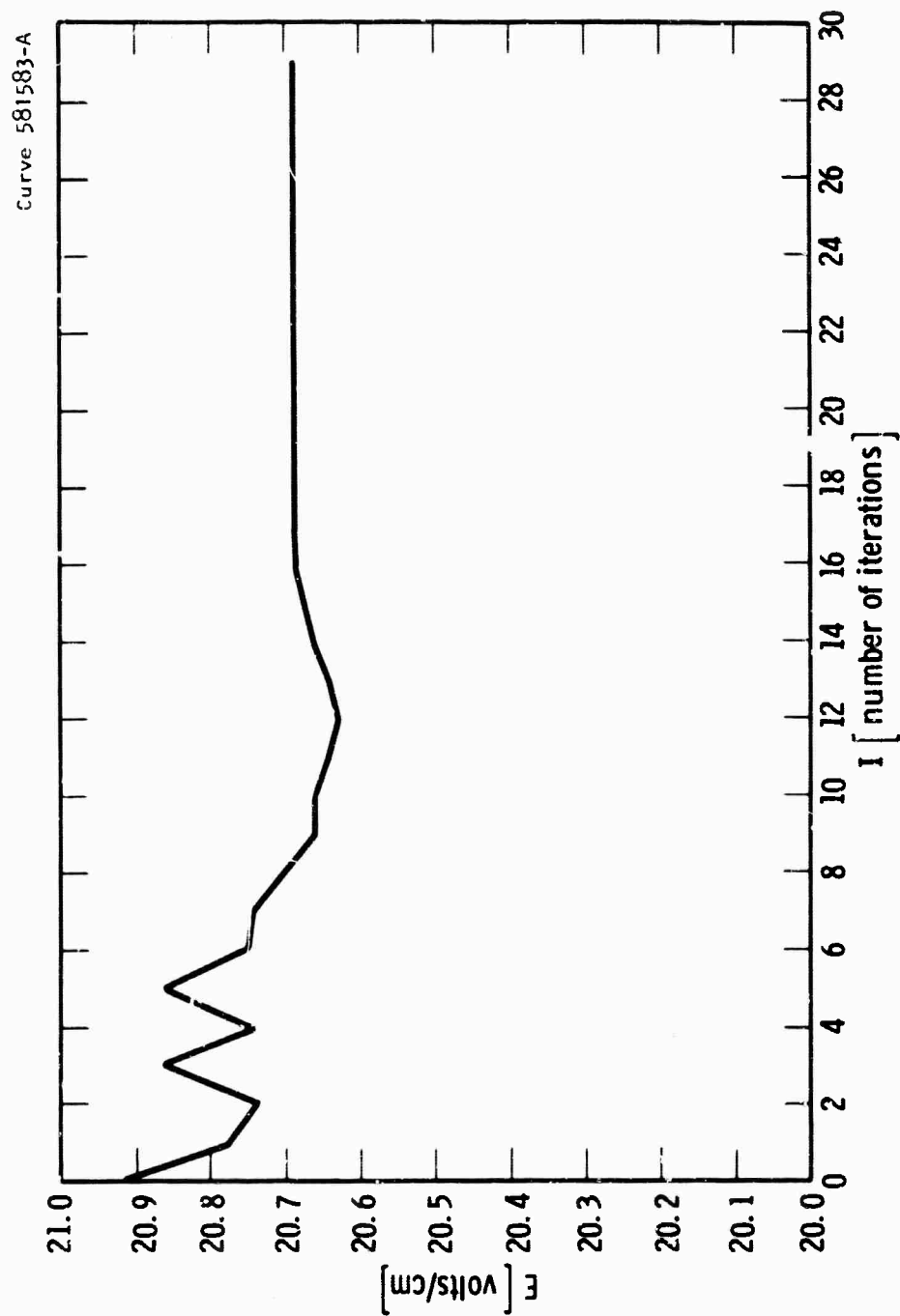


Fig. 7--Variation of E with iteration

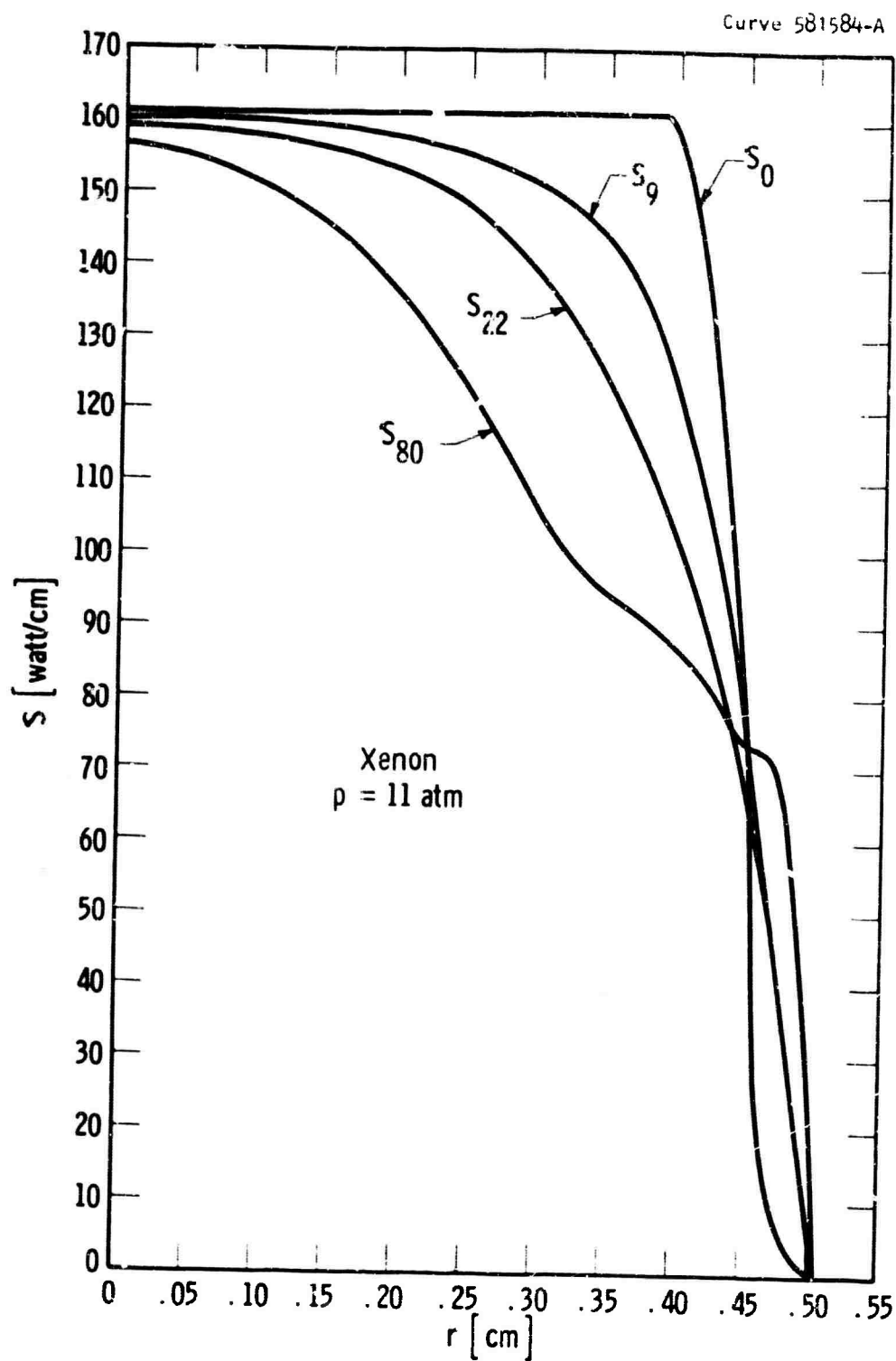


Fig. 8--Iterative S profiles

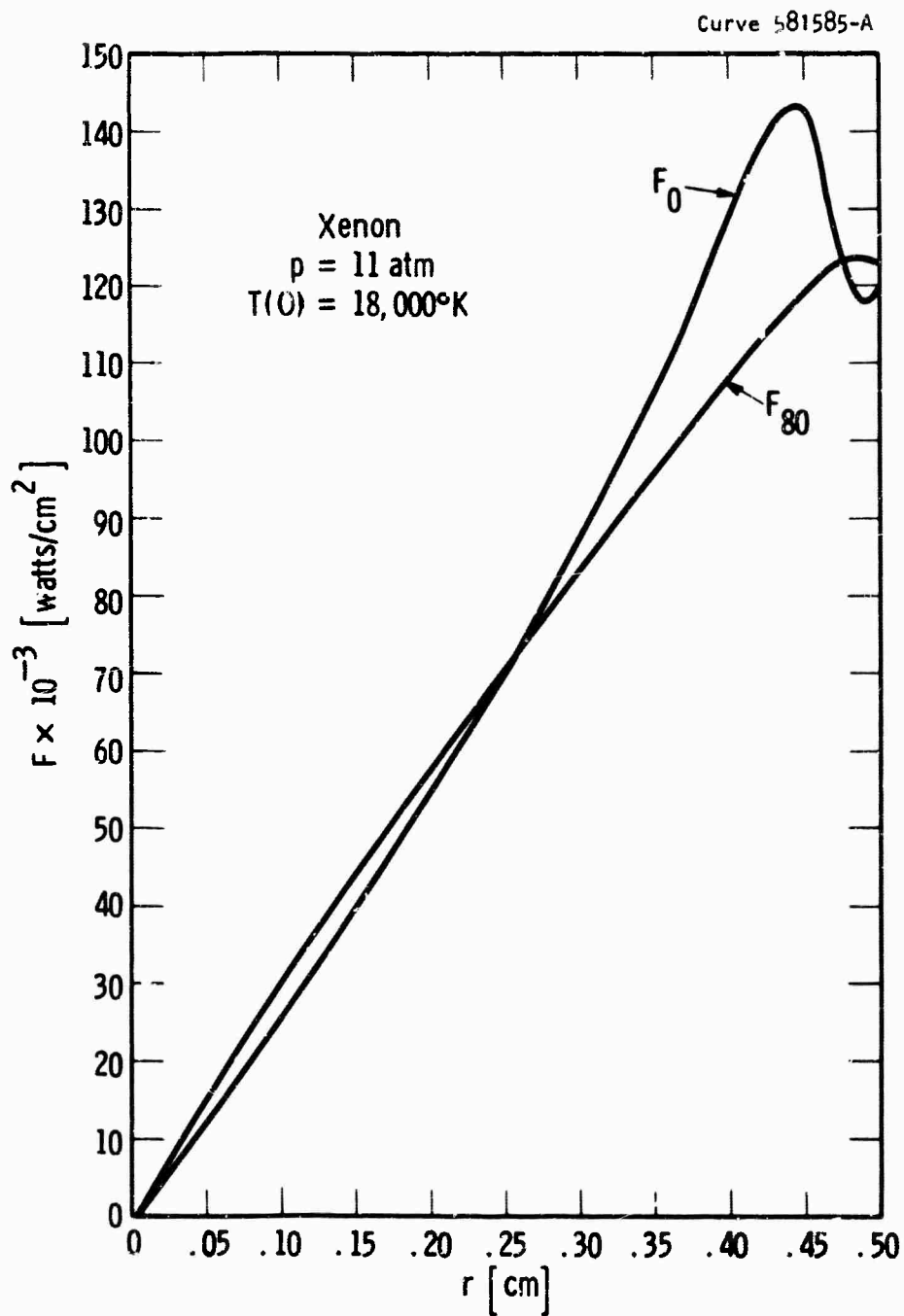


Fig. 9--Iterative flux profiles

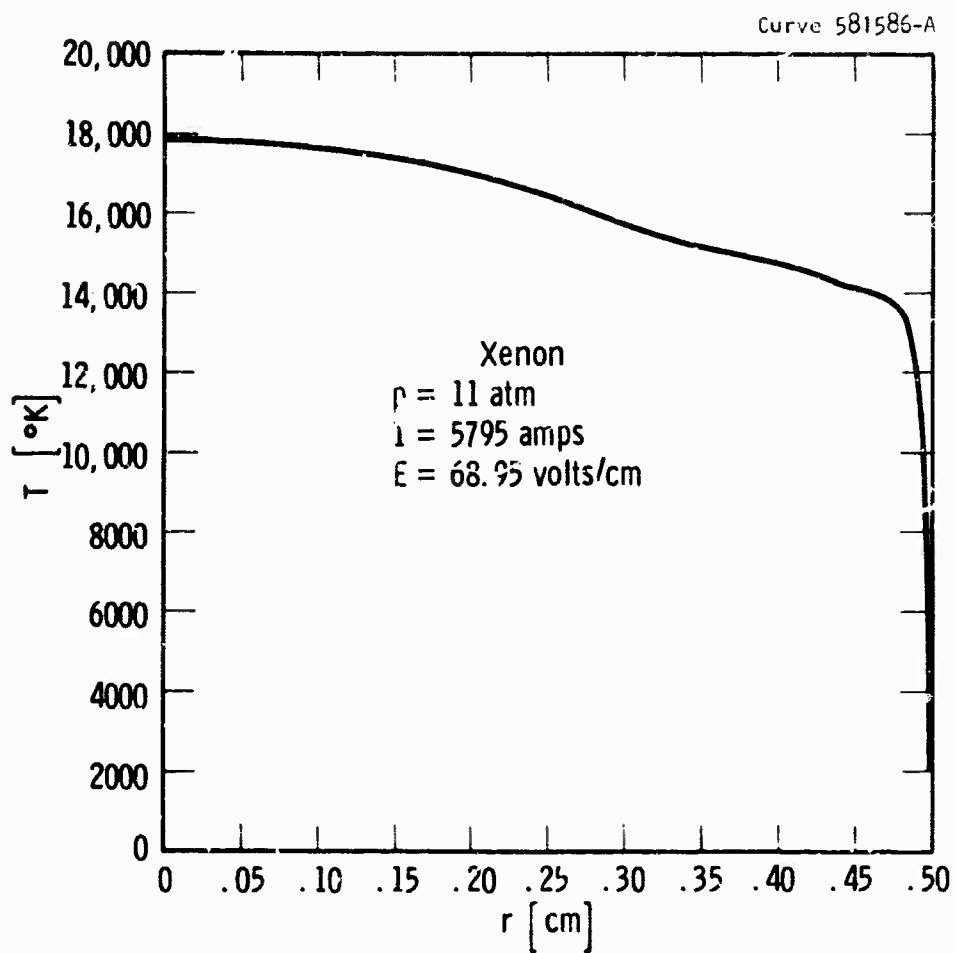


Fig. 10—Steady state temperature profile

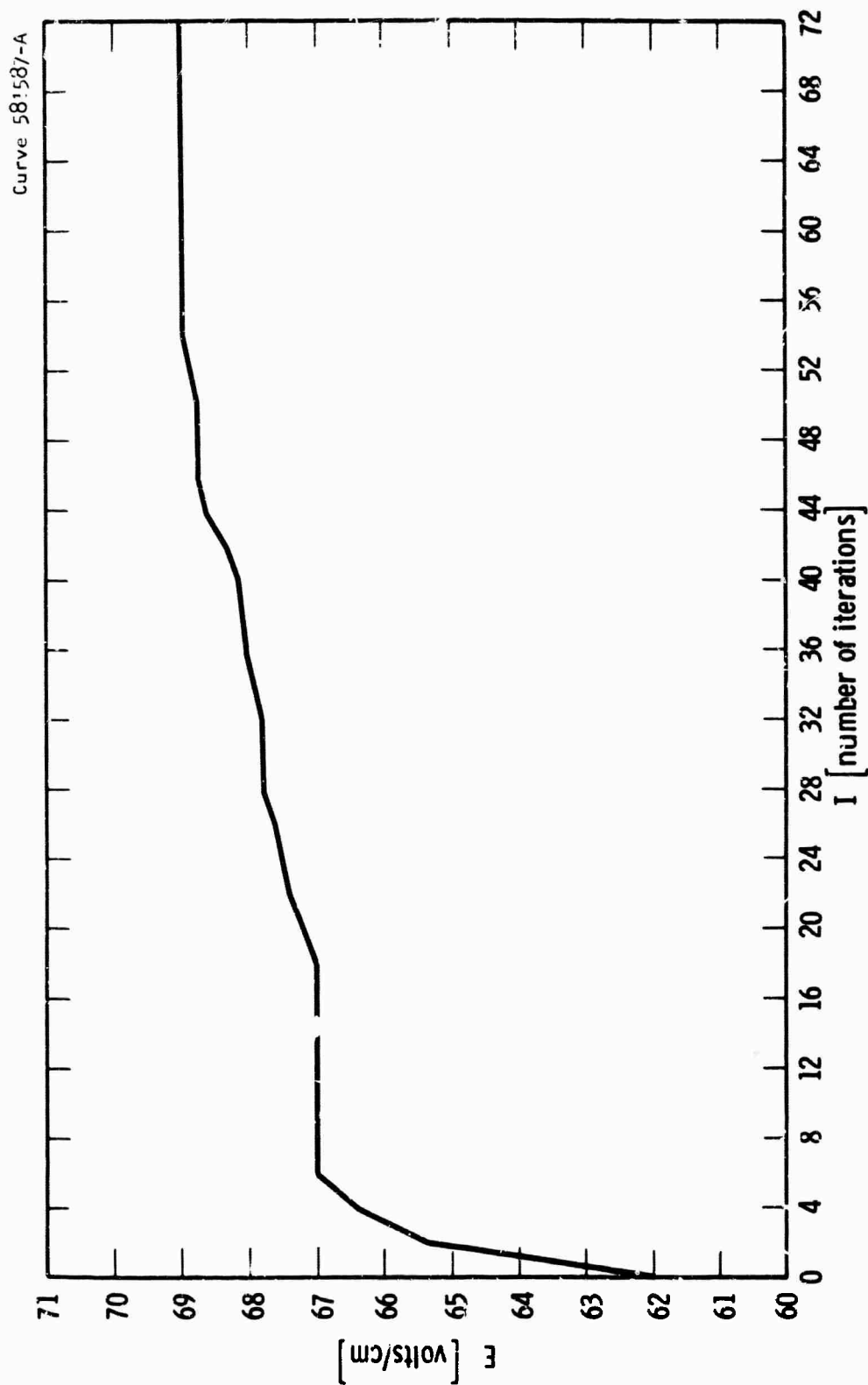


Fig. 11—Variation of E with iteration

BEGIN

SC 11 010

START OF SEGMENT ***** 2

COMMENT

SC 21 010

THIS PROGRAM CALCULATES THE TEMPERATURE PROFILE OF AN ELECTRICAL
ARC COLUMN HAVING CYLINDRICAL SHAPE AND INFINITE LENGTH AND POSSESSING
ASYMMETRICAL SPATIAL VARIANCES ABOUT ITS AXES. THE PROGRAM DETERMINES
THE PROFILE BY AN ITERATIVE PROCESS USING A TIME DEPENDENT DIFFERENTIAL
ENERGY BALANCE EQUATION WHICH INCLUDES RADIATION AS WELL AS THERMAL
TRANSPORT MECHANISMS.

SC 21 010

SC 21 010

SC 21 010

SC 21 010

SC 21 010

SC 21 010

SC 21 010

SC 21 010

SC 21 010

THE PROGRAM CONTAINS NINE READ STATEMENTS. THEY ARE LISTED BELOW IN
ORDER OF CALL.

SC 21 010

SC 21 010

(1)

SC 21 010

RR----- (REAL) THE ARC COLUMN RADIUS (UNITS-- CM) .

SC 21 010

N----- (INTEGER) NUMBER OF STEPS IN R (RADIUS)

SC 21 010

(2)

SC 21 010

DT----- (REAL) TIME STEP SIZE (UNITS-- SEC.) .

SC 21 010

NT----- (INTEGER) NUMBER OF TIME STEPS TO BE RUN

SC 21 010

(3)

SC 21 010

T----- (ARRAY) INITIAL RADIAL TEMPERATURE PROFILE, CONTAINS 51 VALUES
STARTING WITH THE CENTRAL TEMPERATURE AND STEPPING IN
EQUAL INCREMENTS OF RADIUS TO RR (UNITS-- DEG. KELVIN)

SC 21 010

SC 21 010

SC 21 010

(4)

SC 21 010

KT----- (ARRAY) AN ARRAY GIVING THE VALUES OF THE INTEGRAL OF
THERMAL CONDUCTIVITY WITH RESPECT TO TEMPERATURE
(UNITS-- WATTS/CM) .

SC 21 010

SC 21 010

SC 21 010

SWT----- (ARRAY) AN ARRAY OF ELECTRICAL CONDUCTIVITIES (UNITS-- MMHS/CM)

SC 21 010

NOTE

SC 21 010

THE ABOVE TWO ARRAYS ARE READ IN SIMULTANEOUSLY AT CORRESPONDING
TEMPERATURE VALUES .

SC 21 010

SC 21 010

(5)

SC 21 010

NPM----- (INTEGER) NUMBER OF DAYS IN MAKING NUMERICAL APPROXIMATIONS
IN THE FLUX PROCEDURE (USUALLY 40 IN AS SIX) .

SC 21 010

SC 21 010

APPROXDS----- (REAL) APPROXIMATE STEP SIZE TO BE TAKEN ALONG EACH OF THE
THE ABOVE DAYS (USUALLY READ IN AS .05) .

SC 21 010

SC 21 010

(6)

SC 21 010

RT----- (REAL) FIRST TEMPERATURE VALUE OF THE KAPPA TABLE DEFINED BELOW

SC 21 010

DT----- (REAL) TEMPERATURE STEP SIZE OF KAPPA TABLE

SC 21 010

RT----- (REAL) LAST TEMPERATURE VALUE OF THE KAPPA TABLE

SC 21 010

NOTE THE ABOVE THREE TERMS HAVE UNITS OF DEG. KELVIN

SC 21 010

(7)

SC 21 010

RFREQ----- (REAL) FIRST FREQUENCY VALUE OF THE KAPPA TABLE

SC 21 010

DFREQ----- (REAL) FREQUENCY STEP SIZE OF THE KAPPA TABLE

SC 21 010

EFREQ----- (REAL) LAST FREQUENCY VALUE OF THE KAPPA TABLE

SC 21 010

Z----- (INTEGER) FREQUENCY INDEX (WITH 1 CORRESPONDING TO

SC 21 010

RFREQ) WHICH DEFINES THE SPECTRUMS TO BE USED IN

SC 21 010

```

      THE FLUX PROCEDURE FOR THE EXACT AND APPROXIMATE
      CALCULATIONS THEREIN, THE EXACT SOLUTION USES THE
      FREQUENCY SPECTRUM CORRESPONDING TO THE INDICES OF
      Z TO THAT FOR EFREQ,
      NOTE THE UNITS OF FREQUENCY IS CYCLES/SEC.
      ( R )
      KAPPA=((ARRAY / 1 SPECTRAL ABSORPTIVITY VALUES WHICH ARE A FUNCTION OF
      TEMPERATURE AND FREQUENCY RESPECTIVELY 1 UNITS 1/CM )
      ( 0 1 )
      MGT---(REAL / 1 THE FIRST TEMPERATURE VALUE ( DEG. KELVIN )CORRESPONDING
      TO THE FIRST ENTRY OF THE ST FUNCTION OF (S. ,
      MGT---(REAL) LAST TEMPERATURE VALUE CORRESPONDING TO LAST ENTRY OF ST
      DAT---(REAL) THE TEMPERATURE INCREMENT OF THE ST FUNCTION. )
      FILE IN MASSG DISK SERIAL (1,330) )
      FILE IN READER (2, 10) )
      FILE OUT PUNCH (2,101) )
      FILE OUT PRINTER (2,15) )
      LABEL START, FIN, EXIT )
      REAL RHO, LCA, HETA, E, D, OT, RB, RMAX, R1, IFC
      APRAT S, A, R, C, SIGMA, F, OGV, R+0.05(0.95), T(0.15), S(0.190) )
      ARRAY T, ST(0.95) )
      ARRAY SC, OVG, SFG, SE(0.95) )
      INTEGER I, J, K, M, N, COUNT, MN, MT )

      DEFINE SL = STEP 1 UNTIL 0 )
      COMMENT (ARTIME)
      FORMAT FMT(1X, F5.2, R11.4, X2, R11.4, X1, R11.4, X3, F9.4, X3, R11.4, X3,
      START OF SEGMENT ***** A
      011.4, X3, M11.4, X3, R11.4) )
      MDT(1X, "R", X10, "S", X11, "F", X10, "T", X9, "SIGMA", X6, "COND PART",
      X4, "OVGF", X11, "SE", X2, X4, "SUM RATE", / ) )
      A IS 10 LONG, NEXT SFG 2
      REAL PROCEDURE ILAG ( X, YA, N, YO, NY ) )
      COMMENT ORDER 3 LAGRANGE INTERPOLATION, EQUAL DEPENDENT STEP, SINGLE
      INDEPENDENT, DEPENDENT VARIABLE, EXTRAPOLATES IF NOT VARIOUSLY,
      Y = DEPENDENT INDEPENDENT VALUE
      YA = NAME, INDEPENDENT VARIABLE VALUE TABLE (SINGLE SUBSCRIPT)
      N = MAX INDEX OF YA TABLE ( 2 3 )
      YO = FIRST DEPENDENT VALUE (REFERENCE POINT == FOR YAO) )
      NY = STEP SIZE, DEPENDENT VARIABLE )
      VALUE Y, N, YO, DY / REAL Y, YO, DY / INTEGER N / ARRAY YAT / )
      BEGIN INTEGER I / REAL EO, E1, E2, E3, F10, F20, F30, F32, G /
      START OF SEGMENT ***** 5
      EO = SIGN( RAINI - YATN ) )
      FOR I = 0 STEP 1 WHILE (I+1)ASH AND SIGN(X-YAT1+2Y3)NEQ 00 )
      F10 = ( E1 + YAT I + 1 I = N ) = ( EO + YAT I ) = X )

```

```

F20 = ( E2 * XA( 1 + 2 * I - 1 ) - E0 )
F31 = ( E3 * XA( 1 + 3 * J - 1 ) - E1 )
F32 = E3 - A2 )
ILAG = ( ( G + 1 * DY + Y0 ) * E3 / F10 / F20 - ( 3 * DY + 1 * E0
/ F31 / F32 ) * E1 + E2 / ( E3 + E0 ) - ( ( DY + G ) * E2 / F10
/ F31 - ( 2 * DY + G * 1 * E1 / F20 / F32 ) * E0 + F3 / ( E2 + E1 )
END ILAG )

```

```

REAL PROCEDURE LAG ( X , A0 , DX , Y , N )
COMMENT
X = DESIRED INDEPENDENT VALUE
A0 = FIRST INDEPENDENT VALUE OF Y TABLE (FOR Y(0))
DX = TABLE STEP FOR INDEPENDENT
Y = NAME, DEPENDENT VARIABLE VALUE TABLE (MUST BE SINGLE SUBSCRIPT)
N = MAX INDEX OF Y TABLE ( ≥ 0 )
VALUE X , X0 , DX , N )
REAL X , A0 , DX ) INTEGER N ) ARRAY Y(0) )
BEGIN
INTEGER I ) REAL S )

```

```

Y0ENTIC( (S+(X-X0)/DX) )
IF S01 THEN LAG=Y(1) ELSE
LAG=(Y(1)+(Y(2)-Y(1))*N(2-1)+Y(1))

```

```
END LAG )
```

```

REAL PROCEDURE LLAG(XA, Y, N)
COMMENT ORDER 3 LAGRANGE INTERPOLATION, NO EQUAL STEPS, SINGLE DEPENDENT
& INDEPENDENT VARIABLE, EXTRAPOLATES IF NOT XA(0) ≤ X ≤ XA(3) .
X = DESIRED INDEPENDENT VALUE
XA = NAME, INDEPENDENT VARIABLE VALUE TABLE (SINGLE SUBSCRIPT)
Y = NAME, DEPENDENT VARIABLE VALUE TABLE (SINGLE SUBSCRIPT)
N = MAX INDEX OF BOTH XA & Y TABLES ( ≥ 3 )
VALUE X, N)
REAL X)
ARRAY XA, Y(0)
INTEGER N)
BEGIN
INTEGER J)

```

```

REAL E0, E1, E2, E3, F10, F20, F31, F32)
E0 = SIGN(XA(1)-X, X(0))
FOR I = 0 STEP 1 UNTIL (I) > 3 AND SIGN(XA(I+2)-X) < 0 DO
I
F10 = (E1 - XA(I+1)) * (E1 - XA(I+2))
F20 = (E2 - XA(I+2)) * (E1 - E0)
F31 = (E3 - XA(I+3)) * (E1 - E0)

```

```

ILAG 1A SC 51 1711
ILAG 5 SC 51 2011
ILAG A SC 51 2311
ILAG 7 SC 51 2612
ILAG 8 SC 51 2910
ILAG 10 SC 51 3410
I 7 SC 51 3911

```

```

5 IS 46 LONG, NEXT SEG 2
LAG 1 SC 21 2610
SC 21 2610
LAG A SC 21 2610
LAG 5 SC 21 2610
LAG A SC 21 2610
LAG 7 SC 21 2610
LAG 8 SC 21 2610
LAG 9 SC 21 2610
LAG 10 SC 21 2610
LAG 11 SC 21 2610
LAG 12 SC 21 2610

```

```

START OF SEGMENT ***** 6
SC 61 010
SC 61 311
SC 61 512

```

```

LAG 1A SC 61 1110
6 IS 14 LONG, NEXT SEG 2
00009200 SC 21 2610
00009300 SC 21 2610
00009400 SC 21 2610
00009500 SC 21 2610
00009600 SC 21 2610
00009700 SC 21 2610
00009800 SC 21 2610
00009900 SC 21 2610
00010000 SC 21 2610
00010200 SC 21 2610
00010100 SC 21 2610
00010300 SC 21 2610
00010400 SC 21 2610

```

```

START OF SEGMENT ***** 7
00010500 SC 21 010
00010600 SC 21 010
00010700 SC 21 312
00010800 SC 21 1212
00010900 SC 21 1310
00011000 SC 21 1711
00011100 SC 21 2110

```

```

F32= E3-E2)
ULAG=(Y1)*E3/F10/F20+Y1*(3)*E2/F31/F32)*E1+E2/(E3+E0)+(Y1
+1)*E2/F10/F31+Y1*(+2)*E1/F20/F32)*E0+F3/(E1-F2)
END ULAGI
00011200 SC 71 2311
00011300 SC 71 2412
00011400 SC 71 3111
00011500 SC 71 3713
7 15 AB LANA, NEXT SEG 2
PROCEDURE FLUX(SP,FP,R)
VALUE R REAL N
ARRAY SP,FP(01)
COMMENT PROCEDURE FOR EVALUATING FLUX GIVEN S FUNCTION
BEGIN
MODLEAM APPE
START OF SEGMENT ***** 8
INTEGER N,J,PHI
LABEL APPROX,EXACT,EXIT
REAL X,SUN,S,S,A,B,TN,RSNX,TBN,4,VH,LANRDA,TR,TEMP,YMT,XLN,
NPHI,PHI, K,KRINT,K2INT
ARRAY FR(0112)
ARRAY RT,TP,EXPARG(0151) ARRAY MT,TP(0112)
OWN REAL RFREQ,LFREQ,DFREQ
OWN REAL APPROXS
OWN REAL OPHI,Z,LANMAX,BT,ET,GT,EXT,ENT,EXT,LITILEP
REAL O
OWN INTEGER NT,NKT
OWN ARRAY L1,DLANDR(01190)
OWN ARRAY C,MS,LS(0111,0110)
OWN ARRAY S(01300),XAPPA(0150,0135),MAX(0111)
OWN ARRAY R(0136),K,KAP(0135)
REAL TAUP2,TAUR2,P2,KR2,TAUP,TAUR,COUNTS,KPT,KKT,TAUA,PRR
IF COUNT > 1 THEN GO EXACT
READ(HEADER,/,N,MI,APPROXS)
NPHI = 3.1415926536/NPHI * NPHI + 3.1415926536 * NPHI,A
READ(PASSG,301,4(03) (EXIT)
READ(HEADER,/,MI,DT,FT,(EXIT) COMMENT TEMP AT WHICH KAPPA IS GIVEN
READ(HEADER,/,BFREQ,DFREQ,EFREQ,Z (EXIT)
LANMAX = (FFREQ-DFREQ)/DFREQ + 1
FOR N = 1 STEP 1 UNTIL LANMAX DO LANIN= SP10/(DFREQ+(N-5)*DFREQ)
NT = (ET-RT)/DT
FOR N=1 STEP 1 UNTIL LANMAX DO
READ(HEADER,/,FUP J = 0 STEP 1 UNTIL NT DO KAPPA(N,J) (EXIT)
READ(HEADER,/,RPT,EXT,DKT (EXIT)
KKT = (EXT-RPT)/DKT
FOR J = 2 STEP 1 UNTIL LANMAX DO DLANDR(J)=LAN(J-1)
DLANDR(1)= DLANDR(2)
BEGIN
REAL FRI,PHI,PHI,TAN2PHI,TANPHI,SINPHI,COSPHI,COSALPH,SINALPH

```

START OF SEGMENT ***** 9

```

      LENGTH,NDS)
      INTEGER NR,NPHI
      NR=0
      FOR FRI = .1, .2, .35, .5, .6, .7, .8, .85, .9, .95, 1 DO
      BEGIN
        NR = NR + 1
        NPHI = 0
        LPHI = IF FRI = 1 THEN DPHI=.5 ELSE 1.9707963268 * DPHI=.5
        FOR PHI=LPHI STEP DPHI UNTIL NPHI DO
        BEGIN
          NPHI=NPHI+1
          TAN2PHI=(TANPHI+ISINPHI*SIN(PHI))/COSPHI+COS(PHI))*2
          COSALPH=(F/(1-TAN2PHI-SQP(1+TAN2PHI*(1-FRI**2)))/(1+TAN2PHI)
          SINALPH=SORT(1-COSALPH**2)
          IF ABS(SINALPH/(COSALPH-FRI)*TANPHI) >.0000001 THEN
            BEGIN
              COSALPH=(FRI-TAN2PHI+SORT(1+TAN2PHI*(1-FRI**2)))/(1+TAN2PHI)
              SINALPH=SORT(1-COSALPH**2)
            END
            LENGTH = SINALPH*NR/SINPHI
            NDS=ENTIER(LENGTH/APPROXDS) + 1
            NSINR,NPHI=LENGTH-(COSINR,NPHI)*LENGTH/NDS)/2+.8
            COSINR,NPHI=COSPHI
            END
            MAXINR=NPHI
          END
        END
      END

```

```

SC 91 010
SC 91 010
SC 91 010
SC 91 013
SC 91 2311
SC 91 2311
SC 91 2511
SC 91 2912
SC 91 4210
SC 91 4210
SC 91 4311
SC 91 4712
SC 91 5213
SC 91 5510
SC 91 5712
SC 91 5810
SC 91 6311
SC 91 6512
SC 91 6711
SC 91 7010
SC 91 7513
SC 91 7713

```

9 IS AT LONG, NEXT SEG 8

```

EXACT
FOR N=0 STEP 1 UNTIL 50 DO
  BEGIN
    RTIN=NR/50
    TRIN=ILAG(NR*(N+1)*57.4AT, NAT,RT)
    END
  TR151=TR150
  N=0
  FOR X=0.0+.1, .2, .35, .5, .6, .7, .8, .85, .9, .95, 1 DO
  BEGIN
    RTIN=NR
    TRIN=ULAG(XNR,RT,TR,50)
    N=N+1
    END
  FOR N = 1 STEP 1 UNTIL 11 DO
  BEGIN
    A=RIGHT
    SUM=0
    FOR PHI = 1 STEP 1 UNTIL MAX(1) DO
    BEGIN
      SUM=0
    END
  END
  X=BSIN,PHI)
  X=CIN,PHI)
  X=NSIN,PHI)
  FOR J = 1 STEP 1 UNTIL LAMMAX DO FIXARG(J)=0

```

```

SC 81 12810
SC 81 12810
SC 81 12910
SC 81 12910
SC 81 13111
SC 81 13511
SC 81 13712
SC 81 13810
SC 81 13913
SC 81 14411
SC 81 14411
SC 81 14610
SC 81 17010
SC 81 17111
SC 81 18210
SC 81 18310
SC 81 18310
SC 81 18410
SC 81 18413
SC 81 18413
SC 81 18413
SC 81 18413
SC 81 18413
SC 81 18413
SC 81 18413
SC 81 18413
SC 81 18413
SC 81 18413

```

VM = 0 J	SC	01	19912
FOR S=1/2 STEP 1 UNTIL 0 DO	SC	01	20011
BEGIN	SC	01	20512
RSHXY = SORT(CCA) * 2 + 2 * XAXX * R + 5 * 2 J J	SC	01	20512
TMO = LAG(RSHXY, 0, R/50, 1, 0, 51) J	SC	01	21011
IRM = 1.44022/TM J	SC	01	21312
ZMOU J	SC	01	21413
FOR J = 2 STEP 1 UNTIL LAMMAX DO	SC	01	21512
BEGIN	SC	01	21810
LAMRDA = LAM(J) J	SC	01	21810
KLN = LAG(TM, 0, T, KAPP(J, 1, 1, 1) J J	SC	01	21910
IRR = 1.19250 - 12 / (LAMRDA * 5 * (EXP(IRM/LAMPOA) - 1)) J	SC	01	22210
TEMP = KLN * X / 2 + EXPARG(J) J	SC	01	22613
EXPARG(J) = X * KLN + EXPARG(J) J	SC	01	22911
IF TEMP < 30 THEN	SC	01	23113
BEGIN	SC	01	23212
YMT = KLN * IRR * LAG(TEMP, 0, 1, 6, 300) J	SC	01	23310
ZM = YMT * LAMPOA(J) * 2 J	SC	01	23613
END TEMP 30 J	SC	01	23813
END OF LAM-DA LOOP J	SC	01	23813
VM = ZM + VM J	SC	01	24110
END OF S LOOP J	SC	01	24211
SUM = VM * X + SUM J	SC	01	24510
SUM1 = SUM1 + SUM J	SC	01	24613
END OF PH1 LOOP J	SC	01	24812
PR1(N) = SUM1 * X * PH1 J	SC	01	24910
END OF N LOOP J	SC	01	25111
IF ZM1 THEN APPF = FALSE ELSE APPF = TRUE J	SC	01	25312
IF APPF THEN BEGIN	SC	01	25613
IF COUNT > 1 THEN GO APPROX J	SC	01	25712
BEGIN	SC	01	25813
COMMENT FORMING TABLES OF PP(T), PR(T), KP(T) FOR APPROX SOLUTIONS J	SC	01	25813
REAL PRINT, PRINT1	SC	01	25913
START OF SEGMENT ***** 10			
ARRAY PP(0150, 11361) J	SC	101	010
FOR J = 1 STEP 1 UNTIL 2 DO	SC	101	210
BEGIN	SC	101	310
LAMRDA = LAM(J) J	SC	101	310
IRM = 1.44022/LAMRDA J	SC	101	410
TEMP = LAMRDA * 5 J	SC	101	511
I = 1 J	SC	101	712
FOR K = 1 STEP 0.1 UNTIL 1.0	SC	101	812
PPR(J, I + 1) = 1.19250 - 12 / (TEMP * (EXP(IRM/X) - 1)) J	SC	101	1110
PPR(J, I) = 2 * PPR(J, 0) - PPR(J, I) J	SC	101	2011
PPR(J, I + 1) = 2 * PPR(J, I) - PPR(J, I - 1) J	SC	101	2710
END OF PPR TABULATION J	SC	101	3412

FOR I = 0 STEP 1 UNTIL NT DO	SC 101 1613
BEGIN	SC 101 1910
RB11=0	SC 101 1910
FOR J= 1 STEP 1 UNTIL 2 DO	SC 101 4011
RB11= PRRC(J,1)DLAMBDA*RA1(J) +RB11	SC 101 4110
END OF NR TABULATION	SC 101 4712
RR(NT+1)= 2*RR(NT)+RB(NT+1)	SC 101 4813
FOR I = 0 STEP 1 UNTIL NT DO	SC 101 5312
BEGIN	SC 101 5510
KRINT=KPINT+ 0	SC 101 5510
FOR J = 1 STEP 1 UNTIL 2 DO	SC 101 5611
BEGIN	SC 101 5710
KRINT=KRINT+1*PBREJ,I+11-PBREJ,I-11)/(2*DT)*DLAMBDA*RA(J)	SC 101 5710
TEMP= IF A = KAPPA1,J,1=0 THEN A ELSE 0=30	SC 101 4313
KPINT = KPINT + PBREJ,I+1*TEMP*DLAMBDA*RA(J)	SC 101 4910
END OF J LOOP	SC 101 7310
IF I =0 THEN KR(0) = (KR(1)-RB(0))/DT/KRINT ELSE	SC 101 7511
KR(1) = (KR(1)+1-KR(1-1))/(2*DT)/KRINT	SC 101 7913
KR(1)=KPINT/RB11	SC 101 4613
END OF I LOOP	SC 101 4813
COMMENT RB11,KPINT,KR(1) VALUES NOW FORMED	SC 101 9110
LITTLER = 1	SC 101 9110
END	SC 101 9113

APPROX 1	SC 101 24010
BEGIN COMMENT APPROX SOLUTION	SC 101 24010
ARRAY KA,RAZ,TM(1:2001)	SC 101 24010
START OF SEGMENT ***** 11	
FOR N = 1 STEP 1 UNTIL 11 DO	SC 111 211
BEGIN	SC 111 310
A=PI(N)	SC 111 310
SUMF = 0	SC 111 410
FOR PHI = 1 STEP 1 UNTIL MAX(N) DO	SC 111 413
BEGIN	SC 111 813
SUM = 0	SC 111 813
X=DSIN,PHI) * W(C(N,PHI) * COS(SIN,PHI))	SC 111 912
VM = 0	SC 111 1413
TAUP2 = 0	SC 111 1512
TAUH2 = 0	SC 111 1611
RSH=V+SQRT(4+2*TAH=V*(S+D+.15*V)+S+2)	SC 111 1710
TIMP=LAW(RSH*V,0,R/50,TAH,51)	SC 111 2311
KP2= LAW(TEMP,HT,DT,KP,NT)	SC 111 2612
KR2= LAW(TEMP,HT,DT,KR,NT)	SC 111 2911
TAUP = KP2*V/2	SC 111 3210
TAUH = KR2*V/2	SC 111 3313
COUNTS = ENTIER((S+.25*V)/APPROXOS1+2)	SC 111 3512

K0,ANK 1	SC 111 1911
FOR S= U =.1XX STEP =X UNTIL K DD	SC 111 4012
BEGIN	SC 111 4611
COUNTS = COUNTS + 1 1	SC 111 4611
RSHAY = SQRT(A+2 +2*SHAB+4+2) 1	SC 111 4712
TEMP=TH(COUNTS)+LAG(RSHAY,0,R/40,TR,51) 1	SC 111 5211
KPT=LAG(TEMP,RT,DT,KP,NT) 1	SC 111 4612
KRT=LAG(TEMP,RT,DT,RR,NT) 1	SC 111 4911
TAUP2= KKKPT + TAUP2 1	SC 111 4210
TAUR2= AKKRT + TAUR2 1	SC 111 4313
KA(COUNTS)=LITTLER/(TEMP+LITTLER +TAUP2)=(LITTLER+TAUR2)/	SC 111 4512
TEMPKKPT + TAUP/TEMPKKRT 1	SC 111 4613
TEMP=LAG(SQRT(A+2+2*AKKRT(TEMP+S=X/2)+ TEMP+2),0,R/50,TR,51)	SC 111 7119
1	SC 111 7912
KP2= LAG(TEMP,RT,DT,KP,NT) 1	SC 111 4012
KR2= LAG(TEMP,RT,DT,RR,NT) 1	SC 111 4311
TAUP=KP2*X+TAUP 1	SC 111 4610
TAUR=KR2*X+TAUR 1	SC 111 4713
KA2(COUNTS)=LITTLER/(TEMP+LITTLER+TAUP2)=(LITTLER+TAUR2)/	SC 111 4912
TEMPKK2 + TAUP2 /TEMPKK2 1	SC 111 9213
END OF PRE S LOOP 1	SC 111 9513
TEMP=LAG(SQRT(A+2+2*AKKRT(S+A/4)+2+2),0,R/50,TR,51) 1	SC 111 14210
KPT =LAG(TEMP,RT,DT,KP,NT) 1	SC 111 11011
KRT =LAG(TEMP,RT,DT,RR,NT) 1	SC 111 11310
TAUP=(KPT+KP2)/2KA/A 1	SC 111 11313
TAUR=(KRT+KR2)/2X/R 1	SC 111 11412
KA2(1)=(LITTLER/(TEMP+LITTLER+TAUP2)=(LITTLER+TAUR2)/TEMPKKPT	SC 111 12111
+ TAUP/TEMPKKRT)/2 1	SC 111 12510
TAUA =0 1	SC 111 12810
COUNTS= 0 1	SC 111 12813
FOR S= A/2 STEP X UNTIL 0 DD	SC 111 12912
BEGIN	SC 111 13413
COUNTS=1+COUNTS 1	SC 111 13413
RSHAY= SQRT(A+2+2*SHAB+4+2) 1	SC 111 13610
KLM = KA(COUNTS) 1	SC 111 14013
BRR = LAG(TH(COUNTS),RT,DT,RR,NT) 1	SC 111 14113
TEMP +TAUA+ KA2(COUNTS)*A + TAUA 1	SC 111 14413
IF TEMP >30 THEN ZMOG ELSE ZMO=LMRRBRRLAG(TEMP,0,.1,G,300) 1	SC 111 14711
VM= ZM + VM 1	SC 111 15212
END OF S LOOP 1	SC 111 15413
SUM = VMXX +SIMP 1	SC 111 15710
SUMF= SUMRR +SIMP 1	SC 111 15813
END OF PM1 LOOP 1	SC 111 16012
PRX(N)= SUMF+ANPM1 + PRX(N) 1	SC 111 16110
END OF M1 LOOP 1	SC 111 16410
END OF APPPOX FLUX 1	SC 111 16611

END OF APPF ;	11 IS 170 LONG, NEXT SEG 8	
FRN(0)+FRN(1)+0 ;	SC 81 26110	
FOR J= 2 STEP 1 UNTIL 9(NN	SC 81 26110	
FRN(J)+ULAS(NTJ)J+R1,FRN(1) ;	SC 81 26311	
COUNT + 10 ;	SC 81 26410	
EXIT ;	SC 81 27012	
IF COUNT # 10 THEN	SC 81 27111	
WRITE(PNINTER,4 "DATA CARDS FOR FLUX PROCEDURE ARE INCOMPLETE "5) ;	SC 81 27210	
	SC 81 27213	
END OF FLUX ;	12 IS 11 LONG, NEXT SEG 8	
	SC 81 27611	
PROCEDURE DELSQ (N,SC) ;	P IS 296 LONG, NEXT SEG 2	
VALUE N ; INTEGER N ;	SC 21 2610	
ARRAY SC(0) ;	SC 21 2610	
BEGIN	SC 21 2610	
SC(1) + A*(S(2)+S(3))/(OR+2) ;	SC 21 2610	
FOR I=2 SL N DO	SC 21 2610	
SC(I)+(S(I)+1)+S(I-1)+0.5/(OR+R(1)) + (A*((+1)+S(1-1)+S(I)+2))/(OR+2) ;	SC 21 3013	
END OF DELSQ ;	SC 21 3210	
PROCEDURE TRIJAG (N, A,B,C,D) ;	SC 21 4013	
ARRAY A,B,C,D(0) ; INTEGER N ;	SC 21 4610	
COMMENT PROCEDURE FOR INVERTING TRIJAGONAL MATRIX OF N*N ;	SC 21 4610	
	SC 21 4610	
BEGIN REAL Z ; INTEGER J ;	SC 21 4610	
	START OF SEGMENT ***** 13	
O((3 + O((3)/B(1) ;	SC 131 010	
Z= B((3) ;	SC 131 211	
FOR J= 2 SL N DO	SC 131 311	
BEGIN R(J)=1 + C(J-1)/Z ;	SC 131 410	
Z + B(J) = A(J-1) + R(J) ;	SC 131 710	
O(J) + (O(J)- A(J-1)+ B(J-1))/Z ;	SC 131 1012	
END ;	SC 131 1510	
FOR J= SL N=1 DO	SC 131 1711	
D(N=J) + D(N=J) =B(N=J)+ D(N=J+1) ;	SC 131 2112	
END TRIJAG ;	SC 131 2712	
PROCEDURE DVGVT (N,SM, F, DGV) ;	13 IS 30 LONG, NEXT SEG 2	
ARRAY SM, F, DGV(0) ; INTEGER N ;	SC 21 4610	
COMMENT PROCEDURE FOR EVALUATING THE DIVERGENCE OF FLUX ;	SC 21 4610	
BEGIN REAL M,2 ; INTEGER I, J ;	SC 21 4610	
	START OF SEGMENT ***** 14	
P= F(2)+2/OR +A*(S(2)+S(3))/(OR+2) ; P=ANS(P)/E+ SORT(P/SIGMA((3) ;	SC 141 010	
DVG(1) = F(2)+2/OR ;	SC 141 610	
SEQ(1) + SIGMA(1) =E+2 ;	SC 141 1012	
FOR I=2 SL N DO BEGIN	SC 141 1310	
DVG(I) + (F(I)+F(I+1))/(2+OR) + F(I)/R(I) ;	SC 141 1410	

```

      SIGE(I) = SIGNA(I) * E-2  )
      DGV(I) = SEB(I) - DVG(I)  )
      END  I2  )
      DGV(I) = SIGE(I) * E-2 - F(I)*X2/DR  )
      END  DVGVT  )

```

```

SC 141 1913
SC 141 1921
SC 141 1932
SC 141 1943
SC 141 1950

```

```

      COMMENT  XCHANGE (VERSION OF 4/1/66)

```

```

1A 15  1A LONG, NEXT SEG  2
00000000 SL  21  A610
00000000 SC  21  A011
SC  21  A011
SC  21  A011
SC  21  A210
SC  21  A312
SC  21  7513
SC  21  7712
SC  21  R713
SC  21  R910
SL  21  9011
SC  21  9512
SC  21  9713
SC  21  10010
SC  21  10212
SC  21  10A13
SC  21  10613

```

```

      COMMENT  PRELIMINARY CALCULATIONS  )
      TIME1(PRTNTR  ) )
      RETA = 1.0  )  M = 90  )
      READ(READER, //, RB, N  )  )
      COUNT=0  )
      READ(READER, //, OT, NT  )  )
      NM = N + 1  )
      OM = NR/N  )
      FOR I = 1 SL  NM  ON  REFI = (I-1)*DR  )
      RMO = RETA*NT / (DR+2)  )
      LDA = RETA*NT / (2*NR)  )
      L(S1) = 0  )  R(S1) = RB  )
      A(I) = LDA/DR = RMO  )
      C(I) = -A*NRMU  )
      R(I) = 1 + A*NRMO  )

```

```

      FOR I=2 SL  N  ON  BEGIN
      A(I) = (LDA/R1)+1 = RMO  )
      C(I) = -(RMO + LDA/R1)  )
      END  I  )
      READ (HEADER, //, FOR I=1 SL  51  DO  TFFI  )  )
      READ(HEADER, //, FOR I=0 SL  N  DO  (STFI), SWFI  )  )
      K=0  )  TFCI=0  )
      FOR I=1 SL  NM  ON  S(I) = LAG(C(I), 2000, 270, ST, M)  )
      COMMENT  MAIN PROGRAM AND NEW TIME SOLUTIONS START HERE  )
      START  )

```

```

SC  21  10910
SC  21  11010
SC  21  11310
SC  21  11513
SC  21  11810
SC  21  13013
SC  21  14513
SC  21  14713
SC  21  14813
SC  21  14813
SC  21  14910
SC  21  1A811
SC  21  17510
SC  21  17513
SC  21  1A213
SC  21  1A512

```

```

      WRITE(PRTNTR, PNT, //, FOR I=1 SL  NM  DO  S(I)  )  )
      FOR I=1 SL  NM  DO  SIGNA(I) = ULAG(S(I), ST, SWT, M  )  )
      IF K # 0 THEN
      FOR I=1 SL  NM  DO  T(I) = ILAG(S(I), ST, M, 2000, 200  )  )
      WRITE(PRTNTR, LPAGE  )  )
      WRITE(PRTNTR, //, "AT TIME=", R12.5, X3, "SECONDS", //, THEN  )  )

```

```

15 15  17 LONG, NEXT SEG  2
SC  21  19611
SC  21  19812
SC  21  19913
SC  21  20213
SC  21  20411
SC  21  21011

```

```

      FLUX (S, F, RB  )
      IF  COUNT # 10 THEN GO  EXIT  )
      DVGVT (M, SIGMA, F, DGV  )  )
      DELSU (M, SC)  )
      FOR I=1 SL  N  ON  S(I) = SC(I) + SFO(I) = DVG(I)  )
      WRITE(PRTNTR, M01  )  )

```

```

WRITE(PRINTER, PNT), FOR 1+1 SL NN DD INIT, S11, F11, T11,
SIGN(17, SC11), DVB(11), SEQ(11), SS(11) ) )
WRITE(PRINTER, IDBL 1 )
WRITE (PRINTER, <X>, "E 0", F10.0, //>, F ) )
SC 21 21311
SC 21 22610
SC 21 23811
SC 21 24110
16 IS 8 LONG, NEXT SEG 2
A1 = 0.0 )
SC 21 24811
FOR 1+1 SL NN DD BEGIN
SC 21 24910
IFC+ IF 1+1 UR 10NN THEN 1 ELSE IF (1+1) WDD 2 DD THEN 2
SC 21 25010
ELSE 4 )
SC 21 25413
A1 = A1 + 2*3.1415926*(X+R11)*S10*111)*17C )
SC 21 25613
END INT )
SC 21 26110
A1 = A1*DR/3 )
SC 21 26311
WRITE(PRINTER, <X>, X3, "ARC CURRENT 10", R12.5, //>, A1) )
SC 21 26510
17 IS 12 LONG, NEXT SEG 2
TIMEIT(PRINTER) )
SC 21 27311
IF K= NT THEN WRIT (PUNCH, <S(E12.5, " = )>, FOR 1+1 SL NN DD
SC 21 27411
18 IS 7 LONG, NEXT SEG 2
T11 ) )
SC 21 28111
IF K 2 NT THEN GO TO EXIT )
SC 21 28811
THK+11+ THK) + DT ) K= K+1 )
SC 21 28912
FOR 1+1 SL N DD D11) + T11 + DVB11)*RTANDT )
SC 21 29311
B11) = 1 + A*RHDD )
SC 21 29912
FOR 1+2 SL N DD B11) + 1+ 2*RHDD )
SC 21 30113
TRIDAG (N, A, B, C, D) )
SC 21 30712
EXCHANGE( S, D ) )
SC 21 31111
GO TO START )
SC 21 31313
EXIT:
SC 21 31811
TIMEIT (PRINTER) )
SC 21 31910
END.
SC 21 31610
2 IS 319 LONG, NEXT SEG 1

```

CDS	IS SEGMENT NUMBER	0010, PRT ADDRESS IS 0154
EXP	0020	0160
SIN	0021	0154
SORT	0022	0154
OUTPUT(N)	0023	0107
BLOCK CONTROL	0024	0004
INPUT(N)	0025	0144
GO TO SOLVER	0026	0144
ALGOL WRITE	0027	0014
ALGOL READ	0028	0014
ALGOL SELECT	0029	0014

NUMBER OF ERRORS DETECTED = 0
 LAST CARD WITH ERROR WAS SEG #
 PRT SIZE = 156 TOTAL PGM SEG SIZE = 1404 WORDS DISK SIZE = 40 SEGS NO. PGM. SEGS = 30
 ESTIMATED CORE STORAGE REQUIREMENT = 6630 WORDS.
 16150142 WEDNESDAY, JUNE 7, 1967 PROCESSOR TIME = 31.40 SECONDS I/O TIME = 31.62 SECONDS

APPENDIX F

Analysis of Xenon Discharges

J. J. Lowke
Westinghouse Research Laboratories
Pittsburgh, Pennsylvania 15235

I. INTRODUCTION

Calculations have been performed deriving temperature profiles of discharges in xenon flash tubes from given material functions for xenon, at a specified experimental value of current and electric field strength. The calculations include the effects of conduction, radiation, and self absorption of radiation. Comparisons are made of three different methods of doing these calculations. Results of these calculations indicate that for typical values of electric field strength and current the temperature profiles are radiation dominated if the pressure is equal to or higher than four atmospheres, the profiles are relatively flat, the influence of radiation at wavelengths less than 1000Å is negligible, and the effect of self absorption in the visible continuum is of only secondary importance in determining the central temperature.

An analysis has been made of the time dependence of the experimental data of electric field strength, current and radiation. The radiation measurements suggest that the xenon discharge should be treated as a time dependent problem rather than a wall stabilized, steady state arc, which is the basis of the present calculations.

II. TEMPERATURE PROFILE CALCULATIONS

Calculations of the temperature profile for a wall stabilized steady state arc for a given electric field strength, current and gas pressure have been made using (1) the Eddington Approximation, (2) a pseudo time dependent equation and an exact radiation flux calculation and (3) a pseudo time dependent equation and an exact radiation intensity calculation. It is considered that method (3) is the least expensive. However, for comparison of calculated values of central temperature and arc radius with experiment, a simple constant temperature model is adequate.

The material functions for the calculations are those supplied by C. H. Church. The spectral absorptivities are an estimate of the continuum and neglect line radiation. Thermal and electrical conductivities are calculated using a program of De Voto. The effects of radiation were determined by dividing the spectrum into 20 equal frequency bands extending to 5×10^{16} Hz (600Å).

1. Method using Eddington Approximation

This method is outlined in reference (1). The following equations are solved numerically.

$$\nabla \cdot (\vec{F}_C + \vec{F}_R) = \sigma E^2 \quad (1)$$

$$\vec{F}_C = -k\nabla T \quad (2)$$

$$\vec{F}_R = \int \vec{F}_{R\nu} d\nu \quad (3)$$

$$\nabla \cdot \vec{F}_{R\nu} = 4\pi (\epsilon_\nu - J_\nu K_\nu) \quad (4)$$

$$\vec{F}_{R\nu} = -\frac{4\pi}{3K_\nu} \nabla J_\nu \quad (5)$$

The nomenclature is given in Table I.

Equation (5) is the only inexact equation and is known in astrophysics as the Eddington approximation. The equation is in effect a diffusion approximation for the radiation flux and is equal to a constant multiplied by the gradient of the radiation energy density, which is proportional to ∇J_ν . An iterative procedure is used to satisfy the boundary conditions which are as follows

$$\text{at } r = 0 \quad F_{R\nu} = 0 \quad \text{and } F_T = 0$$

$$\text{at } r = R \quad T = T_W \quad \text{and } J_\nu = \frac{2}{\pi} F_{R\nu}.$$

Table I

Nomenclature

\vec{F}_C	Conduction Flux Density	(watts cm^{-2})
\vec{F}_R	Radiation Flux Density	(watts cm^{-2})
k	Thermal Conductivity	(watts $\text{cm}^{-1} \text{ } ^\circ\text{K}^{-1}$)
σ	Electrical Conductivity	(mho cm^{-1})
K_ν	Spectral Absorbtivity	(cm^{-1})
ϵ_ν	Spectral Emission Coefficient	(watts $\text{cm}^{-3} \text{ ster}^{-1} \text{ sec}$)
$\vec{F}_{R\nu}$	Radiation Flux Density per unit Frequency	(watts $\text{cm}^{-2} \text{ sec}$)
J_ν	Radiation Intensity per unit Frequency	(watts $\text{cm}^{-2} \text{ ster}^{-1} \text{ sec}$)
T	Temperature	($^\circ\text{K}$)
E	Electric Field Strength	(volt cm^{-1})
I	Electric Current	(amps)
r	Radius	(cm)
T_w	Wall Temperature	($^\circ\text{K}$)
C_p	Specific Heat at Constant Pressure	(Joules $\text{gm}^{-1} \text{ } ^\circ\text{K}^{-1}$)
ρ	Density	(gm cm^{-3})
ϵ	Integrated Emission Coefficient	(watts $\text{cm}^{-3} \text{ ster}^{-1}$)
t	Time	(sec)
B_ν	Planck Function	(watts $\text{cm}^{-2} \text{ ster}^{-1} \text{ sec}$)
p	Pressure	(Atmospheres)

Input values are the material functions k , σ , K_v and ϵ_v (which are functions of temperature), and the experimental values of I and E . R is determined from

$$2\pi R(F_c + F_R)_{r=R} = IE \quad (6)$$

The solution of these equations giving T , F_R and F_C as a function of radius for $E = 29$ volt/cm and $I = 1140$ amps at a pressure of 11 atmospheres is shown in Fig. 1.

2. Method using a pseudo time dependent equation and an exact radiation flux calculation

This method has been suggested by B. Swanson.

Rather than iterate to satisfy split boundary conditions as in the former method, an assumed initial temperature profile is modified using the time dependent equation to obtain the steady state solution.

The time dependent equation, neglecting effects of mass flow is given by equation (7)

$$C_p \rho \frac{\partial T}{\partial t} = \sigma E^2 - \nabla \cdot \vec{F}_C - \nabla \cdot \vec{F}_R \quad (7)$$

As we are only interested in obtaining the steady state solution, C_p is made equal to 1, a constant. \vec{F}_C is obtained using equation (2) and \vec{F}_R is obtained exactly using the integration procedure of Swanson.² A number of difficulties associated with this method are overcome as described below.

(1) The numerical solution of this equation is unstable for large step sizes in time. This instability is described by Richtmyer³ and in the present method of solving the equation, the size of the time step for stability has been empirically found to closely follow the requirement cited by Richtmyer that

$$\Delta t < \frac{(\Delta r)^2}{2F} \text{ where } F = k/\rho C_p. \quad (8)$$

Generally the small step size requirement makes computing times prohibitively large. However in radiation dominated arcs, the temperature of most of the arc is controlled by the terms $\sigma E^2 - \nabla \cdot \vec{F}_R$ of equation (7) and not by ∇F_C which causes the instability. By initially dividing the term $\nabla \cdot \vec{F}_C$ by a factor of the order of 30 and increasing the step size by the same factor the rate of convergence to the final profile is greatly increased. The multiplying factor is then removed to determine the outer small region of the profile, which is controlled by conduction. In this latter stage of the calculation it is only necessary to recalculate \vec{F}_R , which is the most time consuming part of the calculation, at say every twentieth time step, for \vec{F}_R is determined primarily by

the temperature of the inner region of the arc. With this simplification any initial temperature profile can be made to rapidly converge to the final solution.

(2) In the present problem, current and electric field strength are input values and the radius and the temperature profile are the output. After each time step the radius is recalculated using equation (9), where the temperature profile is regarded as a function of r/R

$$R^2 = I[2\pi E \int_0^1 x \sigma dx]^{-1} \quad (9)$$

where $x = r/R$.

In this way the correct current is maintained as the temperature profile is varied.

(3) It is found that the temperature profile can vary monotonically and very slowly in a way making it difficult to determine the error from the true steady state solution. To test for convergence, after calculating each new temperature profile, equations (1) and (2) are solved to obtain \vec{F}_R as a function of r . If the temperature profile is correct, the values of \vec{F}_R will agree with the values of \vec{F}_R obtained from the spectral absorptivities using the Swanson exact integration procedure.

In the numerical results presented using this method the two values of \vec{F}_R agree to 1% in each case. The method was used for the conditions of Fig. 1 and the temperature profile is shown as the broken curve. The small difference in the profiles near the outer wall is considered to be due to an insufficiently small step size in method 2 and not due to the Eddington approximation. The step size in r/R near the wall in method 2 was 0.01 whereas in the Eddington method it was 0.0001.

The method was also used for $p = 4$ Atmospheres with $E = 29 \text{ volt cm}^{-1}$ and $I = 1140$ amps giving results insignificantly different from those shown in Fig. 2, which were obtained using method 3. Fig 3 gives results obtained using method 2 showing the variation of F_{Rv} with r at two different frequencies. The radiation flux integrated from the absorption edge at $\nu = 2.9 \times 10^{15}$ to $\nu = 5 \times 10^{15}$ Hz attains a maximum of only 2% of the total radiation flux at $r/R = 0.87$ for the conditions of Fig. 2. The inclusion of lines in this region of the spectrum will only decrease the radiation flux as, from the Eddington Approximation, which is equation (5), K_v is increased in the region of lines and $J_v \sim B_v$ (see Fig. 4). Consequently it is concluded that, except for very high powers where the central temperature is greater than 14000°K , the effect of radiation for wavelengths less than 1000\AA can generally be neglected in the present calculations.

3. Method using a pseudo time dependent equation and exact radiation intensity calculations

For the conditions of the present problem it is of considerable advantage to express equation (7) in the form

$$C_p \rho \frac{\partial T}{\partial t} = \sigma E^2 - \nabla \cdot \vec{F}_c - 4\pi(\epsilon - \int J_\nu K_\nu d\nu) \quad (10)$$

where use is made of the continuity equation for radiation, equation (4). From Kirchoff's Law $\epsilon = \int B_\nu K_\nu d\nu$ and ϵ is simply a function of temperature. J_ν can be obtained exactly from a modification of the Swanson integration procedure used to obtain \vec{F}_R .

The advantages of this modification to method 2 are

- a. The increment in temperature does not depend on the gradient of a computed quantity. In method 2 to determine $\nabla \cdot \vec{F}_R$, F_R needs to be calculated to high accuracy and at many radial steps.
- b. For typical experimental conditions in xenon, $\int J_\nu K_\nu d\nu$ is small compared with ϵ , provided that ultraviolet radiation can be neglected. Then the integral need only be calculated at say every 100th step, instead of after every 20th step, as outlined in the latter part of Section

II 2 (1). In fact if the integral in the visible range of the spectrum is set at zero, the central temperature is decreased by only 200°K for Fig. 1 and 300°K for Fig. 2.

Instead of having E and I as the input, as in method 2, E and R are treated as the input and the value of I is calculated as output. The difficulty outlined in II 2 (2) is thus removed and the stability of the numerical solution is also improved.

The profile obtained using this method, with $E = 29$ and $R = 0.1$ as input at a pressure of 4 Atmospheres is shown in Fig. 2. Fig. 4 gives J_v as a function of frequency at two radial points.

4. Constant temperature model

In any comparison of theoretically derived temperature profiles with experiment one of the principal interests is to compare, for any value of I and E , the theoretical central temperature and radius with experimental observations. An assessment can then be made of the accuracy of the input material functions, σ and K_v , assuming that the experimental arc is wall stabilized and in an effective steady state condition. For this purpose, for the experimental conditions considered in this paper, the central temperature and R can be computed to within 5% simply by assuming that the arc is at constant temperature, without computing the temperature profile.

For radiation dominated arcs, loss of energy by conduction at the center of the arc is negligible compared with radiation losses. Thus the input electrical energy equals the net emission of radiation energy, as expressed in equation (11), i.e.,

$$\sigma E^2 = 4\pi(\epsilon - \int J_v K_v dv) \quad (11)$$

At the center of a cylindrical plasma of radius R and uniform temperature T , J_v can be calculated using the two radiation equations (4) and (5) again given below

$$\nabla \cdot \vec{F}_{RV} = 4\pi(\epsilon_v - J_v K_v)$$

$$\vec{F}_R = - \frac{4\pi}{3K_v} \nabla J_v$$

As ϵ_v and K_v are constant the equations can be solved analytically to give

$$J_v(0) = B_v \left\{ 1 - 1/(I_0(y) + \frac{8}{\sqrt{3}\pi} I_1(y)) \right\} \quad (12)$$

where $y = \sqrt{3} K_v R$ and I_0 and I_1 are modified Bessel Functions.

In this way the integral in equation (11) can be evaluated, and the equation used to determine E for any given cylinder of radius R and temperature T . The current I is then obtained from the conductivity equation (13)

$$I/E = \pi R^2 \sigma \quad (15)$$

Curves computed using equations (11), (12) and (13) are given in Figs. 5, 6 and 7 for pressures of 2.5, 4 and 11 atmospheres respectively. The agreement of the central temperature and radius predicted for pressures of 4 and 11 atmospheres for $E = 29$ and $I = 1140$ with the temperature profiles of Figs. 1 and 2 is within 5%.

For $p = 2.5$ Atmospheres, the point at $E = 29$ volt cm^{-1} and $I = 1140$ amperes appears to be just in the folded region of the curves of Fig. 5 where multiple solutions are possible. The existence of multiple solutions has been investigated but for other input material functions and for a different gas and will be reported later. For xenon at 2.5 Atmospheres, for E greater than 30 and $I = 1140$ the only solution that exists is for a conduction dominated arc where the central temperature is controlled by thermal conduction and not by radiation. At $E = 29$ volt cm^{-1} $I = 1140$ amperes the only solution that was found was that of a conduction dominated arc with a central temperature above $19,000^\circ\text{K}$. At these temperatures the input material functions are unknown. No detailed search was made for the existence of a solution corresponding to a radiation dominated arc for this value of E and I .

III. COMPARISON WITH EXPERIMENT

1. Steady state condition

For a tube of $R = 0.63$ cm the peak values of I , E and temperature that have been measured are $E = 29$ volt cm^{-1} , $I = 1140$ amps, central temperature = $11,500^\circ\text{K}$ and pressure = 4.2 atmospheres.⁴ As these quantities apply for a time corresponding to $\frac{\partial T}{\partial t} = 0$ it should be appropriate to compare with the steady state theoretical solution. Upper and lower limits of the possible gas pressure are 11 and 2.5 Atmospheres.

Results obtained from Fig. 6, and for similar curves at 4 Atmospheres but with different values of σ and K_v are given in Table 2.

Table 2 ($p = 4$, $E = 29$, $I = 1140$)

Input		Output	
σ	K_v	R	T
De Votto Values	Normal Continuum	0.4	13,300
De Votto Values	2 x Continuum	0.42	11,700
1/2 x De Votto	Normal Continuum	0.6	11,700
1/2 x De Votto	2 x Continuum	0.62	10,800

If lines are included in the spectral absorbtivity data, the integrated emission coefficient may be increased by a factor of two. However, as is seen from Table 2, the computed radius is still only 0.42 cm and σ would still need to be decreased for the arc to fill the tube.

Unfortunately measurements of the discharge radius are difficult to make. Furthermore no accurate experimental measurements of σ for xenon are known. It is seen that the theoretical predictions are in very approximate agreement with experiment, but if the discharge does indeed fill the discharge tube it would appear that the De Vott³ values of σ are too high. However an analysis of the time dependence of the experimental parameters suggests that the discharge does not fill the tube. Therefore it should not be concluded that we believe that the σ or σ data is in error.

2. Time dependence of the discharge

From the time dependence of the experimentally⁴ observed values of E , I and radiation intensity at 8232Å, the curves of Fig. 8 and 9 have been prepared. In Fig. 8 it is seen that the curves for differing discharge energies are in reasonable coincidence for the latter portion of the discharge time. However it is seen in Fig. 9 that the radiation intensity at a particular value of I varies markedly for discharges of differing input power. If the discharge were to be well stabilized and effectively in the steady state condition, the value of E and central temperature (and thus

the radiation intensity) would be determined for any value of R and I . If the experimental measurements are correct, it appears that the arc cannot be regarded as being wall stabilized and in the steady state at times after the peak radiation intensity.

It is known that the pressure inside of the discharge tube is determined not only by the core temperature, but is controlled to a large extent by the temperature of the gas near the tube wall. It is suggested that this gas is continually heated throughout the duration of the pulse, thus increasing the pressure. The central temperature, which is determined from equation (11), is thus lower at a given I for pulses of high power because the gas pressure is higher. In this way it may be possible to explain the radiation measurements of Fig. 9. It would then be expected that the radius of the central portion of the arc does not fill the tube, and increases throughout the duration of the pulse.

Measurements of the temperature profile at peak power are consistent with the theoretical predictions that the temperature profile is very flat.

IV. CONCLUSIONS

For the experimental parameters typical for the operation of xenon flash tubes, the following generalizations can be made.

1. The temperature profiles are very flat and are radiation dominated, provided the gas pressure equals or is greater than 4 Atmospheres.

2. Except for very high powers where the central temperature is above $14,000^{\circ}\text{K}$, the effect of radiation of wavelengths less than 1000\AA can be neglected.
3. Self absorption effects in the visible continuum generally effect the central temperature by less than 1000°K .
4. The constant temperature model in which account is taken of absorption, can be used to predict the central temperature and outer radius of wall stabilized arcs to within 10%.
5. Of the three methods used to compute temperature profiles of steady state, wall stabilized arcs from input material functions, it appears that the time dependent method using an exact radiation intensity calculation is the most economic.
6. Experimental measurements indicate that the arc discharge is not wall stabilized and that time dependent studies are needed.

V. POSSIBLE FUTURE WORK

1. Experimental

- (1) Time dependent studies of the radiation intensity as a function of radius are needed to determine whether the radius varies with time.
- (2) Improved measurements of the pressure as a function of time.
- (3) Measurements of temperature profiles of a cascade arc in xenon. Such a measurement would enable a determination of electrical conductivity, which is a crucial input parameter in the theoretical calculation of temperature profiles.

2. Theoretical

- (1) If the pressure and E were known as a function of time, a time dependent study using equation (10) could be made to predict the current and the temperature profile as a function of time. The self-absorption integral of equation (10) could be neglected giving very considerable improvement in computation time and an error of only a few hundred degrees in the central temperature. It is proposed that for a given I the temperature of the gas near the quartz walls which contain the arc, is dependent on the total power fed into the pulse, but that the temperature profile of the arc core at late times is relatively insensitive to the initial temperature profile that is assumed for the calculations. The gas pressure as a function of time could be derived from the computed temperature profiles and compared with the input pressure as a function of time.
- (2) A more involved computation could be carried out solving equations (14), (15) and (16)

$$C_p \rho \left(\frac{\partial T}{\partial t} + \underline{v} \cdot \nabla T \right) - \nabla \cdot (k \nabla T) + v \frac{\partial v}{\partial t} + v \underline{v} \cdot \nabla v - \sigma E^2 - 4\pi - \frac{1}{\rho} \frac{\partial p}{\partial t} = 0 \quad (14)$$

$$\rho \frac{\partial \underline{v}}{\partial t} + \rho \underline{v} \cdot \nabla \underline{v} = -\nabla p \quad (15)$$

$$\frac{\partial \rho}{\partial t} + \nabla \cdot \rho \underline{v} = 0 \quad (16)$$

As p and ρ determine T ; p , ρ , v and T can be determined as a function of time and compared with experiments.

VI. ACKNOWLEDGEMENT

Acknowledgement is made for many discussions with A. V. Phelps, B. Swanson, M. A. Uman, C. H. Church, R. Lieberman and P. Buchhave.

VII. REFERENCES

1. J. J. Lowke and E. R. Capriotti, "The Influence of Radiation on High Pressure Arcs", Report 66-1E2-GASES-R1 (1966).
2. B. W. Swanson, "Radiation Flux in a Non-Isothermal Non-Grey Cylindrical Arc", Paper 65-8D8-GASDY-P1 (1965).
3. R. D. Richtmyer, "Difference Methods for Initial Value Problems", Interscience (1957).
4. P. Buchhave, Quantum Electronics Dept., Private Communication.

BLANK PAGE

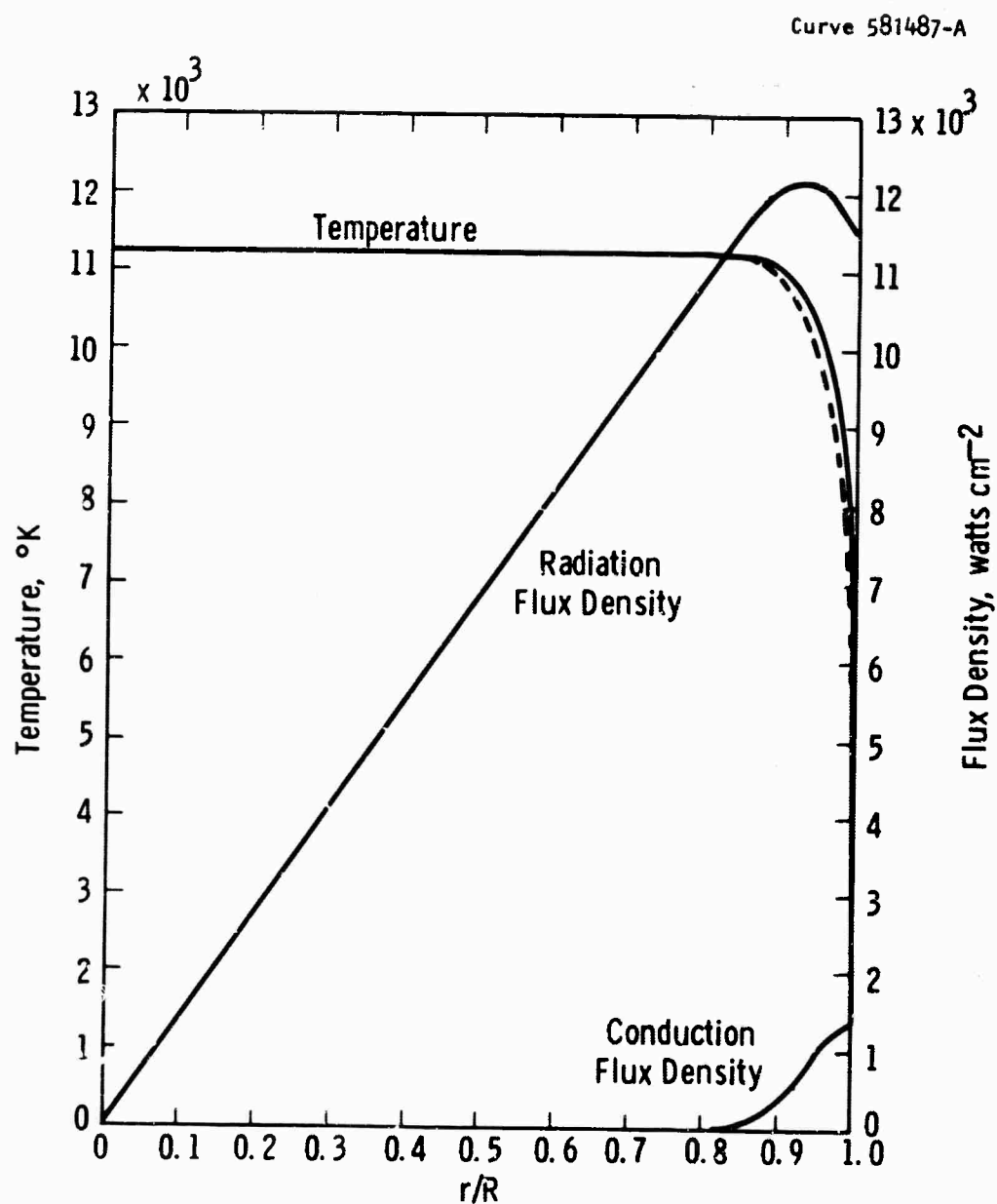


Fig. 1-Xenon arc profile

Input: $p = 11 \text{ atm}$, $E = 29 \text{ V/cm}$, $I = 1140 \text{ Amp}$, $T_W = 2000^{\circ}\text{K}$
 Output: $R = 0.410 \text{ cm}$

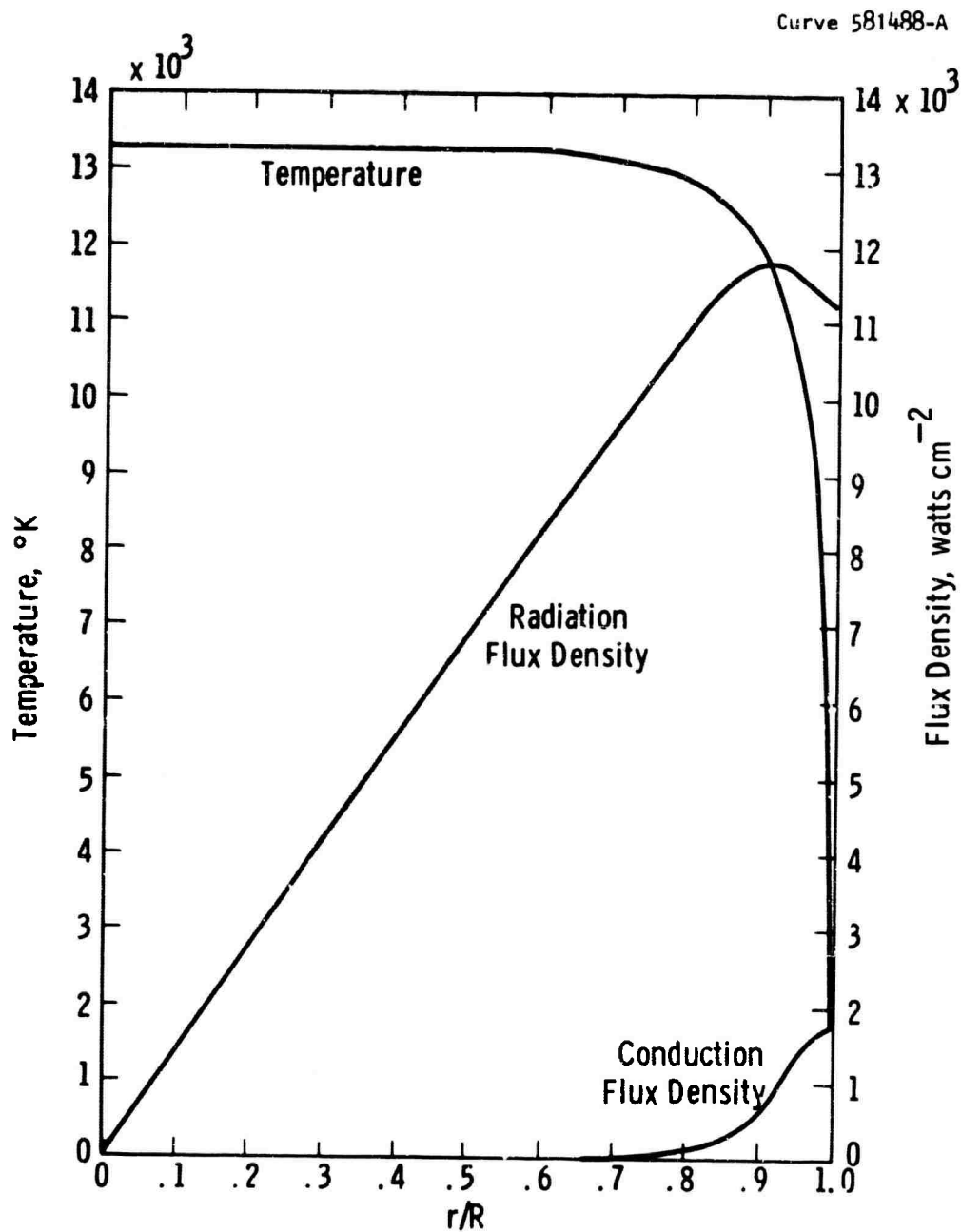


Fig. 2-Xenon arc profile

Input: $p = 4$ Atm, $E = 29$ V/cm, $R = 0.411$ cm, $T_W = 2000^\circ\text{K}$
 Output: $I = 1145$ Amps

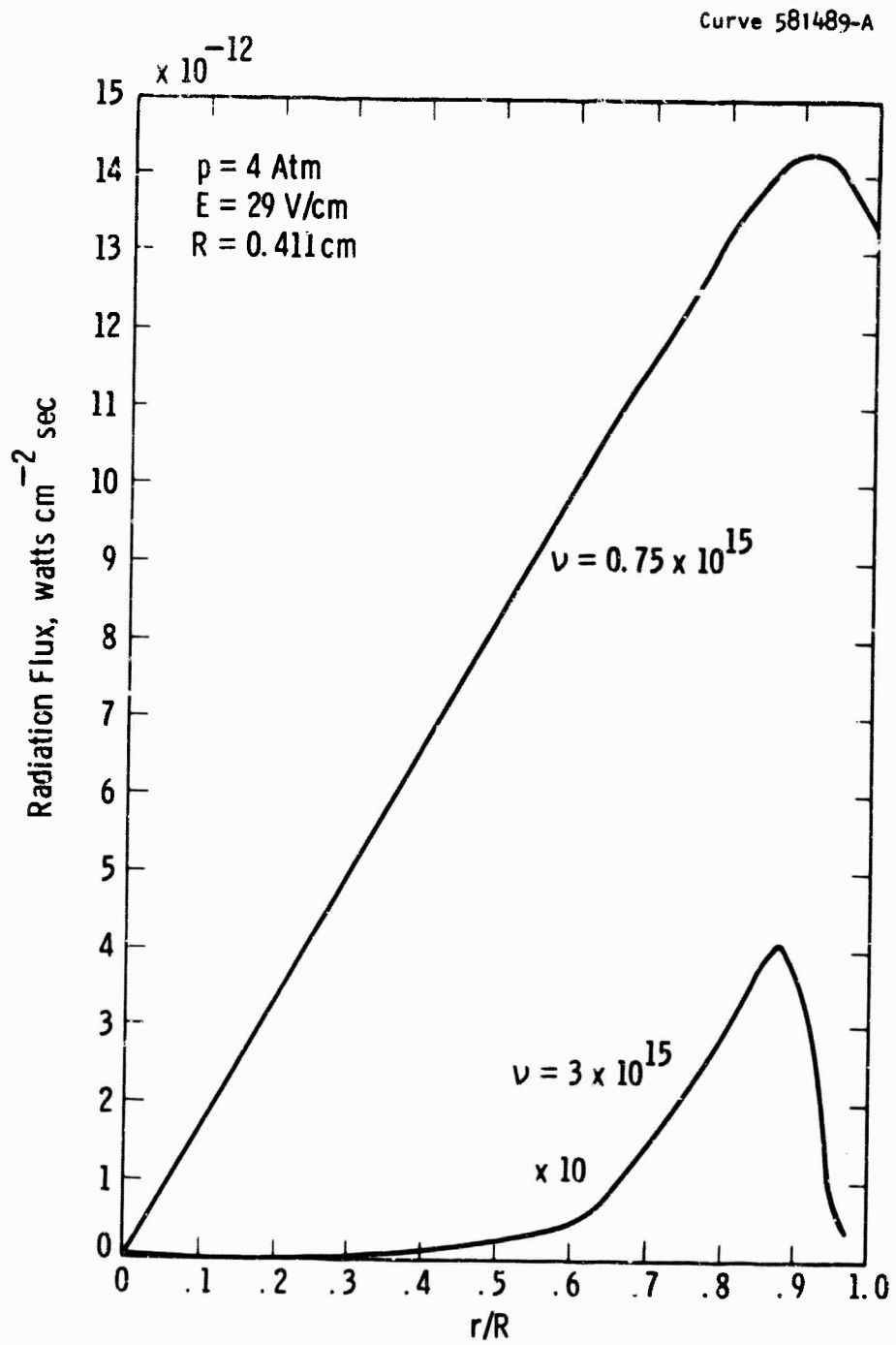


Fig. 3--Radiation flux

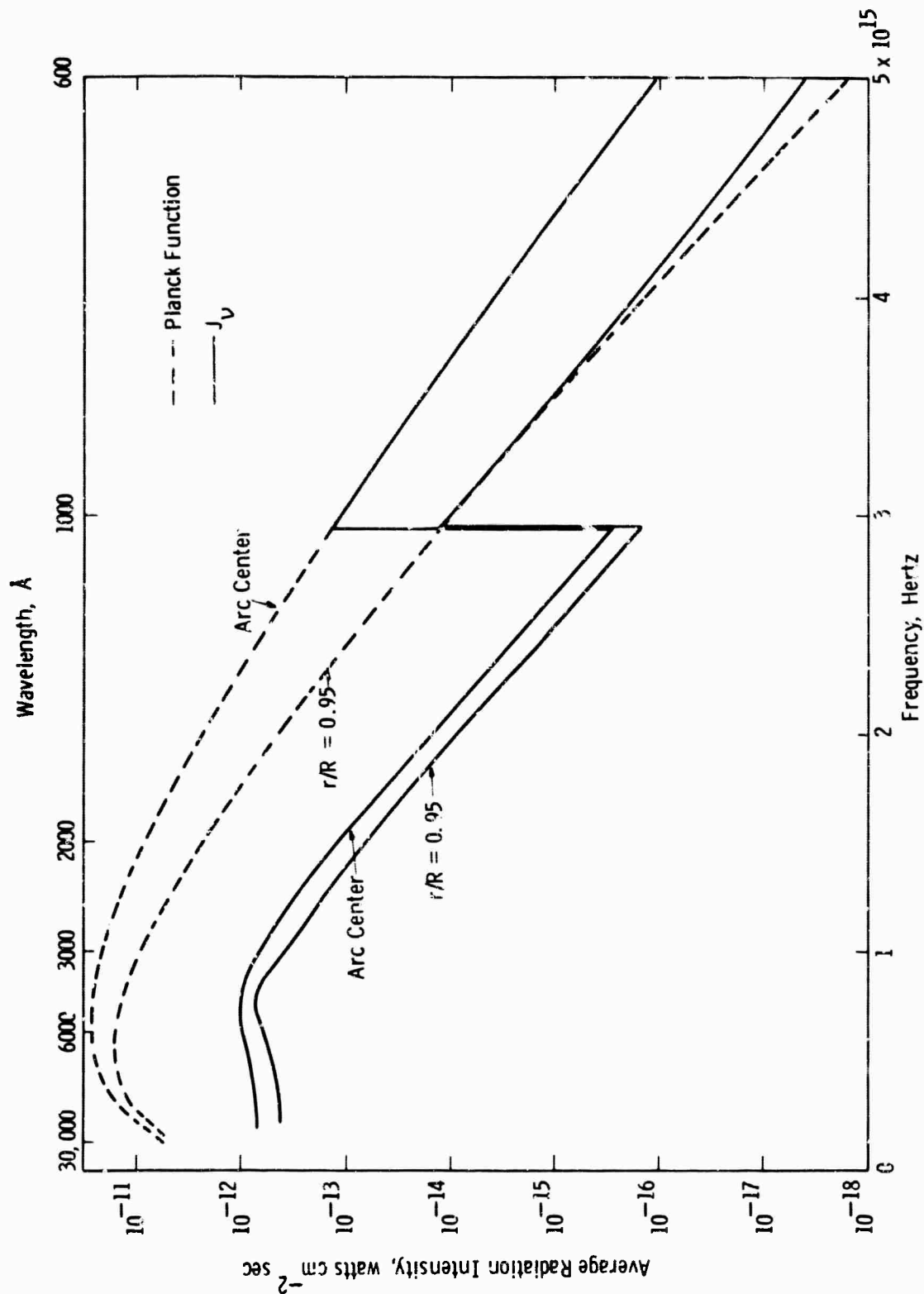


Fig. 4

Curve 581491-A

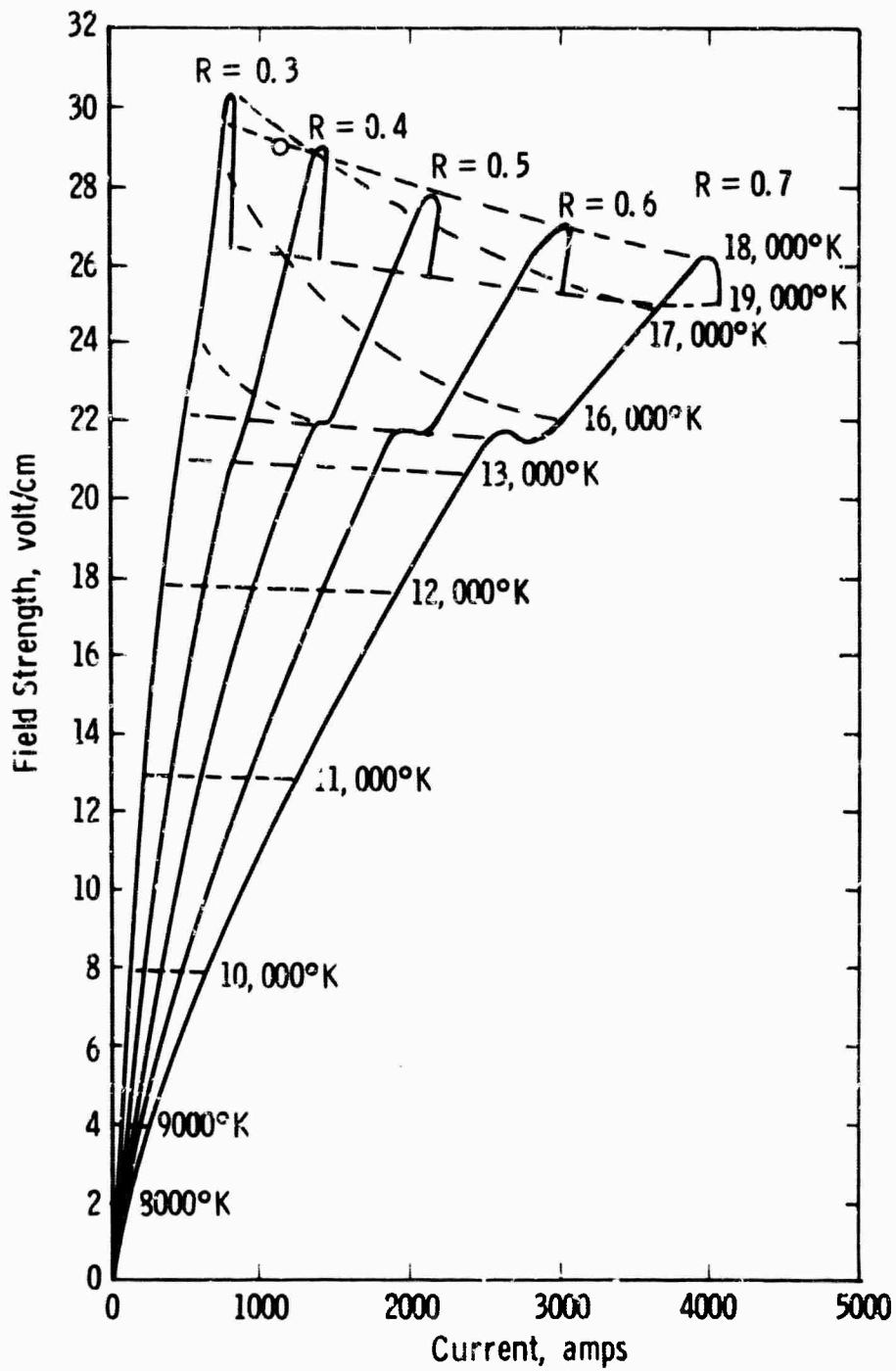


Fig. 5—Xenon, constant temp model, $p = 2.5$ atmospheres

Curve 581492-A

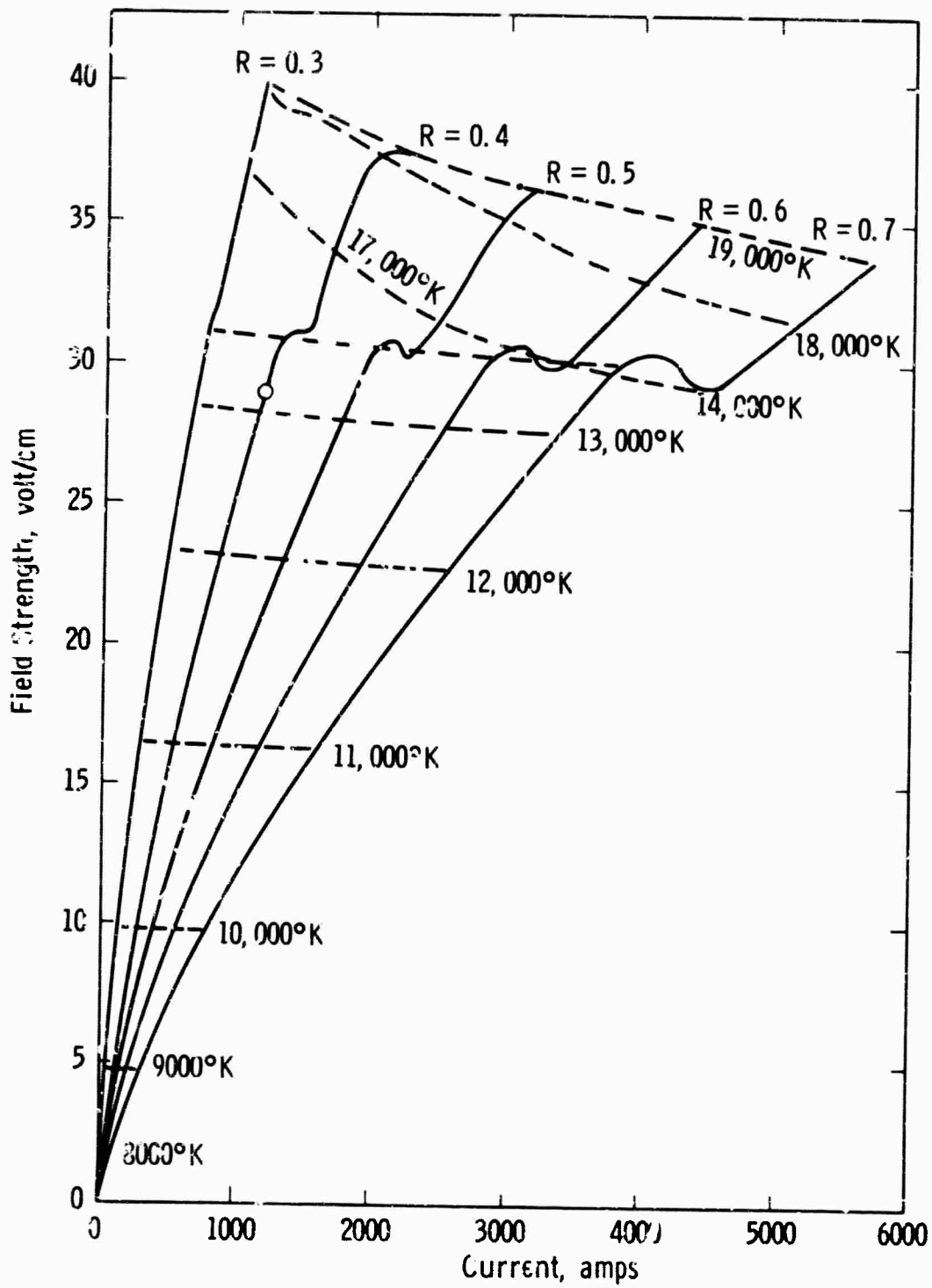


Fig. 6-Xenon, constant temp model, $p = 4$ atmospheres

Curve 581493-B

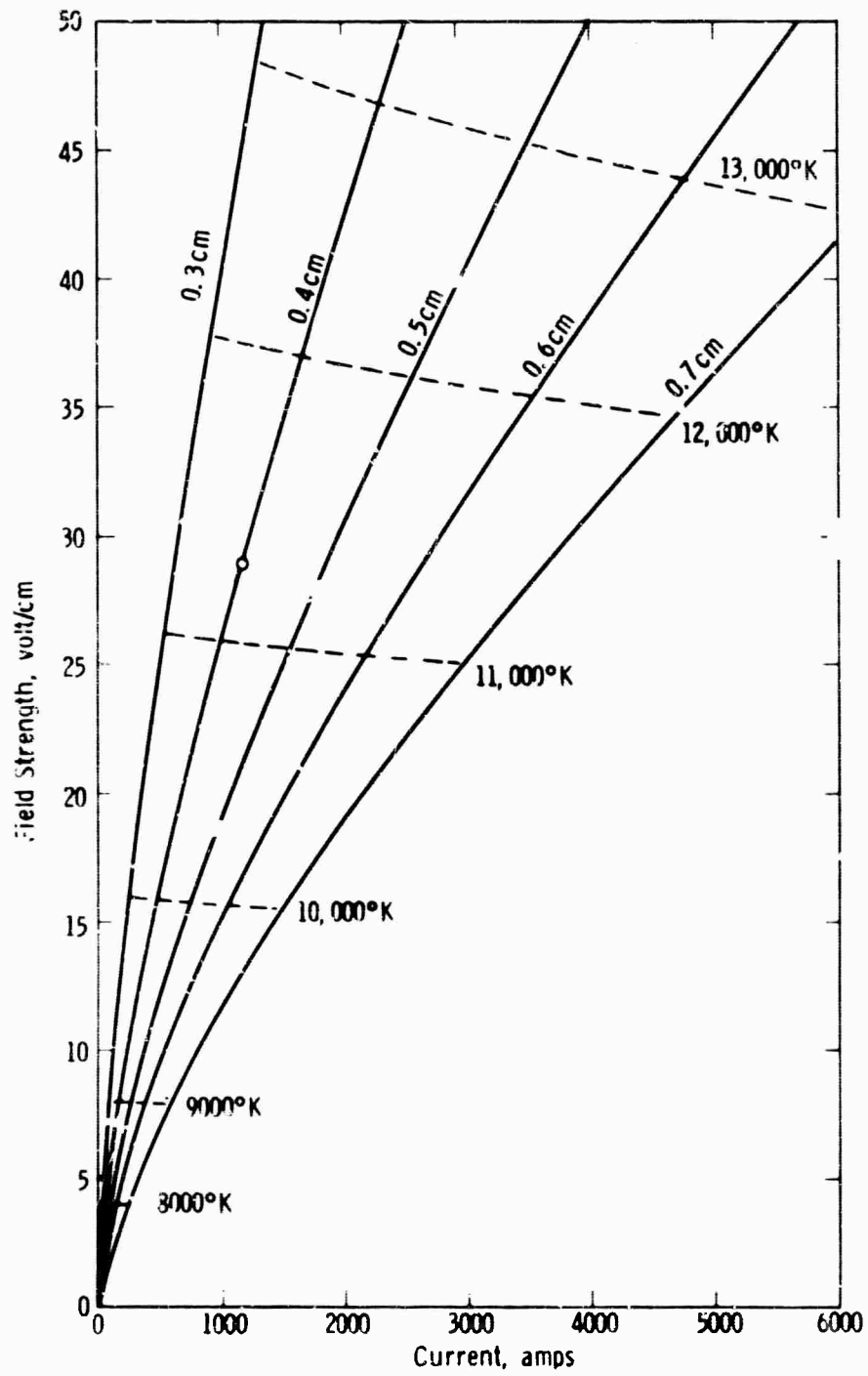


Fig. 7 - Xenon, constant temp model, $p = 11$ atmospheres

Curve 581494-A

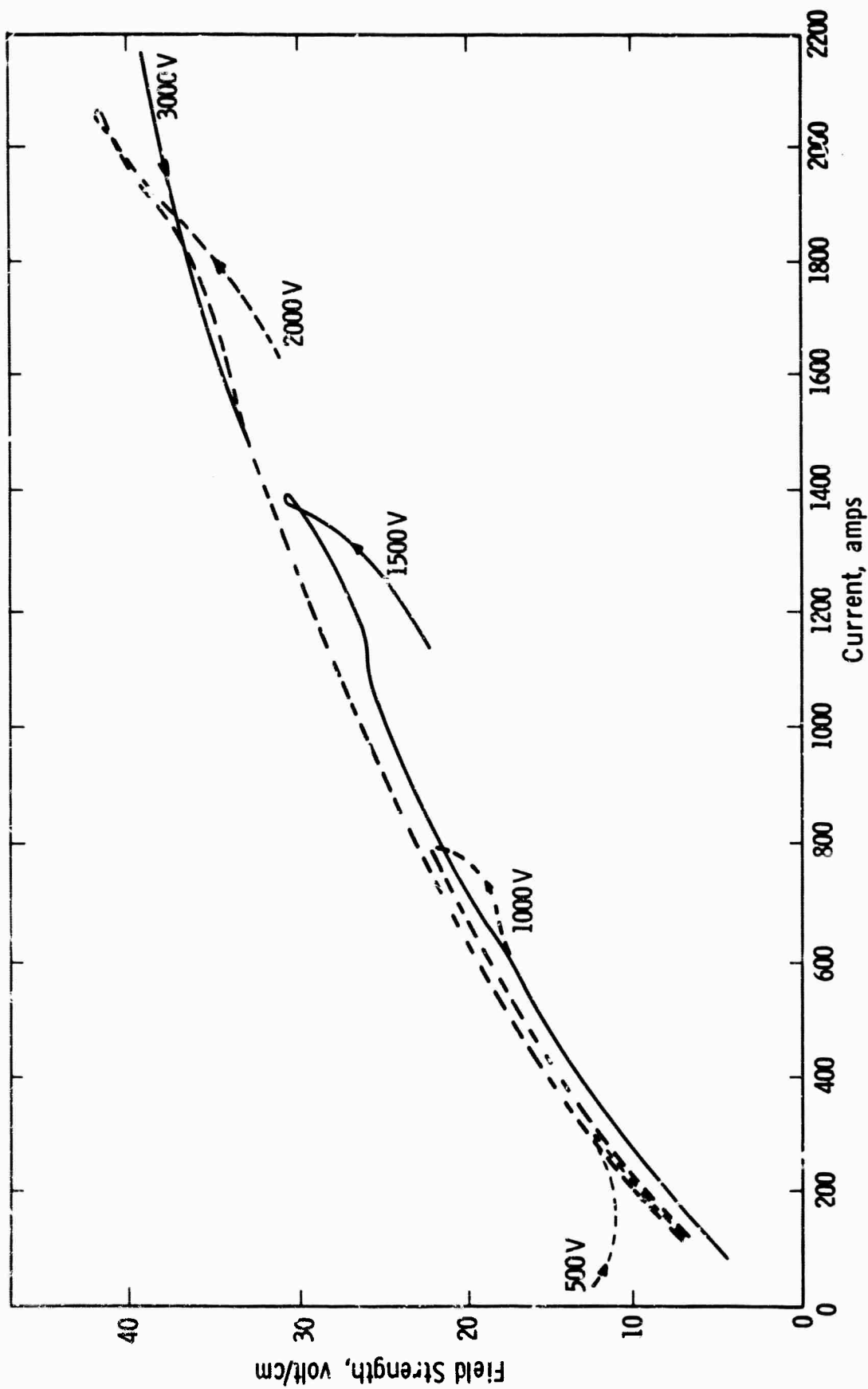


Fig. 8—Volt/current characteristic $R = 0.63$

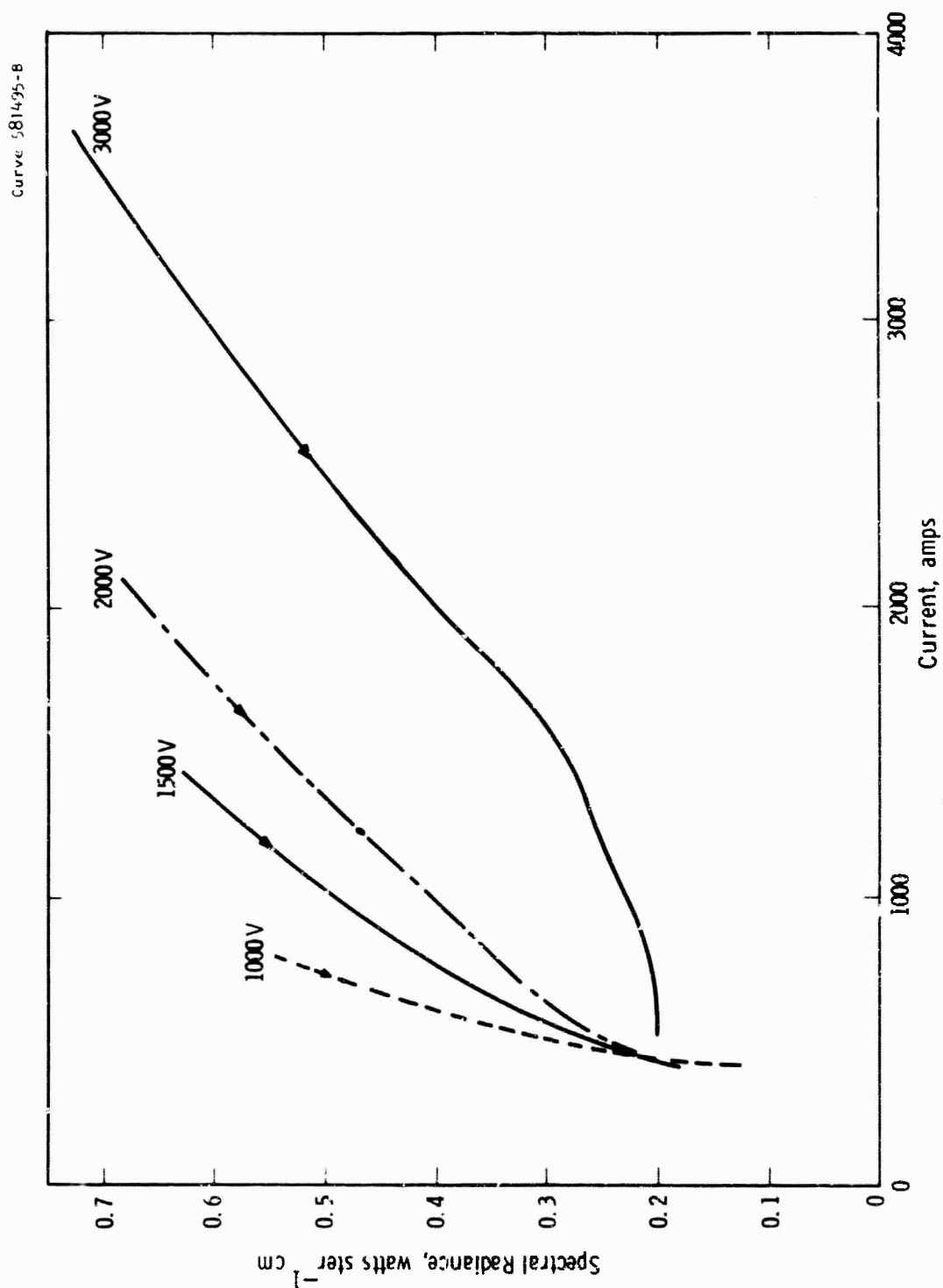


Fig. 9—Spectral radiance 8232 Å

BLANK PAGE

DOCUMENT CONTROL DATA - R&D

(Security classification of title, body of abstract and indexing annotation must be entered when the overall report is classified)

1 ORIGINATING ACTIVITY (Corporate author)		2a REPORT SECURITY CLASSIFICATION	
Westinghouse Electric Corporation		Unclassified	
		2b GROUP	
3 REPORT TITLE Final Report, Arc Discharge Sources, Covering Period from 15 October 1964 to 28 February 1967			
4 DESCRIPTIVE NOTES (Type of report and inclusive dates) Also Semiannual Report covering period from 15 October 1966 to 28 February 1967			
5 AUTHOR(S) (Last name, first name, initial)			
Church, C.H.		Liebermann, R.	Geil, E.
Swanson, B.W.		Buchhave, P.	Armstrong, L.
Lowke, J.		Liberman, I.	Basi, G.
			Sun, D.
			de Voto, R.S.
6 REPORT DATE		7a. TOTAL NO. OF PAGES	7b. NO. OF REFS
31 March 1967		193	52
8a. CONTRACT OR GRANT NO.		9a. ORIGINATOR'S REPORT NUMBER(S)	
Nonr 4647(00)		67-9C1-ARCSO-R1	
b. PROJECT NO.		9b. OTHER REPORT NO(S) (Any other numbers that may be assigned this report)	
c. ARPA Order No. 306-62			
d. Code 4730			
10 AVAILABILITY/LIMITATION NOTICES			
Qualified requestors may obtain copies from DDC			
11. SUPPLEMENTARY NOTES		12. SPONSORING MILITARY ACTIVITY	
Models for Laser Pumps (F. -h Lamps)		Office of Naval Research, Advanced Research Projects Agency, Department of Defense Under Project DEFENDER	
13 ABSTRACT			
<p>This report summarizes the studies made on Contract Nonr 4647(00) towards the development of models for the highly radiative arcs used for the high energy pumping of lasers. The report also presents the experimental and theoretical studies since the last semiannual report. The experimental investigations were primarily concerned with more extensive measurements of the spectral radiance of the plasma to provide verification for the models. The theoretical work has resulted in computer methods, described in the appendices, to calculate the transport properties, the spectral absorptivities for the lines and the continuum of xenon, and the spectral radiance and temperature profiles in cylindrical arcs. Also included as an appendix is a theoretical analysis of the xenon arc using radiative transport techniques developed in other studies.</p>			

14

KEY WORDS

Arc Discharges
Laser Pumping
Flash Lamps
Xenon
Models
Calculation
Computer Programs
Plasmas
Spectral Absorptivity

LINK A

LINK B

LINK C

ROLE

WT

ROLE

WT

ROLE

WT

INSTRUCTIONS

1. ORIGINATING ACTIVITY: Enter the name and address of the contractor, subcontractor, grantee, Department of Defense activity or other organization (corporate author) issuing the report.

2a. REPORT SECURITY CLASSIFICATION: Enter the overall security classification of the report. Indicate whether "Restricted Data" is included. Marking is to be in accordance with appropriate security regulations.

2b. GROUP: Automatic downgrading is specified in DoD Directive 5200.10 and Armed Forces Industrial Manual. Enter the group number. Also, when applicable show that optional markings have been used for Group 3 and Group 4 as authorized.

3. REPORT TITLE: Enter the complete report title in all capital letters. Titles in all cases should be unclassified. If a meaningful title cannot be selected without classification, show title classification in all capitals in parenthesis immediately following the title.

4. DESCRIPTIVE NOTES: If appropriate, enter the type of report, e.g., interim, progress, summary, annual, or final. Give the inclusive dates when a specific reporting period is covered.

5. AUTHOR(S): Enter the name(s) of author(s) as shown on or in the report. Enter last name, first name, middle initial. If military, show rank and branch of service. The name of the principal author is an absolute minimum requirement.

6. REPORT DATE: Enter the date of the report as day, month, year, or month, year. If more than one date appears on the report, use date of publication.

7a. TOTAL NUMBER OF PAGES: The total page count should follow normal pagination procedures, i.e., enter the number of pages containing information.

7b. NUMBER OF REFERENCES: Enter the total number of references cited in the report.

8a. CONTRACT OR GRANT NUMBER: If appropriate, enter the applicable number of the contract or grant under which the report was written.

8b, 8c, & 8d. PROJECT NUMBER: Enter the appropriate military department identification, such as project number, subproject number, system numbers, task number, etc.

9a. ORIGINATOR'S REPORT NUMBER(S): Enter the official report number by which the document will be identified and controlled by the originating activity. This number must be unique to this report.

9b. OTHER REPORT NUMBER(S): If the report has been assigned any other report numbers (either by the originator or by the sponsor), also enter this number(s).

10. AVAILABILITY/LIMITATION NOTICES: Enter any limitations on further dissemination of the report, other than those

imposed by security classification, using standard statements such as:

- (1) "Qualified requesters may obtain copies of this report from DDC."
- (2) "Foreign announcement and dissemination of this report by DDC is not authorized."
- (3) "U. S. Government agencies may obtain copies of this report directly from DDC. Other qualified DDC users shall request through _____."
- (4) "U. S. military agencies may obtain copies of this report directly from DDC. Other qualified users shall request through _____."
- (5) "All distribution of this report is controlled. Qualified DDC users shall request through _____."

If the report has been furnished to the Office of Technical Services, Department of Commerce, for sale to the public, indicate this fact and enter the price, if known.

11. SUPPLEMENTARY NOTES: Use for additional explanatory notes.

12. SPONSORING MILITARY ACTIVITY: Enter the name of the departmental project office or laboratory sponsoring (paying for) the research and development. Include address.

13. ABSTRACT: Enter an abstract giving a brief and factual summary of the document indicative of the report, even though it may also appear elsewhere in the body of the technical report. If additional space is required, a continuation sheet shall be attached.

It is highly desirable that the abstract of classified reports be unclassified. Each paragraph of the abstract shall end with an indication of the military security classification of the information in the paragraph, represented as (TS), (S), (C), or (U).

There is no limitation on the length of the abstract. However, the suggested length is from 150 to 225 words.

14. KEY WORDS: Key words are technically meaningful terms or short phrases that characterize a report and may be used as index entries for cataloging the report. Key words must be selected so that no security classification is required. Identifiers, such as equipment model designation, trade name, military project code name, geographic location, may be used as key words but will be followed by an indication of technical context. The assignment of links, rules, and weights is optional.